To Seda and Destina,

PEPTIDE BASED LIGAND DISCOVERY TO PREVENT PROTEIN AGGREGATION IN NEURODEGENERATIVE DISEASE CONDITIONS

A THESIS SUBMITTED TO

THE GRADUATE SCHOOL OF ENGINEERING AND SCIENCE

OF BILKENT UNIVERSITY

IN PARTIAL FULFILLMENT OF THE REQUIREMENTS FOR

THE DEGREE OF

MASTER OF SCIENCE

IN

MATERIALS SCIENCE AND NANOTECHNOLOGY

By

ÖZGE BEĞLİ

SEPTEMBER 2019

PEPTIDE BASED LIGAND DISCOVERY TO PREVENT PROTEIN AGGREGATION IN NEURODEGENERATIVE DISEASE CONDITIONS

By Özge Beğli

September 2019

We certify that we have read this dissertation and that in our opinion it is fully adequate, in scope and in quality, as a thesis for the degree of Master of Science.

_____

Urartu Özgür Şafak Şeker (Advisor)

_____

Michelle Marie Adams

_____

Çağdaş Devrim Son

Approved for the Graduate School of Engineering and Science:

_____

Ezhan Karaşan

Director of the Graduate School

ABSTRACT

PEPTIDE BASED LIGAND DISCOVERY TO PREVENT PROTEIN AGGREGATION IN NEURODEGENERATIVE DISEASE CONDITIONS

Özge Beğli

M.S. in Materials Science and Nanotechnology

Advisor: Urartu Özgür Şafak Şeker

September, 2019

Neurodegenerative diseases such as Alzheimer's disease, Parkinson's disease and Huntington's disease are cognitively and physically debilitating and progressive diseases due to the gradual and irreversible loss of discrete neuronal populations in the brain. In addition to millions of people worldwide suffering from them, the prevalence of the neurodegenerative diseases dramatically increases with the increasing lifespan of the population. Most of the current therapeutic strategies either target toxic aggregates in neurons or support the healthy cells in diseased region. However, these interventions provide only symptomatic relief and deceleration of disease progression. Besides, aggregation involves a locking phase in which irreversible transition of soluble monomeric and oligomeric molecules into insoluble fibrous structures occurs. During aggregation, fragmentation of mature fibrils leads to the formation of new oligomeric structures possessing seeding

activity. The seeds behaving as a nucleation unit trigger other structures to join the accumulated proteins.

Synthetic biology is an emerging field that suggests therapeutic solutions for several diseases. Development of synthetic proteins such as artificial transcription factors and improved antibodies, artificial cell transplants with controlled secretion, designed inhibitory RNA molecules and antisense oligonucleotides, gene circuits and logic gates, synthetic viruses as an advanced delivery system and genome editing technologies using programmable nucleases are revolutionary approaches for the diagnosis and treatment of diseases. With the utilization of a variety of advanced tools, synthetic biology is extremely promising to treat neurodegenerative disorders too. In this study, biotechnological approaches and tools such as gene cloning, yeast surface display and phage display library have been used to target neurodegenerative proteins before aggregation takes place. Neurodegenerative proteins were cloned into a plasmid DNA within bacteria and displayed on the surface of *Saccharomyces cerevisiae* cells. A phage display library has been screened against those neurodegenerative proteins and binding peptides of these proteins have been selected following recursive rounds of binding and washing steps. Peptides that bind to neurodegenerative proteins with high affinity possess the potential to block them and prevent the initiation of aggregation. Beside to the promising results of neuroprotective and neurorestorative interventions, this strategy can provide prevention of aggregation which is the underlying cause of neurodegeneration.

Keywords: Neurodegenerative diseases, synthetic biology, amyloid, yeast surface display, phage library display, protein-ligand interactions

ÖZET

NÖRODEJENERATİF HASTALIK KOŞULLARINDA AGREGASYONU ÖNLEMEK İÇİN PEPTİT TEMELLİ LİGAND KEŞFİ

Özge BEĞLİ

Malzeme Bilimi ve Nanoteknoloji, Yüksek Lisans

Tez Danışmanı: Urartu Özgür Şafak Şeker

Eylül, 2019

Alzheimer Hastalığı, Parkinson Hastalığı, Huntington Hastalığı gibi nörodejeneratif hastalıklar, beyindeki farklı nöron popülasyonlarının kademeli ve tersine çevrilemez şekildeki kaybına bağlı olarak gelişen, bilişsel ve bedensel olarak zayıflatıcı ve ilerleyici hastalıklardır. Dünya üzerinde bu hastalıklara sahip olan milyonlarca insanın yanı sıra, ortalama yaşam süresinin de artmasıyla bu hastalıkların yaygınlıkları artmaktadır. Var olan terapötik stratejilerin çoğu ya toksik kümelenmeleri hedeflemektedir ya da beynin hastalıklı bölgesindeki sağlıklı hücreleri desteklemeyi amaçlamaktadır. Fakat bu girişimler sadece semptomların hafifletilmesini ve hastalığın ilerleyişinin yavaşlatılmasını sağlamaktadır. Buna ek olarak, protein agregasyonu, çözülebilir monomerik ve oligomerik yapılardan çözülemez fibröz yapılara tersine çevrilemez bir geçişin görüldüğü kenetlenme fazını (locking phase) içerir. Agregasyon sırasında, olgunlaşmış fibrillerin fragmentasyonu yeni oligomerik yapıların oluşumuna sebep olur. Bu oluşumlar birer çekirdeklenme

birimi gibi davranır ve diğer yapıları da tetikleyerek kümelenmiş proteinlere katılmalarına yol açar.

Sentetik biyoloji birçok hastalığa tedavi edici çözümler sunan ve hızla gelişmekte olan bir alandır. Artifisiyel transkripsiyon faktörleri ve geliştirilmiş antikorlar gibi sentetik proteinler,, artifisiyel hücre transplantasyonu ile kontrollü molekül salınımı, tasarlanmış inhibitör RNA molekülleri ve antisens oligonükleotidler ile gen baskılama, gen devreleri ve mantık kapıları, gelişmiş taşıma sistemleri olarak kullanılan sentetik virüsler ve programlanabilir nükleazlar kullanılarak genom düzenleme teknolojileri, hastalıkların teşhis ve tedavisinde devrimsel nitelikte yaklaşımlar sunmaktadır. Çeşitli gelişmiş araçları kullanması yönüyle, sentetik biyoloji, nörodejeneratif hastalıkların da tedavisi için fazlasıyla umut vadedmektedir. Bu çalışmada, nörodejeneratif proteinleri agragasyon oluşmadan önce hedeflemek için gen klonlama, mayada yüzey gösterimi ve faj gösterim kütüphanesi gibi biyoteknolojik yaklaşım ve araçlar kullanılmıştır. Nörodejeneratif proteinler bakteri hücrelerinde plasmid DNAsına klonlanmış ve *Saccharomyces cerevisiae* hücrelerinin yüzeyinde gösterilmiştir. Birbirini izleyen bağlama ve yıkama aşamalarıyla, faj gösterim kütüphanesi içerisinden bu proteinlere karşı peptid seçimi yapılmıştır. Nörodejeneratif proteinlere yüksek afiniteyle bağlanan peptidler, bu proteinleri bloke edecek ve agregasyonu önleyecek nitelik taşımaktadır. Nöroprotektif ve nörorestoratif müdahalelerin umut vadeden sonuçlarına ek olarak, bu çalışmadaki strateji nörodejenerasyonun altında yatan sebep olan agregasyonu önleme potansiyeline sahiptir.

Anahtar kelimeler: Nörodejeneratif hastalıklar, sentetik biyoloji, amiloid, maya yüzey gösterimi, faj gösterim kütüphanesi, protein ligand etkileşimleri

Acknowledgement

Being a part of Synthetic Biosystems Laboratory under the supervision of Asst.Prof.Urartu Özgür Şafak Şeker is one of the greatest chances of my life. I want to express my deepest gratitude to my advisor for his guidance and mentorship throughout my master's degree. I will never forget his understanding and patience when I was dealing with lots of failures. I am so lucky to have such a role model doing his best to provide opportunities to his students and to encourage young scientists.

I am thankful to my jury members, Michelle Marie Adams and Çağdaş Devrim Son for their helpful and understanding attitudes and for their invaluable feedbacks.

I especially want to thank to my project mate, Cemile Elif Özçelik for her important contributions to improve my thesis. I am thankful to Recep Erdem Ahan for being a great iGEM advisor and all his helps in the experiments.

I am grateful to Synthetic Biosystems Laboratory for bringing a lot of valuable people in my life. During my undergraduate years, some senior students of our lab were my first guides. I am grateful to Ebru Şahin Kehribar, Behide Saltepe and Elif Duman for their informative and helpful attitudes and nice friendships. I am very happy to know Esra Yuca, Ebuzer Kalyoncu and Onur Apaydın who have always been helpful and kind to me. I am thankful to Tolga Tarkan Ölmez for his advices on yeast experiments and nice talks about life and science. It is great to know such a person like Eray Ulaş Bozkurt with a fantastic sense of humor and music taste. I want to thank for all good times I have shared with İlkay Çisil Köksaldı, Merve Erden, Gökçe Özkul, and Zafer Koşar. I want to thank Ahmet Hınçer for his friendship, contributions to this study and the motivation he has given. Additionally, being an iGEM advisor was an unforgettable experience thanks to Göktuğ Attar, Deniz Çayırtepe, İlayda Şenyüz, Ahmet Hınçer and Mehmet Ali Hoşkan.

It is a great feeling to have lots of special friends to mention here. I feel very lucky to have unforgettable memories with Nedim Hacıosmanoğlu during our iGEM advanture

in Boston. Saygın Bilican will always be my biggest protective factor. I will never feel alone as long as I have Sinem Uluocak in my life. I owe most of the great times I have spent during my master's to Sinem and Erdem Dinçer. Efe Işılak is the most colorful personality in my life. I will never forget our unique friendship initiated with a single gossip. I would like to thank Didem Dede for our unforgettable memories as house mates and for her matchless music lists. I will always remember our rich breakfast sessions with Engin Can Sürmeli, Koray Yavuz, Didem Dede and Efe Işılak. I want to express my admiration to musician and traveler friend, Erkin Hadimoğlu. I have listened to his compositions more than he can imagine.

I want to declare my deep love to Kukumber team. I have already missed the puzzle sessions that Büşra Merve Kırpat has introduced to us. Our coffee times, finding her grammatical mistakes and our one-to-one therapy sessions were unforgettable. Despite of the mystery behind her poker face, Merve Yavuz has always been a reliable friend. I will remember her as a talented musician with a smiling face, sarcastic tone and the grocery store that she hides in her office cabinet. I can listen to Julian's speaking in Turkish for hours. I had never thought that I could establish a strong friendship within such a short time until I met with Julian Ostaku. I hope all of his positive foresights will come true. Sıla Köse is my biggest support in the lab and my fellow traveler during our great trips to London and İstanbul. Her truthful criticisms, beautiful smile, scientific achievements, love for animals and artistic personality are just some of the things that I admire about her.

I have a lot of special people in my life that are proud of me. Being successful is much more meaningful to me when shared with those people. I am thankful to Rüstem Ayhan, Havva Ayhan, Salim Kahraman, Hüseyin Çelik, Sabiha Ayhan, Emel Atamaner, Süleyman Kınalı, Aysel Taşer and Hayriye Demir Açıkgöz for their endless support. I am grateful to my psychologist friends Aylin Şahin and İlknur Avcı Yurtsever who make Dışkapı a prestigious and enjoying place. Additionally, I feel very lucky to meet

Önder Albayram who is a great scientist and has enlightened me in the fields of molecular psychiatry and neuroscience.

We have a much more special connection beyond friendship with Filiz Durgun. We had shared a room for five years which were the happiest times of my life. I am sure that we will always make each other motivated by listening to Çıtır Kızlar and laugh a lot whenever we remember the ‘egg family’. I am also thankful to Durgun family for their supports through phone calls and for their hospitality.

I am grateful to my family for their eternal support. Seyhan Beğli is my guardian angel, Habib Beğli is my irreplaceable guide and my rabbit, Destina is the meaning of my life. Also, I want to thank the best psychologist ever. In addition to being a great sister, Seda Beğli is the person that cares about me most. Without her support and motivation, I could not finish this thesis.

I would like to thank TUBİTAK for financially supporting this study with project number 216S127.

1 Table of Contents

List of Figures

List of Tables

INTRODUCTION

1.1 Neurodegenerative Diseases

Neurodegenerative diseases are progressive diseases associated with a gradual and irreversible loss in discrete neuronal populations of central nervous system [1]. Once neuronal loss reaches a severe stage that affects the cognitive functioning, patients develop dementia which is characterized with behavioral impairments and the problems in cognitive capabilities such as language, memory, reasoning and decision making [2, 3]. To enlighten the underlying causes of neurodegenerative diseases, numerous studies have suggested possible explanations disruption in different mechanisms or abnormalities in cell functioning such as oxidative damage due to free radicals [4], neuroinflammation [5], mitochondrial dysfunction [6], endoplasmic reticulum (ER) stress [7] and so on.

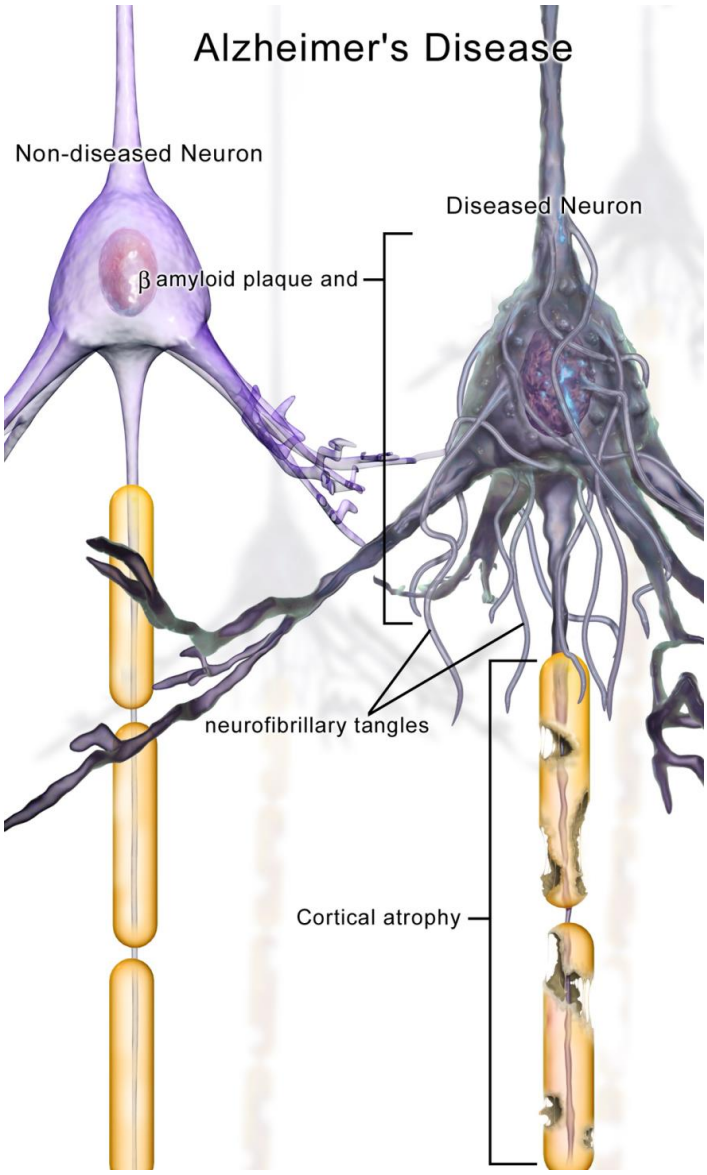

Figure 0.1.1: An illustration depicting the neuronal pathology in Alzheimer's Disease (image credit Bruce Blausen; commons.wikimedia.org/wiki/File:Blausen_0017_AlzheimersDisease.png).

Alzheimer's Disease (AD), Parkinson's Disease (PD), Huntington's Disease (HD), Amyotrophic Lateral Sclerosis (ALS), Metachromic Leukodystrophy (MLD), and Spinal Muscular Atrophy (SMA) are some examples of neurodegenerative diseases [8]. Despite of the fact that there are differences between the sites where the diseases initiate, the types of neurons that are affected, behavioral, motor and cognitive symptoms and the progress, there is a common factor leading to neurodegeneration in these diseases. Protein aggregation and the formation of inclusion bodies are

shared characteristics of neurodegenerative diseases. The behavior of misfolded proteins as a nucleation unit triggering the formation of polymeric structures accelerates the aggregation [9, 10].

1.2 Synthetic Biology Based Solutions for Neurodegenerative Diseases

Synthetic biology has the potential to create solutions to existing limitations in detection and treatment. Most of the current approaches focus on the alleviation of the symptoms and clearance of the toxic accumulations. However, synthetic biology tools can target the underlying factors such as disease causing genes, and monomeric and oligomeric structure involved in aggregation. Genome editing technologies are promising especially in diseases caused by a single gene like Huntington's disease. Logic gates can be utilized to recognize the agents causing the disease and to respond them by producing signals or genes to eliminate disease related formations. RNA inhibition systems and use of antisense oligonucleotides can silence the genes contributing to the diseases. Synthetic proteins such as artificial transcription factors and improved antibodies can decelerate the aggregate formation. Artificial cells can be programmed to release growth factors to support healthy neurons in the diseased brain regions. Stem cells can be engineered and transplanted to the region of interest as a neuroprotective and neurorestorative strategy. Synthetic viruses enable a safe and controlled delivery method. Gene circuits constructed with special parts can provide a controlled and temporal or constant expression of specific genes. Re-establishment of a healthy gut microbiome leads to neuroprotection by sending signals via gut-brain axis. Considering all advanced technologies, a comprehensive therapeutic intervention thanks to synthetic biology can target the real source of the neurodegeneration [11].

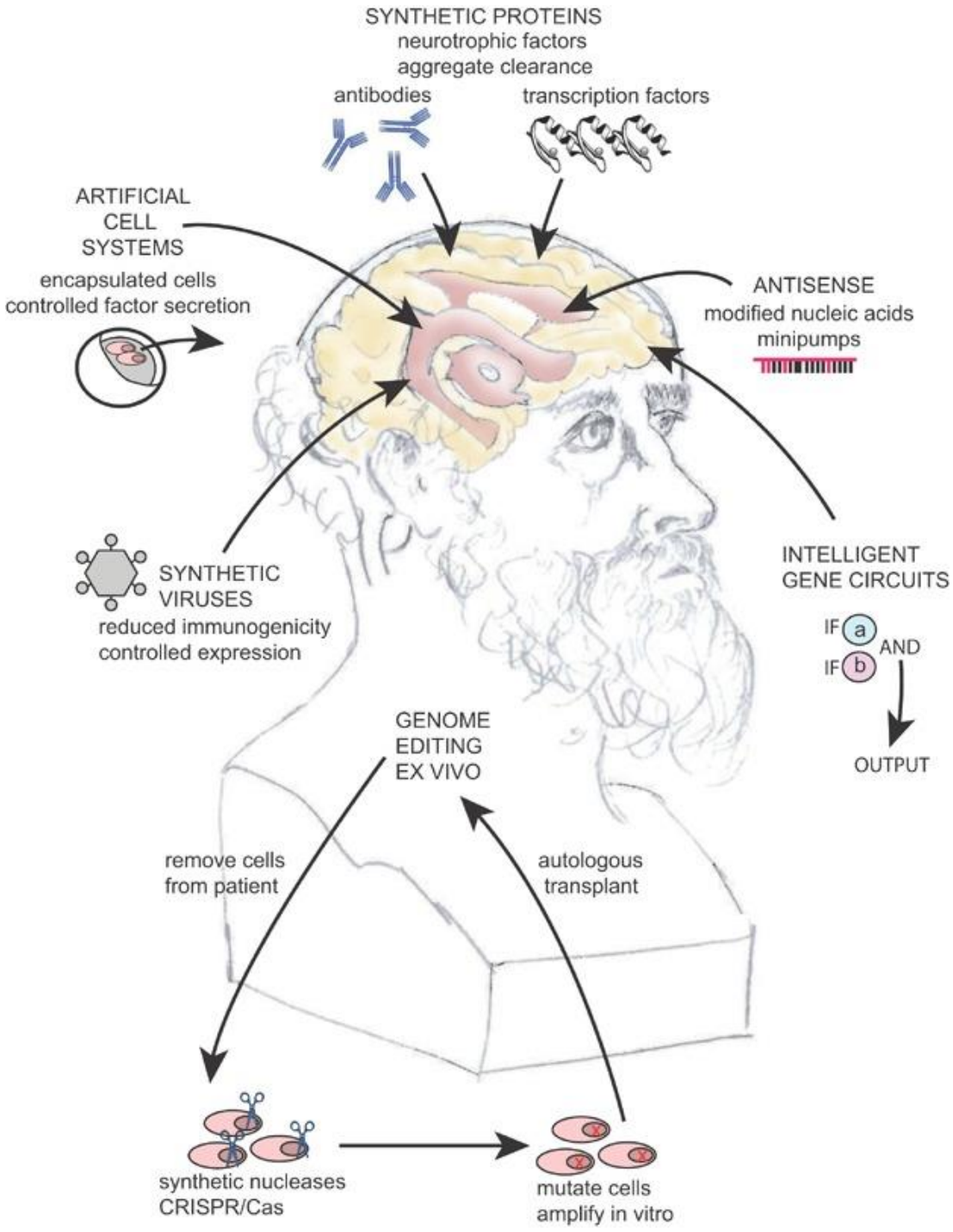

Figure 1.0.2:An overview of synthetic biology based solutions for the treatment of neurodegenerative diseases. Reprinted with permission from reference [11].

1.3 Accumulation of Proteins in Neurodegenerative Diseases

Amyloid beta (aβ) and tau in AD, alpha-synuclein (α-syn) in PD and mutant huntingtin (mHtt) in HD are the proteins causing the formation of aggregates in

different neuronal populations of the brain [12]. Despite the contribution of different genes and proteins in different neurodegenerative diseases, misfolding, conformational changes in protein structure, disruptions in clearance mechanisms, accumulation of toxic aggregates considerably resemble to each other. Discovery of self-propagating behavior and seeding activity of misfolded proteins has been a milestone for the developments of diagnostic and therapeutic approaches [12, 13].

Accumulated proteins, known as amyloids, leading to neurodegeneration mostly contain structures called cross-β which are composed of intermolecular β-sheets [14]. From another perspective, protein misfolding involves a process of the rearrangement of the protein into an array of β-strands that are stabilized through hydrophobic interactions and hydrogen bonds. β-strands provide places for triggering other molecules to join the misfolded structure [13].

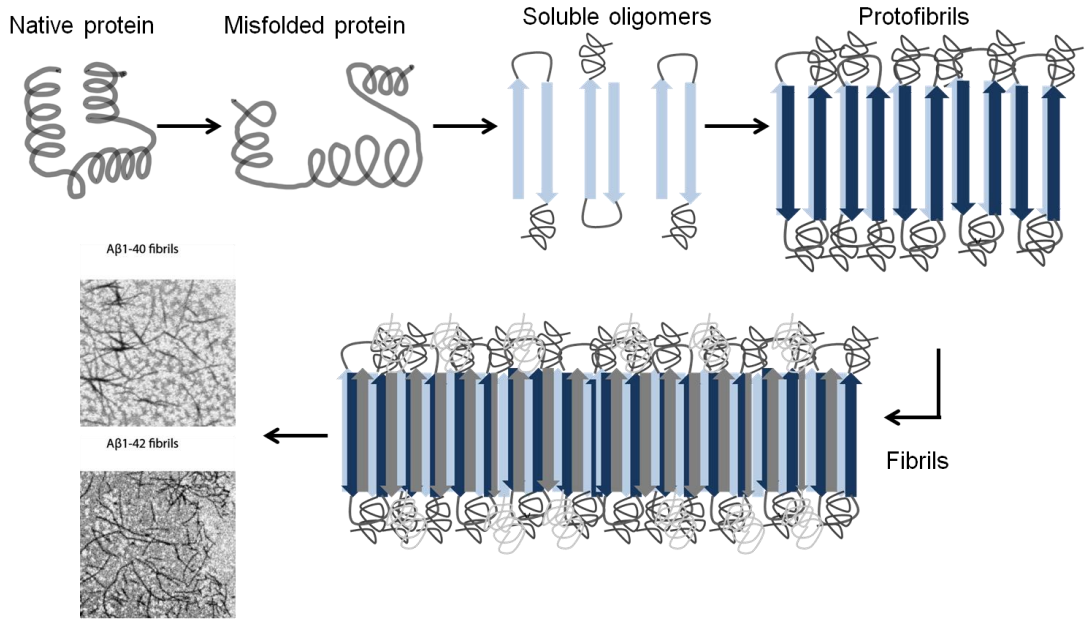

1.0.3: An illustration depicting the formation of insoluble fibrils from soluble oligomeric structures because of misfolding.

Dock-Lock mechanism explains the formation of insoluble aggregates from soluble monomeric and oligomeric structures in two main steps. The first step called ‘dock’ when the soluble monomeric structures dock to an amyloid template is a reversible

phase. However, in the ‘lock’ phase, conformational changes in the monomeric structures takes place and irreversibly associated fibrous structures are formed [14, 15].

Seeding-nucleation model proposed by Lansbury and colleagues explains aggregation in two stages. In the nucleation stage, a stable seed as a nucleation unit is formed. In the elongation stage, the seeds formed in nucleation phase grow rapidly since they trigger soluble monomeric structures to be incorporated into polymeric structures [16, 17]. Fragmentation of long polymers gives rise to the more seed structure leading to the acceleration of aggregation.

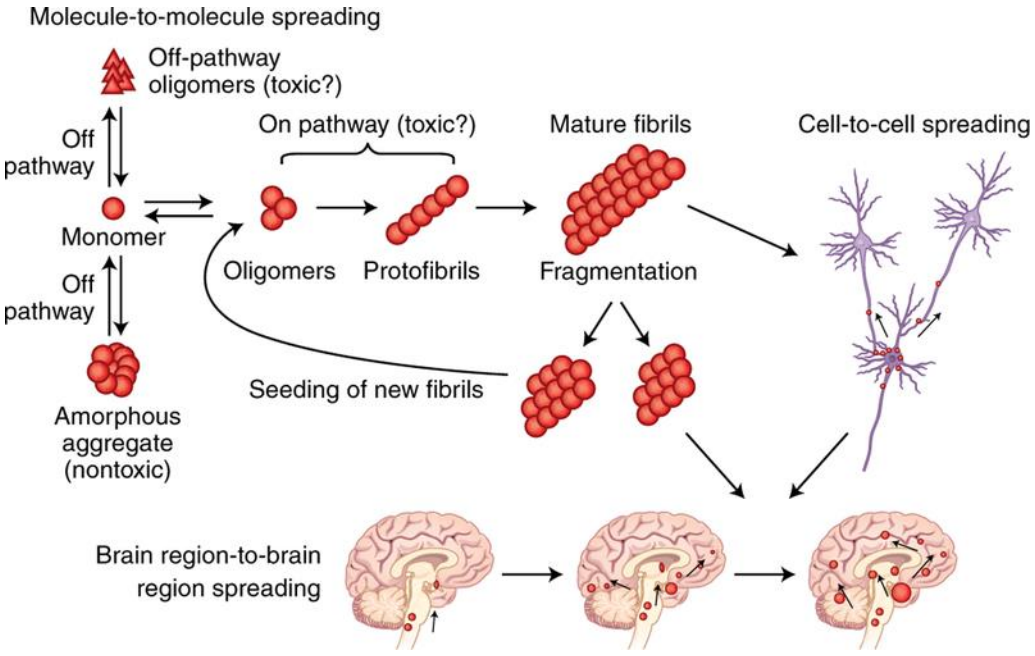

Figure 1.0.4: An illustration summarizing the process of formation and propagation of aggregation in neurodegenerative diseases. Reprinted with the permission from publisher of the study [13].

Another hypothesis claims that misfolded proteins behaving as infectious agents can be transmitted like prions. Several pathways have been suggested to mediate cell-to-cell transmission of improperly folded seeds such as exosome mediated transport, transmission via tunneling nanotubes, transfer through protein-protein interactions, mechanisms of endocytosis and exocytosis and so on [18-21]. Although it seems

logical to target the cell-to-cell transmission of the seeds, it is complicated to manipulate general mechanisms that can be involved in other cellular processes [13].

1.4 Diagnostic Studies for Neurodegenerative Disorders

In order to make effective therapeutic interventions, early diagnosis of neurodegenerative diseases is essential. However, neuropathy as a one of the most reliable diagnostic can be applied only after patients' death [11, 22]. A major difficulty to detect neurodegenerative diseases is that protein biomarkers of neurodegenerative diseases are present in the body fluids like blood and cerebrospinal fluid in small amounts [23]. Limited understanding of neural circuits, complexity of the brain, presence of the blood brain barrier and difficulties of bypassing it for targeted delivery indicate that there is a need for a comprehensive theranostic approaches to diagnose and cure these diseases [11].

To track polyglutamine aggregation, traditional methods utilizes microscopy or detergent insolubility which do not clarify the mechanisms leading to protein misfolding. As a combination of fluorescence energy transfer (FRET) system and cell imaging, Pollitt et al. constructed a reporter system to track polyglutamine aggregation in HEK293 cell line and showed that aggregation-prone proteins with polyglutamine repeats gave FRET positive signal when they were fused with fluorescent proteins. In the study, 2800 biomolecules have been screened and the ones with a inhibitory activity that reversed the process of polyglutamine aggregation were characterized using Drosophila model for polyglutamine disease [24]. In a similar study in 2017, a biosensor cell line has been developed using fusions of tau domain with P301S mutation with two different fluorescent protein, cyan fluorescent protein (CFP) and yellow fluorescent protein (YFP). Application of tau seeds exogenously trigger the initiation of aggregation that results in close proximity of

fluorescent proteins and FRET-positive signal [25]. Holmes et al. designed a FRET-based sensor and assessed taupathy and tau seeding activity in the brains of transgenic P301S mice. They also carried out assays on cross-seeding activity between tau and a-synuclein [26].

yTRAP (yeast transcriptional reporting of aggregating proteins) is another novel system that has been constructed in yeast cells with a theranostic approach. The sensor system has been established in order to give an output depending on the solubility state of the protein of interest. Protein of interest that is prone to aggregation is fused to a synthetic promoter which can activate its cognate promoter only if the cell is not in aggregation state [27].

Since the cells undergoing neurodegeneration are located at different regions in the brain depending on the type of the disease, spatial and temporal control of gene expression is essential for gene therapies. Convection-enhanced delivery was first described in the study of Bobo et al [28]. This method facilitates direct delivery of the therapeutics to the brain by creating a pressure gradient at the tip of a catheter with a small diameter. The method has been developed with the integration of the interventional magnetic resonance imaging (iMRI) technology [29]. There are studies using iMRI-CED technology that focus on neurorestorative therapies for the delivery of neurotrophic factors to support brain health and gene replacement therapies to deliver genes responsible for GABA production and gene encoding the rate limiting enzyme in dopamine synthesis converting levodopa to dopamine to provide symptomatic relief to the patients with Parkinson’s disease [8, 30].

1.5 Therapeutic Interventions

1.5.1 Gene Therapy

Gene therapy is an approach with the purpose of prevention and treatment of the neurodegenerative diseases by means of neuroprotection, neurorestoration and disappearance of neuropathology. The main purpose of gene therapy is to either compensate a defective gene by replacing with a transgene or correcting it or supporting the healthy cells in the diseased region [8, 31]. There are viral and nonviral vectors being used as gene therapy agents [32]. Non-viral vectors including nucleic acids and especially naked plasmid DNA are mostly delivered as complexed with some delivery vehicles such as cationic polymers and lipids [33]. Due to rapid clearance and transient gene expression profile, non-viral vectors are not convenient agents to confer sufficient dosage effect for chronic neurodegeneration [31, 34].

Viral vectors have the ability to invade the cells and deliver the DNA content they are loaded with to the host cell. Their genome is altered to prevent their replication for safety issues [35]. Commonly used viral vectors are lentiviral vectors and adenoviral vectors. Lentiviruses which have larger DNA loading capacity are designed to be integrated into the genome apart from the adeno-associated viruses (AAV) [31, 36]. This unique feature provides stable expression pattern in long-term, but also brings the risk of insertional mutagenesis [37]. AAVs have been commonly used in clinical trials to deliver genes to the brain. There are several serotypes of AAVs; however, some of the serotypes have been so widespread that numerous people have developed immunity against them [38, 39]. Among those serotypes, AAV2 is one of the most preferred ones due to its clinically safe profile whereas AAV9 is more capable of crossing the blood-brain barrier as compared to the other

serotypes. It has been indicated that intravenous administration of AAV9 provides the opportunity for transgene delivery to adult motor neurons [40].

1.5.2 Cell-based therapies

Transplantation of engineered cells that secrete neurotrophic factors promoting growth and maintenance of neurons or enzymes that are deficient in neurodegenerative disease conditions is a neuroprotective and neurorestorative strategy [11, 41, 42]. Despite promising results for treating and preventing neurodegenerative diseases, there are still problems such as immunorejection of grafted cells, lack of stromal support and required growth factors and insufficient integration of the grafted cells. There are two technical concerns about cell replacement therapies for neurodegenerative diseases: which cell type should be convenient and which transplantation method leads to effective functioning of the grafted cells [43]. Human retinal pigment epithelial cell line engineered to secrete NGF has been indicated as an encapsulated therapeutic agent since it displays contact-independent growth characteristics and low nutritional requirements[44].

With the self-renewal capacities and ability to differentiate into several cell types, stem-cells are ideal sources for cell replacement therapies.

In addition to embryonic stem cells which are obtained during embryonic stages and induced pluripotent cells derived from adult somatic cells, glial cells and neurons originated from stem cells such as neural stem cells (NSC) and mesenchymal stem cells can be used in transplantation therapies. NSCs are advantageous regarding their rapid growth characteristics and stable gene expression pattern of therapeutic genes [45-47].

Vascular endothelial growth factor (VGEF) which is a growth factor with neuroprotective effects especially in case of brain injury has been promising in the

treatment of ALS. When VGEF is coupled with stem cell transplantation technology, improvements in therapeutic effects have been seen. Transplantation of NSCs that overexpress VEGF resulted in functional improvements, increased survival and delay in the disease onset [48].

As a therapeutic intervention to metachromatic leukodystrophy which is caused by a deficiency of an enzyme called arylsulfatase A, programmed haematopoietic cells that expressed the enzyme were transplanted and migrated to the brain. Complemented enzyme activity resulted in the clearance of the toxic clusters composed of the substrate of the enzyme [49].

1.6 Alzheimer's Disease

World Health Organization (WHO) has reported that there are approximately 50 million cases of dementia increasing with the addition of 10 million cases each year. 60-70% of cases with dementia arise from Alzheimer's disease. During the disease progression, degeneration of cholinergic neurons and accumulation of amyloid beta plaques have been observed. Familial Alzheimer's disease is rare form being inherited in a Mendelian fashion and caused by mutations in either amyloid precursor protein or the enzymes that are responsible for its cleavage whereas both genetic and environmental factors contribute to the sporadic form of the disease [50, 51].

As a neuroprotective intervention, nerve growth factor (NGF) which supports cholinergic neurons in the basal forebrain that undergo degeneration due to the disease was delivered using AAV2 vector [52]. Safe profile of the vector and NGF expression in an active form have been indicated; however, the clinical trial failed to meet the expectations [53].

Neuroinflammation is one of the underlying factors in Alzheimer's disease. Interleukin-2 as an inflammation controller was delivered within AAV vector to

mouse model for AD. Improvements in memory due to the alleviations in hippocampus have been observed [54, 55]. Another strategy to prevent aggressive progression of AD is to reduce the levels of tau and amyloid beta which have a tendency to form clusters within neurons. To do so, antisense oligonucleotides (ASO) was used to prevent tau aggregation, but this strategy needs to be assessed in animal models to make conclusions about their role in disease progression [56]. AAV mediated miRNA delivery to knockdown acyl-CoA:cholesterol acyltransferase 1 has succeeded in reducing amyloid beta levels [57, 58]. To reverse the effects of reduction in neprilysin enzyme that has a role in amyloid beta catabolism, AAV9 mediated delivery of the enzyme into hippocampus resulted in reduced amyloid beta levels [59]. Indeed, improved memory and learning skills reported by Iwata et al. [60].

Delivery of growth factors is another promising strategy to prevent neuropathology and to provide neuroprotection. The level of insulin growth factor (IGF) in the hippocampus of AD patients has been indicated. AAV8 mediated delivery of IGF caused a significant decrease in the levels of amyloid beta in a mouse model overexpressing amyloid precursor protein [61]. Lentiviral delivery of glial cell-line derived neurotrophic factor (GDNF) that supports brain cells resulted in the preservation cognitive skills such as memory and learning [62].

There are cell transplantation studies for AD that have focused on either the toxicity caused by amyloid beta or neuroprotective and neurorestorative precautions using growth factors to alleviate the symptoms. For instance, glucagon-like peptide-1 secreted by mesenchymal stem cells reduced amyloid beta deposition and toxicity [63-66]. While the secretion of vascular endothelial growth factor (VGEF) by encapsulated cells resulted in improvements in cognition and reduction in amyloid

beta deposition and hyperphosphorylated tau [67], secretion of ciliary neurotrophic factor resulted in improved cognition and stabilization of synaptic proteins [68].

1.7 Parkinson's Disease

According to European Brain Council (EBC), approximately 6.3 million people worldwide have Parkinson's Disease (PD) which is the second most common neurodegenerative disease after AD. Parkinson's Disease (PD) is characterized by symptoms such as impairments in motor function, resting tremor, slow movements and stiffness. Loss of dopaminergic neurons in the brain region called substantia nigra that modulates movement and the reduction in dopamine levels in the striatum are underlying factors of neuropathology. Lewy bodies which are cytoplasmic inclusion bodies are composed of abnormal fibrillar assemblies [69].

In 1998, Spillantini et al. have indicated the composition of lewy bodies are ubiquitin and mostly a-synuclein through several immunostaining experiments[70].

Current therapies include deep brain stimulation (DBS) and supplying dopamine via drugs such as levodopa which is a dopamine precursor. Although these therapies are effective interventions considering symptomatic relief to some extent, they are insufficient to target the underlying pathology of the disease. Levodopa that is used for dopamine replacement gets less effective as PD progresses and DBS can be emotionally and cognitively deteriorating [71].

At early stages of the disease, dopamine replacement therapy is efficient; however, even increased dosages do not result in same therapeutic outcome as PD progresses. One strategy to overcome this insufficiency is to deliver the rate-limiting enzyme of the dopamine synthesis as a pro-drug approach [8]. The enzyme is called aromatic L-amino acid decarboxylase (AACD) which catalyzes the conversion of levodopa to dopamine during dopamine synthesis. AAV2 mediated delivery of AACD resulted in

statistically significant improvements in behavioral symptoms, lowered the need for levodopa and its side effects [72-76].

There are also neurorestorative strategies focusing on the delivery of GDNF to support neurons. Viral mediated delivery has been combined with iMRI-guided CED technology and utilized in phase 1 trial [77].

There are also studies focusing on cell transplantation strategies for neuroprotective and neurorestorative purposes. Encapsulated cells supplying dopamine precursor and dopamine were transplanted into striatum to alleviate the syptoms of PD. Although this intervention had been effective for several years, it eventually became ineffective since degeneration of dopaminergic neurons continued during this period [78-81]. It has been indicated that dopamine supply is temporarily effective, thus protective precautions before the neurodegeneration takes place can be more successful [82]. Supporting this claim, loss of dopaminergic neurons could be prevented by implating encapsulated cells that released certain dose of GDNF daily into the substantia nigra [83].

1.8 Huntington's Disease

Huntington's Disease (HD) shares similarities with AD and PD regarding the improper processing of proteins and neurons that are vulnerable to these proteins forming clusters. However, in contrast to complex and unknown underlying mechanisms of AD and PD, HD is an autosomal dominant disorder with a single cause which is a mutation leading to the expansion of trinucleotide CAG repeat coding glutamine [84, 85]. In healthy individuals' genome, the number of CAG repeats on the exon 1 of chromosome 4 varies between 6 and 34. Repeat size longer than 36 repeats leads to a problematic, unstable and improperly expanded protein [86, 87].

HD is one of the nine polyglutamine diseases that result in neurodegeneration [85, 88]. As a disease inherited with an autosomal dominant pattern, there is 50% risk of transmitting the disease to the offspring. HD occurs less frequently compared to AD and PD with a ratio of 1:10000 people. Symptoms include cognitive impairments, incoordinate involuntary muscle contractions, behavioral changes and chorea which can be defined as unpredicted body movements [89].

AAV mediated generation of a novel mouse model for HD not only enlightened the mechanism of neuropathology but also enabled the exploration of novel therapeutic interventions. AAV-DJ model indicated changes in behavior, increased in the expression of inflammatory cytokines, and occurrence of neural apoptosis.

AAV9 mediated miRNA delivery targeting exon 48 of human mutant huntingtin eliminated 50-60% of mutant HTT mRNA and mutant huntingtin protein six months after the injection in striatum of sheep model [90]. AAV mediated SIRT3 gene displayed neuroprotective effects by preventing mitochondrial oxidative stress and providing neuronal support [91]. Evers et al, also reported reduced levels of mutant huntingtin protein and mRNA in minipigs as a response to delivery of AAV5 mediated delivery of Huntington-lowering gene [92].

Since disruption of a single gene causes HD, the disease is in the focus of therapeutic applications using gene editing technologies such as CRISPR/Cas9. There are several strategies to silence mHtt expression. One approach is to target promoter region or the beginning of the gene; however, preclinical studies have suggested a global silencing of the mutant and wild-type alleles since it has been shown that complete deletion of HTT gene is not deleterious [93-95]. Exon 1 coding the protein with polyglutamine repeats can be removed completely by using two guide RNAs to

targeting the both sides of the exon [96, 97]. Using next generation sequencing technology, allele-specific strategies can also be developed [98].

Taking neuroprotective precautions is more probable in case of HD since genetic screening can determine the individuals carrying the risk of developing the disease [82]. Implantation of cells producing NGF and CNTF not only preserved neuronal populations of striatum such as GABAergic and cholinergic neurons, but also improved motor and cognitive capabilities [99-101]. CNTF secreting cells encapsulated within polymer structures were transplanted into striatum of monkey models and reduced the striatal damage while protecting and increasing the GABAergic and cholinergic neurons [102, 103].

1.9 Biotechnology Tools for Protein Studies

1.9.1 Yeast Surface Display

Displaying recombinant proteins on the cell surface of *Saccharomyces cerevisiae* is an advanced technology to study and engineer proteins, to optimize affinity of antibodies, to improve catalytic activity of enzymes, to discover binding epitopes, to assess interactions of proteins with small molecules or other proteins and so on [104-107]. Among several proteins anchored to the yeast cell surface such as Flo1p, Cwp1p, Agα1p, Aga2p is the most preferred protein for the fusion of protein of interest [108].

Utilization of yeast display technology provides some advantages over the other display methods. In addition to the ease of handling of a unicellular organism, machineries for eukaryotic expression, protein translation and processing make it possible to study a range of recombinant proteins with proper folding and functions. The protein translation and secretion mechanisms of yeast cells resembling

mammalian cells have made this single-cell microbe a convenient platform to perform library applications and to study eukaryotic proteins too [107]. Yeast two-hybrid system has enabled the studies on protein-protein interactions [109]. Thanks to innate homologous recombination mechanism, genetic manipulations can be done on yeast genome via transformation of a PCR product with upstream and downstream homologies of the target site as short as 40-50 nucleotides for purposes like gene deletion, gene insertion or tag addition [110, 111]. To be classified as 'generally regarded as safe', *Saccharomyces cerevisiae* cells are ideal organisms for applications of food and pharmaceutical industry [112]. However, different glycosylation pattern as compared to mammalian cells [113, 114] and the limited library size as compared to platforms using phage and bacteria [115] are some drawbacks of yeast display system.

Aga1p and Aga2p are proteins that are anchored to the cell surface of yeast cells with mating type a. Those proteins are subunits of a-agglutinin which modulates cell adhesion during yeast cell mating [116, 117]. While Aga1p is anchored to the surface through beta-glucan covalent bonds, Aga1p and Aga2p form two disulfide bonds before being secreted into the extracellular space and placed on the cell surface [107]. This placement results in the display of the protein of interest that is conjugated to Aga2p on the yeast surface.

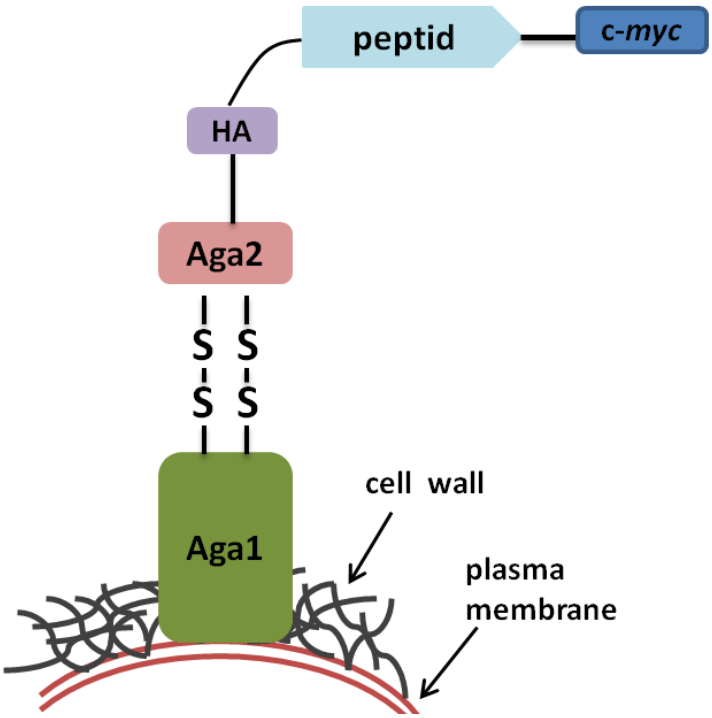

Figure 1.0.5: A drawing that depicts the proteins involved in a-agglutination system in *Saccharomyces cerevisiae* cells and the fused peptides and tags to be displayed on the surface. Figure is adapted from the reference [107].

Aga1 gene that encodes Aga1p is integrated into the genome of the strain of *Saccharomyces cerevisiae* designed for surface display applications. A circular plasmid with an auxotrophic marker for the selection contains Aga2 gene encoding the Aga2p is fused with the protein of interest. Both Aga1 and Aga2 are regulated by a galactose inducible promoter. Therefore, surface display of the proteins is not constitutive. The conditional expression prevents the potential formation of cytotoxic protein products [107, 114].

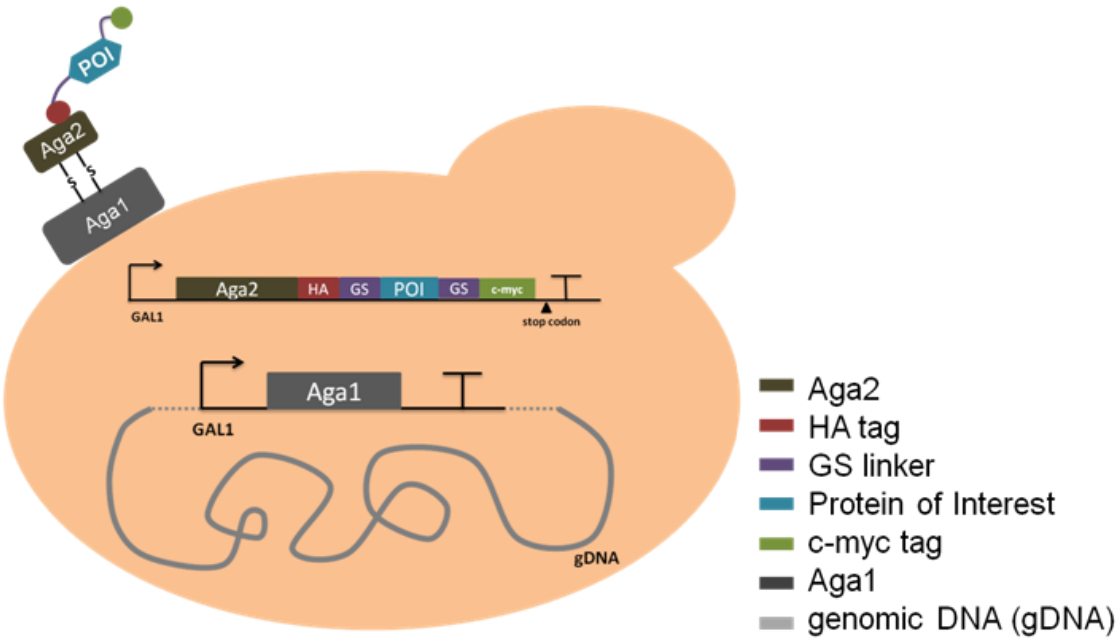

Figure 1.0.6: An illustration of *Saccharomyces cerevisiae* strain, EBY100. Aga1p is expressed on its genomic DNA and Aga2p fused with protein of interest (POI) is expressed on the plasmid DNA to establish surface display system with the POI.

1.9.2 Phage Display Library

Phages, also known as bacteriophages, are the viruses that infect the bacterial cells. These biological entities have numerous unique features such as resistance to harsh environments, ease of handling, inexpensive production in large quantities and immunostimulatory effects [118, 119].

Phage display is an advanced biotechnology tool that utilizes phage particles to display foreign peptides on their surface by fusing the sequence encoding the peptide into the genes encoding viral coat protein [120]. Phage libraries which are constructed by integrating randomized oligonucleotides into the sequence of viral coat proteins have the potential to display a variety of peptides. The technique has been used in several applications such study of protein-protein interactions, drug development and discovery of target molecules like antigens, antibodies and receptors [119].

Phages have a safe profile since viruses have had interactions with mammalians throughout an evolutionary period. Additionally, the genetic diversity of the phages and the large library size are the advantageous sides of this tool over the other display platforms [119, 121, 122].

Screening strategy for phage display libraries is based on biopanning which is a process of recursive binding and washing steps to find the peptides which bind to the target with high affinity. In biopanning, phages with a pool of peptides are incubated with the protein of interest. Then, harsh washing steps are applied to eliminate nonspecific and weak binders. Several methods such as changing pH, use of a proteolytic enzyme addition of a competitive ligand or a denaturing agent can be used for retrieval of the phages. They are not damaged upon these applications since they are stable under tough conditions [123]. Following the retrieval step, bacterial cells are infected with phages; however, the library might be still heterogeneous. Therefore, a few affinity selection steps improve the peptide selection process. DNA sequence encoding the selected peptides can be obtained via DNA sequencing [119].

1.10 Aim of the study

Most of the current studies on the treatment of neurodegenerative diseases focus on the alleviation of the symptoms and clearance of the toxic accumulations after the aggregates has been formed. The purpose of this study is to develop peptides that can block the monomeric structures before the aggregation takes place. The proteins that have been used in this study are amyloid β, α-synuclein and mutant Huntingtin proteins causing aggregate formation in Alzheimer's Disease, Parkinson's Disease and Huntington's Disease, respectively. To develop blocking peptides as drug candidates, methods of biotechnology such as gene cloning, yeast surface display and phage library display have been used. Disease causing proteins have been displayed

on the surface of *Saccharomyces cerevisiae* cells. The peptides interacting with disease causing proteins have been selected among a library displayed on the phages. The potential of those candidate peptides will be assessed through ex vivo binding assays and using neural cell lines and animal models. Peptides that have been selected are also promising to be integrated into biosensors as recognition units.

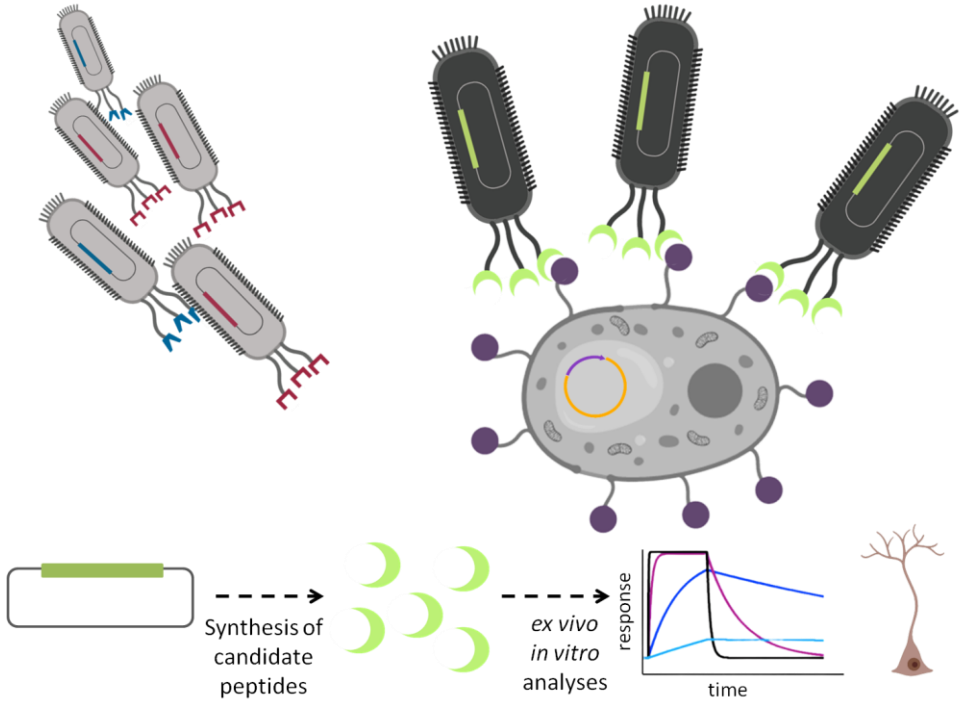

Figure 1.0.7: An illustration of *Saccharomyces cerevisiae* strain, EBY100. Aga1p is expressed on its genomic DNA and Aga2p fused with protein of interest (POI) is expressed on the plasmid DNA to establish surface display system with the POI.

CHAPTER 2

2 EXPERIMENTAL

2.1 Yeast maintenance and growth conditions

Yeast cells can be grown both in liquid medium and on agar plates. A minimal medium including a nitrogen source, a carbon source like glucose, and trace metals is enough to grow the wild-type strain. Yeast cells have the metabolic pathways to produce all amino acids they need; however, extra suppliance of proteins, amino acids, yeast extract, vitamins or nucleotide precursors accelerates the growth.

The wild type yeast strains that have the capacity of meeting nutritional requirements are named as prototroph. The mutant strains with mutations in the genes that belong to the pathways being responsible for the synthesis of the nutritions with survival importance are called auxotroph. The genes coding the enzymes of these pathways that are involved in the production of metabolically crucial monomers are called auxotrophic markers. Auxotrophic genes do not only meet nutritional requirements but also have a role as biological parts within cassettes utilized in genomic manipulations or plasmids as a marker genes. The presence of auxotrophic mutant strains enables doing complementation assays by meeting the auxotrophy deficiency via a DNA fragment to be inserted into the genome or a plasmid including the missing auxotrophy marker. LYS2, URA3, MET15, TRP1, LEU2, HIS3 are the examples of commonly used auxotrophy markers.

Tablo 2.1: Components reqiured for growing yeast cells

Component	Final concentration (mg/L)
Adenine	10
Arginine	50
Aspartic acid	80
Histidine	20
Isoleucine	50
Leucine	100
Lysine	50
Methionine	20
Phenylalanine	50
Threonine	100
Tryptophan	50
Tyrosine	50
Uracil	20
Valine	140

- **+ 2% glucose**
- **+ 6.7 g/L Yeast Nitrogen Base (without amino acid)**
- **+20 g/L agar (for solid medium)**

The steps were followed after the arrival of cells within ampoule in dry ice:

1. EBY100 strain (ATCC® MYA-4941™) being stored at -80^{o}C was immediately thawed in water bath at 30 ^{o}C for 5 minutes.

2. Lid of the ampoule was wiped with %70 ethanol and approximately 50 µl of the cells were inoculated into SD-trp medium and onto SD-trp agar plates under aseptic conditions.

3. Cells were grown under recommended conditions.

Yeast cells are heavier in comparison to the bacterial cells. They have a tendency to precipitate at the bottom of the tube, so constant shaking at higher RPM values is ideal for yeast cells. Optimum growth temperature might change depending on the heat sensitivity of the strain. For EBY100 strain, optimum temperature for growth is 30^{o}C. Yeast cell stocks to be stored at -80^{o}C containing 15% glycerol are prepared by

mixing the same volume of overnight yeast growth and 30% sterilized glycerol near flame. For cell growths, 1:1000 dilution of ampicillin (stock concentration: 100 mg/ml) is used to eliminate bacterial contamination.

2.2 Bacterial cell maintenance and growth conditions

Escherichia coli cells are grown in Lysogeny Broth (LB) solution as liquid cultures or on LB-agar plates containing additional 15 g/L agar. Depending on the plasmid they have, 1:1000 dilution of the stock of the corresponding antibiotic is added into the medium. DH5α PRO strain contains a PRO cassette providing spectinomycin resistance. Optimum growth temperature for E.coli cells is 37^{o}C. Cell stocks to be stored at -80^{o}C containing 25% glycerol are prepared by mixing the same volume of overnight yeast growth and 50% sterilized glycerol near flame.

2.3 Preparation of Mediums

2.3.1 LB (Lysogeny Broth) and LB-agar

8 g peptone, 8 g NaCl and 4 g yeast extract are weighed. Powder mix is dissolved in distilled water and the volume is completed to 800 ml. Mixture is sterilized through autoclave. For agar plates, 15 g/L agar powder is added to LB mix. After autoclave, LB-agar is melted on heat block and waited in approximately 55^{o}C water bath to cool down. Proper antibiotics are added and 20 ml LB agar is poured into each plate and left to solidify near flame.

2.3.2 YPD (Yeast Extract, Peptone, Dextrose) and YPD-agar

10 g peptone and 5 g yeast extract are weighed. Powder mix is dissolved in distilled water and the volume is completed to 500 ml. Mixture is sterilized through autoclave. For agar plates, 10 g agar powder is added to the YPD mix. After

autoclave, YPD-agar is melted on heat block and waited in approximately 55^{o}C water bath to cool down. Proper antibiotic is added and 20 ml YPD agar is poured into each plate and left to solidify near flame.

2.3.3 Synthetic Drop-out Medium

10X Yeast Nitrogen Base without amino acids (YNB w/o aa) and Synthetic Dropout Medium Supplements without tryptophan (SD-trp)

2.01 g YNB and 0.576 g SD-trp are weighed. Powder mix is dissolved in distilled water and the volume is completed to 30 ml. This mixture should be sterilized using 0.2 mm filter instead of autoclave and stored at +4^{o}C. 10X mixture can be diluted in the ratio of 1:10 while using in liquid or solid medium.

SD-trp-agar

6 g agar and 54 g sorbitol are weighed. Powder mix is dissolved in distilled water and the volume is completed to 240 ml. Mixture is sterilized through autoclave.

10X Glucose

22 g glucose monohydrate is weight and dissolved in distilled water and the volume is completed to 100 ml. Mixture is heated, stirred and sterilized using 0.2 mm filter. 10X glucose is stored at +4^{o}C.

10X Galactose

20 g galactose is weight and dissolved in distilled water and the volume is completed to 100 ml. Mixture is heated, stirred and sterilized using 0.2 mm filter.10X galactose is stored at +4^{o}C

10X Phosphate Buffer

8.6 g Sodium dihydrogen phosphate ($NaH_2PO_4.H_2O$) and 10.2 g Disodium hydrogen phosphate ($Na_2HPO_4.7H_2O$) are weighed and dissolved in distilled water, and the

volume is completed to 100 ml. Mixture is sterilized using 0.2 mm filter.10X phosphate buffer is stored at +4^{o}C.

2.3.4 Growth medium

5 ml of each of 10X YNB and SD-trp mix, 10X phosphate buffer and 10X glucose are all 1:10 diluted 50 ml by adding them into 35 ml sterilized ddH_2O. 50 µl ampicillin is added to the mix.

2.3.5 Induction medium

5 ml of each of 10X YNB and SD-trp mix, 10X phosphate buffer and 10X galactose are all 1:10 diluted 50 ml by adding them into 35 ml sterilized ddH2O. 500 µl 10X glucose and 50 µl ampicillin are added to the mix.

2.4 Preparation of Buffers and Solutions

- Annealing Buffer

Tris, pH 7,5 – 8.0	10 mM
NaCl	50 mM
EDTA	1 mM

- 50X Tris-Acetic acid-EDTA (TAE)

242 g Tris is weighed and dissolved in distilled water. 100 mL of 0,5 M EDTA is added. Then, 57 ml of 100% acetic acid is added to the mixture. The volume is completed to 1 L with distilled water. 50X TAE is diluted into 1X for the preparation of agarose gel.

- 10X Phosphate Buffer Saline (PBS) (1X pH 7.4)

80 g sodium chloride,14,4 g sodium dihydrogen phosphate, 2 g potassium chloride and 2,4 g potassium dihydrogen phosphate are weighed. Mixture is dissolved in distilled water and the volume is completed to 1 L. 10X phosphate buffer is autoclaved and diluted to 1X with sterilized distilled water before using.

- ICC: Blocking, Primary Antibody and Secondary Antibody Solutions

0.3 g BSA is dissolved in 1X PBS by vortexing. 10 ul of anti-c-myc antibody is added to 3 ml blocking solution to prepare primary antibody solution. This amount is sufficient for six ICC samples. 6 ul of anti-mouse secondary antibody conjugated with horseradish peroxidase (Abcam) is added to 3 ml blocking solution to prepare secondary antibody solution. This amount is sufficient for six ICC samples. 1X PBS can be directly used for washing steps.

- Protein Isolation from Yeast Cells

  - 0.4 M NaOH

400 µl of 10 M NaOH is diluted in the ratio of 1:10 by adding 9.6 ml distilled water.

  - 1 M LiOAc

3.3 g LiOAc is weighed and dissolved in distilled water, and the volume is completed to 50 ml. Once dissolved, mixture is sterilized using 0.2 mm filter.

- Laemmli Buffer 6X, 10 ml

0.5 M Tris-HCl pH 6.8	1.2 ml
ddH2O	2.1 ml
SDS	1.2 g
Bromophenol Blue	6 mg
100% glycerol	4.7 ml

- Genomic DNA Isolation from Yeast Cells

❖ 200 mM LiOAc 1% SDS

2 ml of 1 M LiOAc and 1 ml of 10% SDS are added to 7 ml ddH_2O. This solution should be stored at room temperature.

❖ 70% Ethanol

7 ml of Ethanol and 3 ml of ddH2O are mixed.

- Preparation of Competent Yeast Cells
- Freezing buffer

0.111 g CaCl2 and 3.6 g Sorbitol are weighed and put into 7 ml of distilled water within a beaker on ice since CaCl2 and ddH_2O undergo exothermic reaction. 2 ml of 50 mM HEPES is added and pH is adjusted to 7.5. The volume is completed to 10 ml with water and the solution is filter-sterilized using 0.2 mm filter.

- Electroporation of Competent Yeast Cells
- 1 M Sorbitol

18 g sorbitol is weighed and dissolved in distilled water. The volume is completed to 100 ml. Solution is filter-sterilized or autoclaved.

- Chemical Transformation of Yeast Cells
- PEG4000 (50% w/v)

10 g PEG4000 is dissolved in distilled water and the volume is completed to 20 ml. Solution is filter-sterilized.

- 1 M LiOAc

3.3 g LiOAc is weighed and dissolved in distilled water, and the volume is completed to 50 ml. Once dissolved, mixture is sterilized using 0.2 mm filter.

- 100 mM LiOAc

1 M LiOAc solution is diluted in the ratio 1:10 using sterile distilled water.

- 12% SDS Gel

Separating Gel (10 ml for 2 gels)

H2O	3.4 ml
Acrylamide/ Bisacrylamide (30% / 0.8 % w/v)	4 ml
1.5 M Tris- HCl (pH 8.8)	2.6 ml
10% (w/v) SDS	100 µl
10% (w/v) APS	100 µl
TEMED	10 µl

Stacking Gel (5 ml for 2 gels)

H2O	2.975 ml
Acrylamide/ Bisacrylamide (30% / 0.8 % w/v)	670 µl
0.5 M Tris- HCl (pH 6.8)	1.25 ml
10% (w/v) SDS	50 µl
10% (w/v) APS	50 µl
TEMED	5 µl

- Western Blot

- 10X TBS

60.6 g Tris and 87.6 NaCl are weighed and dissolved in distilled water. pH is adjusted to 7.6 using 1 M HCl. Volume is completed to 1 L. Solution is diluted in the

ratio of 1:10 to obtain the working solution. TBST solution being utilized in blocking and antibody solutions contains 0,1% Tween 20 in 1X TBS. Blocking solution is prepared by dissolving 1 g skim milk powder in TBST. Primary and secondary antibody solutions are prepared within this solution as 1: 5000 1:10000 dilutions, respectively. TBST is directly used in the washing steps.

- Preparation of Competent *E.coli* cells

- Transformation & Storage Solution (TSS)

5 g PEG8000 and 0.143 g MgCl2 are weighed and dissolved in LB within a beaker on ice since MgCl2 can lead to exothermic reaction. The volume is completed to 47.5 ml with LB. Mixture is filter-sterilized using 0.2 mm filter. 2.5 ml DMSO is added afterwards because it might disrupt the filter. 5-10 ml aliquots are distributed to the sterile falcons near flame and stored at -20^{o}C.

- Polymerase Chain Reaction

Composition of PCR mix with Q5 polymerase:

Q5 Reaction Buffer	5 µl
dNTPs	0.5 µl
Forward Primer	1.25 µl
Reverse Primer	1.25 µl
Q5 polymerase	0.25 µl
DNA	x
ddH2O	(16.75-x) µl

Composition of PCR mix with pfu polymerase:

pfu Buffer	2.5 µl
dNTPs	0.5 µl
Forward Primer	1.25 µl
Reverse Primer	1.25 µl
pfu polymerase	0.25 µl
DNA	x
ddH2O	(19.25-x) µl

Composition of the mixture of double restriction enzyme digestion:

Restriction Buffer	5 µl
Restriction Enzyme 1	1 µl
Restriction Enzyme 2	1 µl
DNA	x µl (1000-2000 ng)
ddH2O	(43-x) µl

Composition of the mixture of restriction enzyme digestion:

Restriction Buffer	5 µl
Restriction Enzyme	1 µl
DNA	x µl (1000-2000 ng)
ddH2O	(44-x) µl

Table: Composition of the mixture of ligation reaction with T4 ligase

T4 ligation buffer	2 µl
T4 ligase	1 µl
total(insert + backbone)	x µl (~100 ng)
ddH2O	(17-x) µl

2.5 METHODS

2.5.1 Immunocytochemistry (ICC)

Cells that are induced overnight are centrifuged at 1500 RPM for 3 minutes and washed with 1X PBS buffer in the same amount of initial volume of the cell suspension. 8 µl of cells are mixed with 12 µl of PBS (2:5 dilution). Slides are prepared in advance. Positively charged slides are heated on a heat block adjusted to 80-90^{o}C and a parafilm frame with an empty rectangular space inside is sticked to each slide. 10 µl of cell suspension is spreaded onto the empty space. Slide is left to air-dry. 500 µl of blocking solution is added onto the space and slides are incubated 30-45 minutes on benchtop shaker at room temperature. After incubation, blocking solution is removed with the help of a pipet. 1:300 dilution of primary antibody (anti c-myc) is added onto the cells. Slides are incubated on benchtop shaker either overnight at +4^{o}C or for 2-3 hours at room temperature. After incubation, primary antibody solution is removed and slides are washed with 500 µl of 1X PBS for 3 times. Washing steps take place at room temperature on benchtop shaker for five minutes. In the end of each washing, used PBS is removed and replaced by fresh 1X PBS. Following washing steps, 1:500 dilution of secondary antibody solution is added and slides are incubated for 2 hours on benchtop shaker at room temperature. During this incubation, it is important to keep slides in dark to get higher signals. Slides are washed 3 times with PBS as in the previous washing steps. Once PBS is removed, slides are left to dry preferably near flame to speed up the process. Then one drop of mounting medium is added. Parafilm is removed and coverglass is put

onto each slide. Nail polish is applied to the borders of the coverglass. Slides can be stored at +4^{o}C.

2.5.2 Protein Isolation from yeast cells

Cells that have been induced overnight are centrifuged at 3000 g for 3 minutes. Pellet is washed with 1 ml 1x PBS and cell suspension is centrifuged again at 3000 g for 3 minutes. Supernatant is removed by pipetting. 1 ml of 1M LiOAc is added. Samples are waited on ice for 5 minutes and centrifuged at 3000 g for 3 minutes. LiOAc is removed via by pipetting. Pellet is dissolved in 1 ml of 0.4M NaOH, and samples are incubated at room temperature for 5 minutes. Following incubation, cells are centrifuged at 3000 g for 3 minutes. Supernatant should be carefully removed to not have any remaining NaOH at the next steps. After removal of the supernatant, approximately 60 µl of ddH2O is added to complete the volume to 80 µl. Pellet is resuspended in ddH_2O. 16 µl of 6X SDS loading dye and 1 µl dTT (~10 mM final concentration) are added to the cell suspension. Cells are incubated on heat block at 37^{o}C for 30-45 minutes with constant shaking at 300 RPM. After incubation, cells are heated at 95^{o}C and centrifuged at 10000 RPM for 3 minutes and spinned down. Supernatant is transferred to a new eppendorf without touching the pellet. 10-20 µl of the supernatant can be loaded into SDS gel.

2.5.3 Genomic DNA isolation from yeast cells

As the cell source either a colony is picked from agar plate near flame or a 1 ml overnight liquid culture is pelleted at 3000 g for 3 minutes and supernatant is discarded. Cells are suspended in 100 µl of 200 mM LiOAc 1% SDS solution. 300 µl of 96-100% ethanol is added to the cell suspension. Cell debris including DNA is spinned down at 15000 g for 3 minutes. Pellet is washed with 70% ethanol. Pellet

which is hard to dissolve at this step is gently resuspended in 100 µl of H_2O or TE buffer. Cell suspension is pelleted at 15000 g for 15 seconds. 1 µl of supernatant is enough for PCR based applications [125].

2.5.4 Preparation of electrocompetent yeast cells

This protocol was adapted from the protocol optimized by Suga and Hatakeyama [126].

S.cerevisiae cells are grown in YPD medium overnight until the cell density reaches to $1x10^7$ cells/ml. Overnight cultures are placed on ice for 15 minutes before centrifugation. Cells are pelleted at 4000 g for 5 minutes. Pellet is washed with ice-cold sterile water three times. (same volume of the initial culture twice, half volume of the initial culture once) Pellet is suspended in ice-cold freezing buffer composed of 2M sorbitol, 10 mM CaCl2 and 10 mM HEPES (pH 7.5) to adjust the final cell concentration to $5x10^8$ cells/ml. 100 µl aliquots are distributed into 1.5 ml microcentrifuge tubes. Competent cells can be stored in a -80^{o}C freezer.

2.5.5 Transformation of/into yeast cells via electroporation

A competent cell aliquot is immediately thawed in water bath 30^{o}C and washed with 1 ml of ice-cold sorbitol by centrifugation at 3000 g for 3 minutes. Pellet is suspended in 1M sorbitol to adjust the cell density to $1\text{-}2x10^8$ cells/ml. 10-50 ng of purified plasmid DNA is added to the cell suspension, resuspended and transferred into a cuvette with a 2 mm gap size which is previously chilled. Electric pulse is applied to the cell suspension. 1 ml 1M ice-cold sorbitol is quickly added to the electroporated cells. 100-200 µl of the cell suspension is spreaded onto agar plates. If

selective plates are used, agar mix should contain 1M sorbitol as osmotic stabilizer. Plates are incubated at 30°C.

Parameters of electroporation:

Voltage	2 kV
Resistance	200 Ω
Capacitance	25 μF
Cuvette gap size	2 mm

2.5.6 Chemical transformation of DNA into yeast cells

Yeast cells are inoculated into 5-10 ml YPD and incubated overnight at 30°C 200 RPM. OD_{660} is measured and required amount of overnight culture is diluted into 50 ml fresh YPD medium to adjust the cell concentration to $5x10^6$ cells/ml. Cells are incubated again at 30°C 200 RPM until cell concentration reaches $2x10^7$ cells/ml. This growth last approximately 4-5 hours and the yield of 50 ml culture is enough for ten transformation. After dilution it is important for the cells to complete at least two divisions. Cells are transferred into a 50 ml falcon and centrifuged at 3000 g for 5 minutes. Supernatant is discarded. Cells are washed with 25 ml sterile ddH_2O and centrifuged again at 3000 g for 5 minutes. Supernatant is removed, pellet is dissolved in 1 ml of 100 mM lithium acetate (LiOAc) and the cell suspension is transferred into a sterile 1.5 ml microcentrifuge tubes. Cells are pelleted at top speed for 5 seconds and LiOAc is removed with a micropipette. Pellet is suspended in 400 μl of 100 mM LiOAc by completing the volume 500 μl to adjust the cell density to $2x10^9$ cells. (The volume of LiOAc can be adjusted according to the cell titer of the cell growth after the dilution.) According to the protocols, 1 ml single-stranded carrier DNA is

boiled, chilled and used at this step. However, in the experiments, I used purified RNA instead. Cell suspension is vortexed and 50 µl aliquots are distributed into 1.5 ml microcentrifuge tubes. Cells are centrifuged at 3000 g for 1 minute and LiOAc is removed. Transformation mix is carefully added onto the cells in the following order:

- 240 µl PEG (50% w/v)
- 36 µl of 1M LiOAc
- 25 µl of RNA (~500 ng/µl)
- 50 µL of sterlie ddH_2O
- DNA (1-10µg)

Cells are dissolved in the transformation mix by using vortex. Samples are incubated at 30°C for 30 minutes. Heat shock is applied to the samples at 42°C for 20-25 minutes. Samples are centrifuged at 6000 RPM for 15 seconds and the transformation mix is removed. Pellet is dissolved in 500 µl of sterile ddH_2O. 200 µl of cell suspension is spreaded onto the selective plates [125].

2.5.7 Polymerase Chain Reaction (PCR)

1	2	3	4	5	6
Initial denaturation	Denaturation	Annealing	Elongation	Final Elongation	On hold
98°C	98°C	Annealing temperature *	72°C	72°C	4°C
30 seconds	10 seconds	30 seconds	30 seconds/kb	2 minutes	∞

25-30 cycles

Figure 2.1: Reaction conditions of Polimerase Chain Reaction with Q5 polymerase

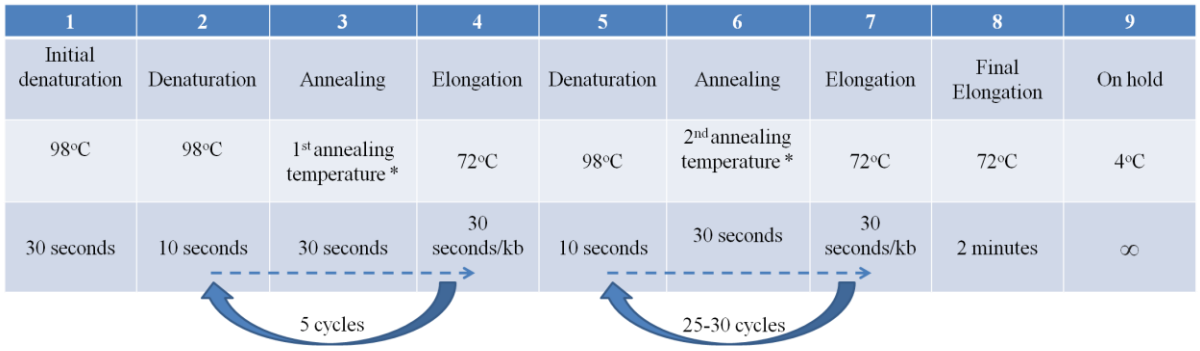

Figure 2.2: Reaction conditions of Polimerase Chain Reaction with Q5 polymerase in case primers with long overhang regions are used

2.5.7.1 Colony PCR

A colony is picked from agar plate and is either mixed PCR mix directly or dissolved in sterile ddH_2O and added to the mix. pfu polymerase and its buffer are used in colony PCR.

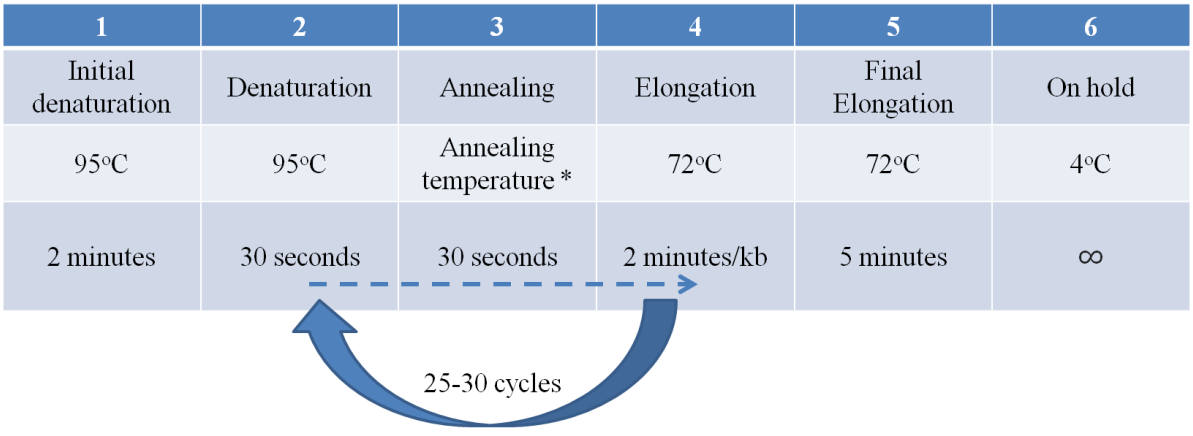

Figure 2.3:Reaction conditions of Polimerase Chain Reaction with pfu polymerase for verification of clonings by using the colony to serve as the template.

2.5.8 Plasmid isolation from bacteria

Plasmid purification from bacterial cells was performed by using Plasmid DNA Miniprep kit of Thermo Fisher Scientific. Manufacturer's protocol was followed for

the purification experiments. After washing, columns are left to air-dry for 5 minutes at room temperature. For the elution of the plasmid DNA, ddH_2O being preheated to 65^oC was used. After adding the water, columns were waited at room temperature for 3-5 minutes. Final centrifugation was at the maximum speed for 5 minutes. Concentration of the purified plasmid, A260, A280 values and their ratios were measured with Nanodrop. Purified plasmids can be stored at -20^oC freezer.

2.5.9 DNA extraction from agarose gel

DNA purification from agarose gel was performed by using GeneJET Gel Extraction kit of Thermo Fisher Scientific. Manufacturer's protocol was followed for the purification experiments. After washing, columns are left to air-dry for 3 minutes at 70^oC. For the elution of the DNA fragments, ddH_2O being preheated to 70^oC was used. After adding the water, columns were waited at room temperature for 3-5 minutes. Final centrifugation was at the maximum speed for 5 minutes. Concentration of the purified DNA fragments, A260, A280 values and their ratios were measured with Nanodrop. Purified DNA fragments can be stored at -20^oC freezer.

2.5.10 Plasmid Isolation from Yeast Cells

Plasmid purification from bacterial cells was performed by using Zymoprep Yeast Plasmid Miniprep II kit (Cat# D2004) of Zymo Research. Manufacturer's protocol was followed for the purification experiments. Buffers were shaken before using because they had a tendency to precipitate. Longer incubation at 37^oC at step 2 resulted in better yields. Neutralizing buffer was pre-chilled on ice for 20-30 minutes. After washing, columns are left to air-dry for 2 minutes at room temperature. For the elution of the plasmid DNA, ddH2O being preheated to 50^oC

was used. After adding the water, columns were waited at room temperature for 2-3 minutes. Final centrifugation was at the maximum speed for 2 minutes. Concentration of the purified plasmid, A260, A280 values and their ratios were measured with Nanodrop. Purified plasmids can be stored at -20^{o}C freezer.

2.5.11 Western blot

After running the samples on SDS gel, the proteins on the gel is transferred onto polyvinylidene difluoride (PVDF) membrane by using Trans-Blot Turbo (Bio-Rad). Membrane is treated with small amount of methanol to get activated. Wattman papers are waited in transfer buffer for 3-4 minutes to get wet. PVDF membrane is placed on one of the Wattman papers. SDS gel is put onto the PVDF membrane in an aligned orientation. The other Wattman paper is placed at the top of them. As the transfer protocol, Trans-Blot Turbo transfer system lasting 7 minutes is used. After transfer, the membrane is incubated in blocking solution composed of %5 milk powder dissolved in TBST buffer to eliminate nonspecific bindings for 1-2 hours at room temperature. Following blocking step, blocking solution is transferred into a falcon and primary antibody solution is added onto the membrane. Primary antibody solution contains 1:1000 dilution of anti c-myc antibody (9E10) (Santa Cruz Biotechnology) within %5 milk powder dissolved in TBST buffer. Primary antibody incubation takes place either -at 4^{o}C overnight or at room temperature for 1 hour. After primary antibody incubation, membrane is washed in TBST buffer 3 times and each washing step lasts 10 minutes. TBST buffer is removed and the membrane is incubated in 1:10000 dilution of anti-mouse secondary antibody conjugated with horseradish peroxidase (Abcam) within %5 milk powder TBST buffer at room temperature for 1 hours in the dark. Following the incubation, washing steps are repeated. To visualize the

membrane, luminescence substrate kit and ChemiDoc Imaging System of Bio-Rad are utilized.

2.5.12 Plasmid construction and cloning of constructs

Htt-25Q, Htt-46Q, Htt-103Q sequences were previously synthesized. Htt-25Q sequence was amplified with the addition of HA tag, SpeI and PstI restriction sites to the upstream region and XhoI site to the downstream region. Htt-25Q was cloned into pETcon vector by digesting both the insert and the backbone at PstI and XhoI restriction sites and ligating them. Components of digestion reaction is written in the Materials section. Digestion reaction with these enzymes takes place at 37^{o}C for 2 hours. Htt-46Q and Htt-103Q were digested and ligated at SpeI and XhoI restriction sites that had been added via PCR. Components of ligation reaction is written in the Materials section. Ligation reaction takes place at room temperature for 15 minutes.

Sequences of amyloid β_{40} and amyloid β_{42} were constructed by annealing two complementary oligos to construct the common 60 bp region in the middle using annealing buffer and extending that region using PCR primers. Both the inserts and pETcon plasmid were digested at SpeI and XhoI restriction sites and ligated.

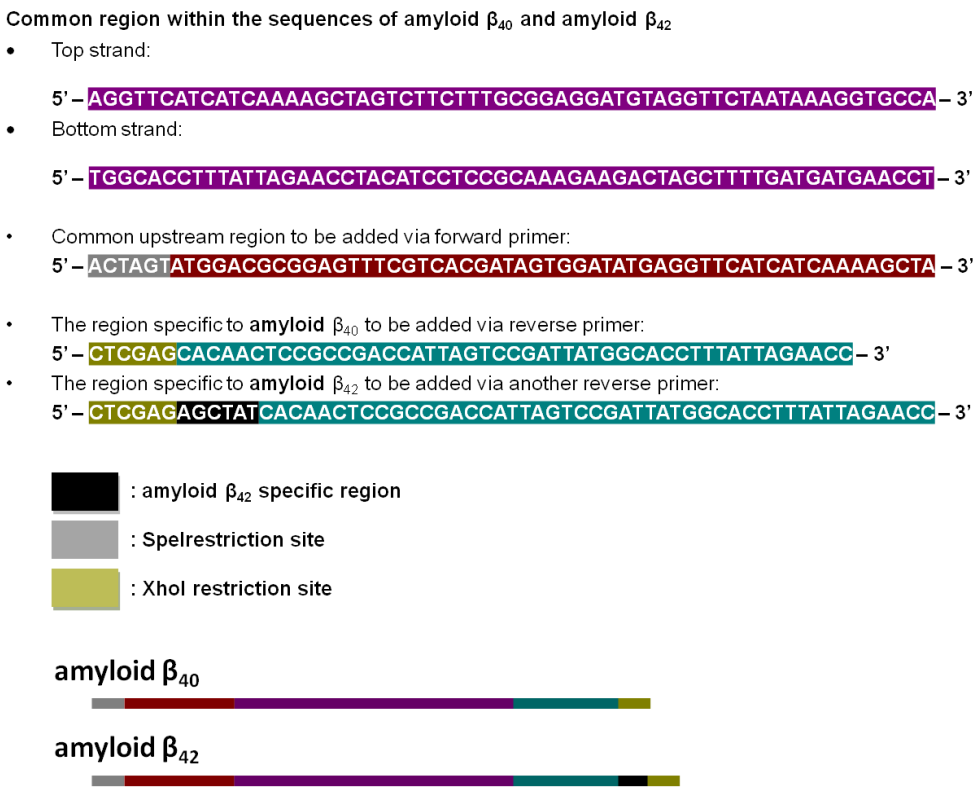

Figure 2.4: The flow chart indicating the construction of double-stranded amyloid β sequences

Repeats of amyloid beta$_{40}$ and amyloid beta$_{42}$ were constructed with the addition of homology domains and by joining a pair of identical amyloid beta sequences and pETcon backbone via Gibson assembly. Components of Gibson mix is written in the Methods section. Gibson assembly reaction takes place at 50^{o}C for 1 hour.

alpha synuclein sequence was synthesized by Genewiz company with the addition of Gibson homology domains. Proper amount of the sequence was directly used in gibson assembly reaction mix.

2.5.13 Surface Display of Neurodegenerative Proteins

Saccharomyces cerevisiae EBY100 strain is inoculated into 3-5 ml selective growth medium (SD-trp) and incubated overnight with constant shaking at 260 RPM at

30°C. OD660 value is measured and cells are diluted in fresh selective medium to adjust the cell concentration to approximately $4.63x10^6$ cells/ml. This concentration is enough to have a cell culture with OD660=1 after 4-hour-incubation at 260 RPM at 30°C. Once OD_{660} value gets 1.0, cells are pelleted at 4000 g for 5 minutes. Supernatant is discarded and cell pellet is dissolved in selective induction medium. Cell suspension is incubated at 20-25°C for 16-20 hours.

2.5.14 Preparation of Chemically Competent Bacterial Cells

E.coli cells are inoculated into 3 ml LB medium and incubated at 37°C overnight. Following incubation, 500 µl of the overnight culture is diluted into 50 ml fresh LB. Cells are left to incubation at 37°C for approximately 2 hours. After incubation, OD_{600} value is measured. Once it reaches 0.2-0.5, cell culture is transferred into 50 ml falcon and waited on ice for 10 minutes. Cells are centrifuged at 13000 RPM for 10 minutes. Supernatant is discarded and the pellet is dissolved in 5 ml TSS buffer. 100 ul aliquots of cell suspension is distributed into sterile, pre-chilled 1.5 ml microcentrifuge tubes. Competent cells can be stored at -80°C freezer.

2.5.15 Transformation of DNA into Chemically Competent E.coli Cells

Competent cells are taken from -80°C freezer and thawed for 20 minutes on ice. Approximately 100 ng plasmid DNA is added onto the cells and cells are waited on ice for 20 minutes. Heat shock is applied by waiting cells at 42°C for 45 seconds and then on ice for 2 minutes. 500 µl LB is added onto the cells and cells are resuspended. Cell suspension is incubated in microcentrifuge tubes at 37°C at 200 RPM for 45 minutes. After incubation, cells are centrifuged at 5800 g for 6 minutes. 500 µl of the supernatant is discarded and cells are suspended in the remaining

supernatant. Cell suspension is spreaded onto the proper selective plates near flame. Plates are incubated at 37^{o}C incubator in upside-down orientation.

3 RESULT AND DISCUSSION

3.1 Cloning of Constructs

pETcon is a shuttle vector with three different origin of replication parts unique to yeast, phage and bacteria. It has an ampicillin resistance gene as a selection marker for bacteria and TRP1 gene as an auxotrophic selection marker for yeast. Aga2 gene codes for Aga2 surface protein that is responsible for cell adhesion during yeast mating. Aga1 is anchored to the yeast cell wall and forms disulfide bonds with Aga2 before being placed on the cell wall. EBY100 strain used in this study has Aga1 in its genome with a modification. Promoter regulating Aga1 transcription is replaced with a galactose-inducible promoter: GAL1. EBY100 strain is Aga2 knockout, and absence of Aga2 is complemented by the presence of Aga2 on pETcon plasmid under the control of GAL1 promoter. An EBY100 cells transformed with pETcon plasmid and induced with galactose is able to re-establish a-agglutination system. Therefore, display on the surface is controlled through galactose presence.

3.1.1 Cloning of Htt-25Q

While cloning into pETcon plasmid, HA tag to be placed between Aga2 and Htt-25Q was added to N-terminus of Htt-25Q using a PCR primer. To include HA tag in the pETcon backbone for the next clonings, a SpeI restriction site was added after HA tag. These additions were made through two successive PCRs. The number of CAG repeats which is abnormally high in patients with Huntington's disease in in the range of 16 and 20. Therefore, polyglutamine repeats consisting 25 CAG provide a basis for comparison with the other variants containing 46 and 103 repeats which were linked severe disease conditions [127].

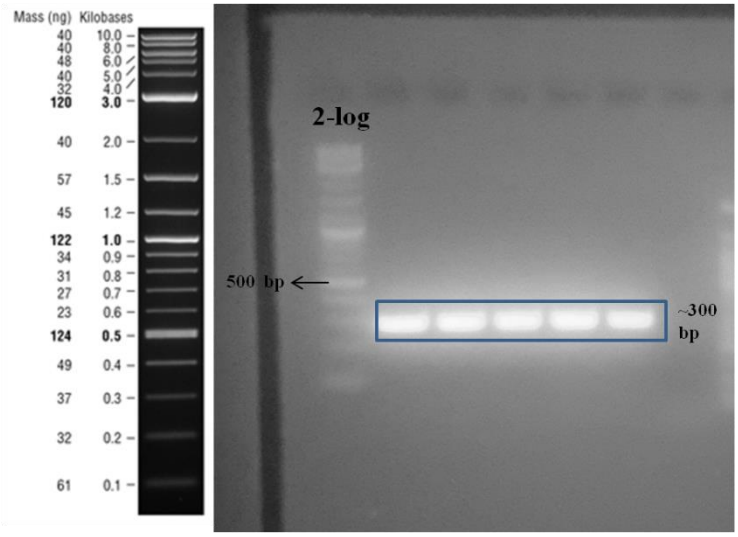

Figure 3.1: Agarose gel image of the first PCR to amplify Htt-25Q sequence by using forward primer 1 (to add HA tag and PstI restriction site) and reverse primer (to add XhoI restriction site) Lane 1: 2-log ladder Lane2-6: 25Q (Expected band length ~300 bp) Lane 7: negative control

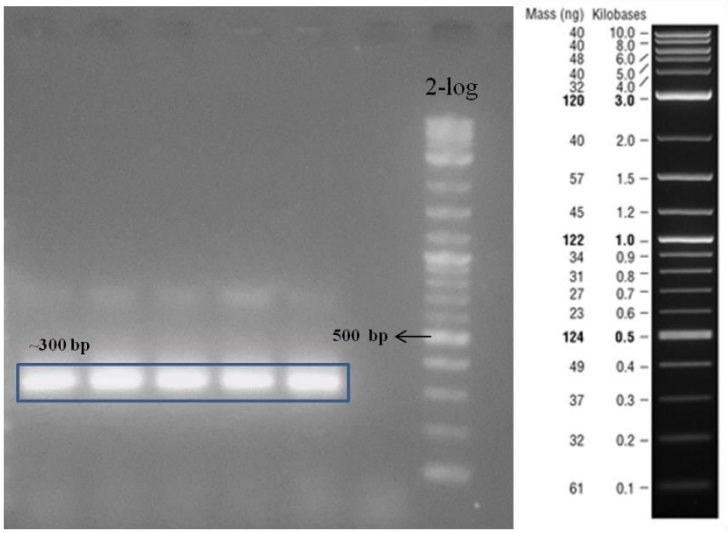

Figure 3.2: Agarose gel image of the second PCR to amplify Htt-25Q by using forward primer 2 (to add SpeI restriction site) and reverse primer Lane 1-5: 25Q (Expected band length ~300 bp) Lane 6: negative control Lane7: 2-log ladder

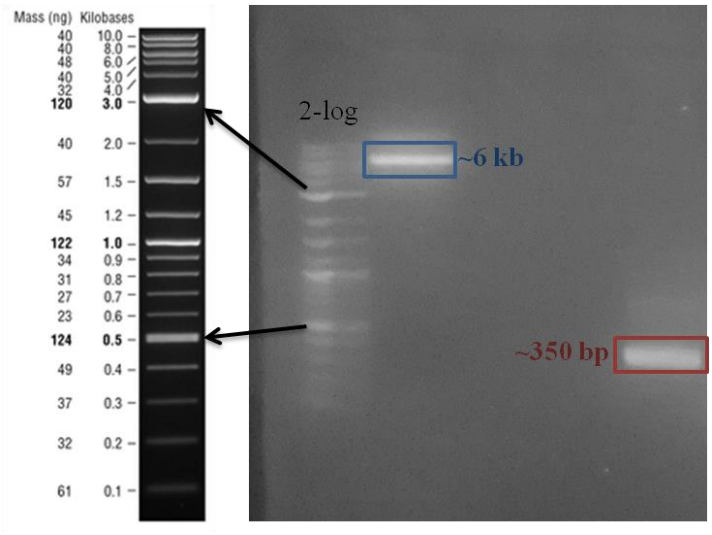

Figure 3.3: Agarose gel image of the restriction enzyme digestion of pETcon backbone and Htt-25Q sequence. Lane 1: NEB 2-log ladder, lane 2: digested pETcon, lane 3: empty, lane 4: digested Htt-25Q. Expected band lengths: 6 kb and 350 bp.

3.1.2 Cloning of Htt-46Q

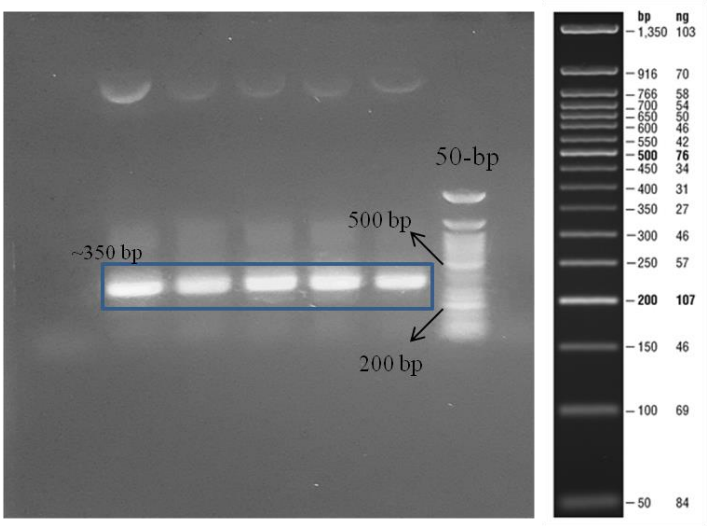

Figure 3.4: Agarose gel image showing the result of PCR to amplify Htt-46Q. Lane 1: negative control, Lane2-6: 46Q (Expected band length ~350 bp) Lane 7: 50-bp ladder

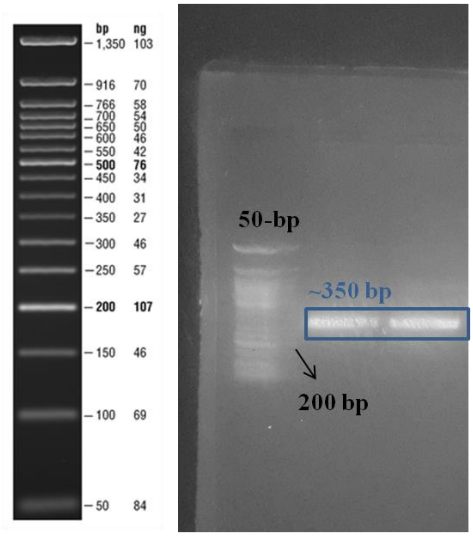

Figure 3.5: Products of double restriction enzyme digestion of Htt-46Q by using XhoI and SpeI. Lane 1: 50-bp ladder, Lane2-3: digested 46Q (Expected band length ~350 bp)

3.1.3 Cloning of Htt-103Q

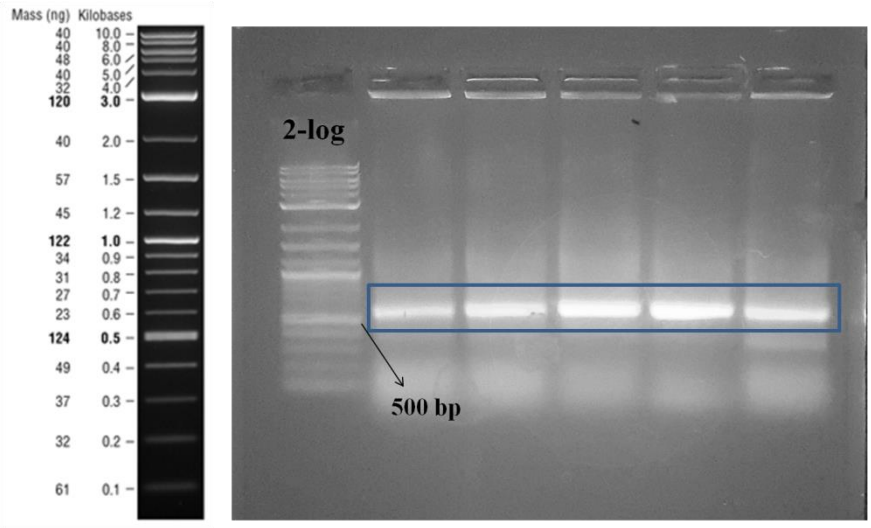

Figure 3.6: Agarose gel image showing the result of PCR to amplify Htt-103Q. Lane 1: NEB 2-log ladder, Lane2-6: 103Q (Expected band length ~500 bp)

3.1.4 Cloning of amyloidβ_{40} and amyloid β_{42}

amyloid β_{40} and amyloid β_{42} are underlying factors that trigger aggregation in Alzheimer's disease. amyloid β_{42} is a more toxic form in comparison to amyloid β_{40}. The difference between their nucleotide sequences is extra six nucleotides in the

sequence of amyloid β_{42}. Therefore, there is a common region that is 120 base pairs in length. 60 bp region in the centre was formed by annealing two complementary single stranded oligos and extended through two successive PCRs. First PCR was for the complementation of the peptide sequences and the other was to add homology regions for Gibson assembly.

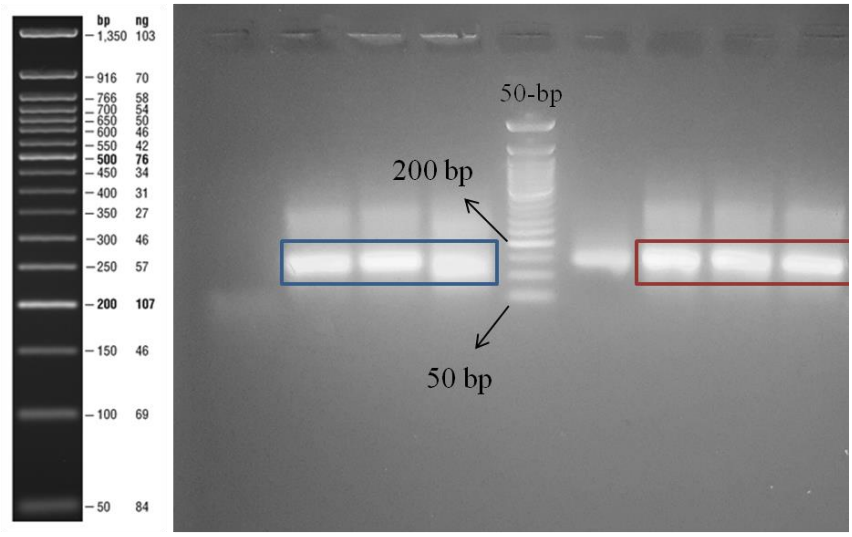

Figure 3.7: Agarose gel image showing the result of the PCR to amplify amyloid β_{40} and amyloid β_{42} after annealing complementary oligo sequences form the double stranded DNA piece. Lane 1: negative control, lane 2-4: amyloid β_{40}, lane 5: 50 bp ladder, lane 6: negative control, lane 7-9: amyloid β_{42}. Expected band length: ~140 bp

There was a band in the negative control for amyloid β_{42}. It was weak but problematic since it was in the sample length with the desired amplicon. To eliminate the formation of nonspecific double stranded structure, gradient PCR was done with varying temperatures ranging from 59.3^{o}C to 71^{o}C. The results showed that 71^{o}C was ideal to do PCR for the amplification of amyloid β_{42} since the nonspecific band was almost disappeared and the signal from the desired amplicon was highest.

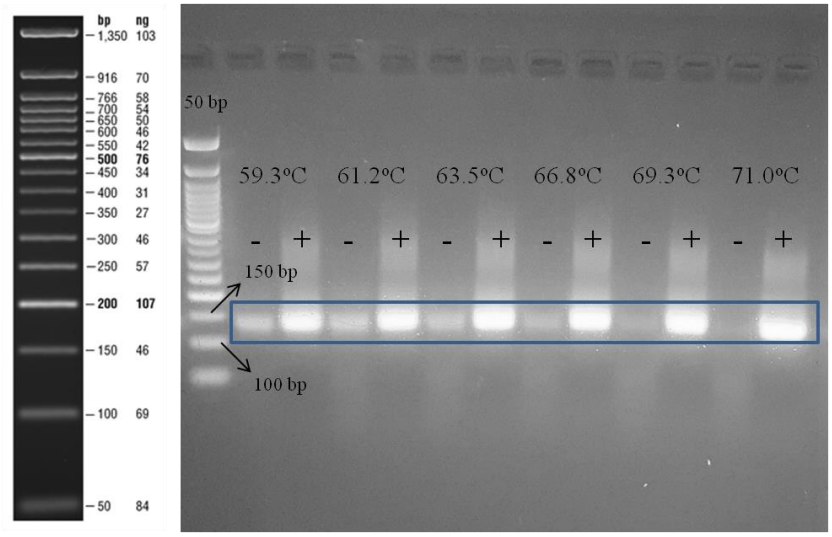

Figure 3.8: Agarose gel image showing the result of gradient PCR to find the optimum annealing temperature to eliminate the formation of amplicon in the negative controls for amyloid β_{42}. Nonspecific bands disappeared at higher temperatures like 71°C which was used as the annealing temperature in the next experiments.

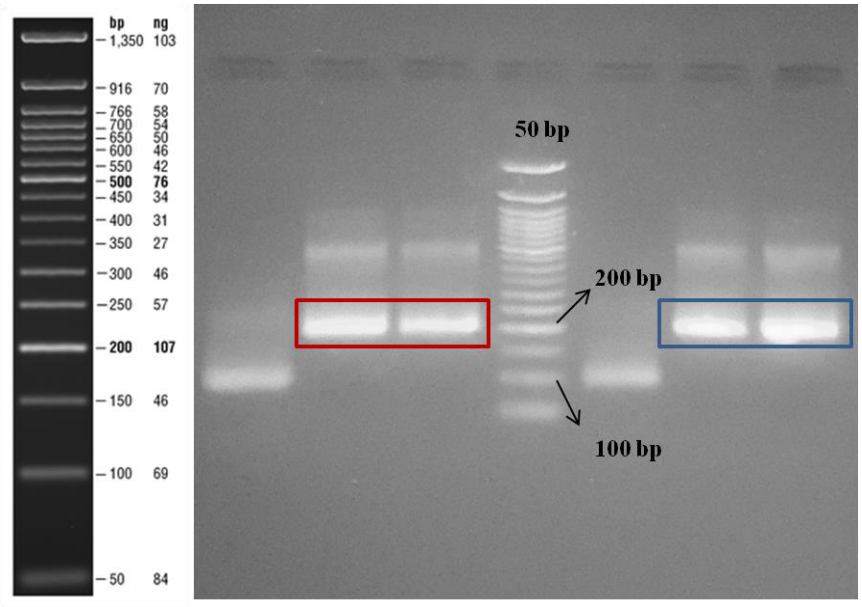

Figure 3.9: Agarose gel image showing the result of PCR to amplify amyloid β_{40} and amyloid β_{42} sequences and add homology regions corresponding to pETcon backbone for Gibson assembly. Expected band lengths: ~200 bp.

3.1.5 Cloning of repeated amyloid β_{40} and amyloid β_{42}

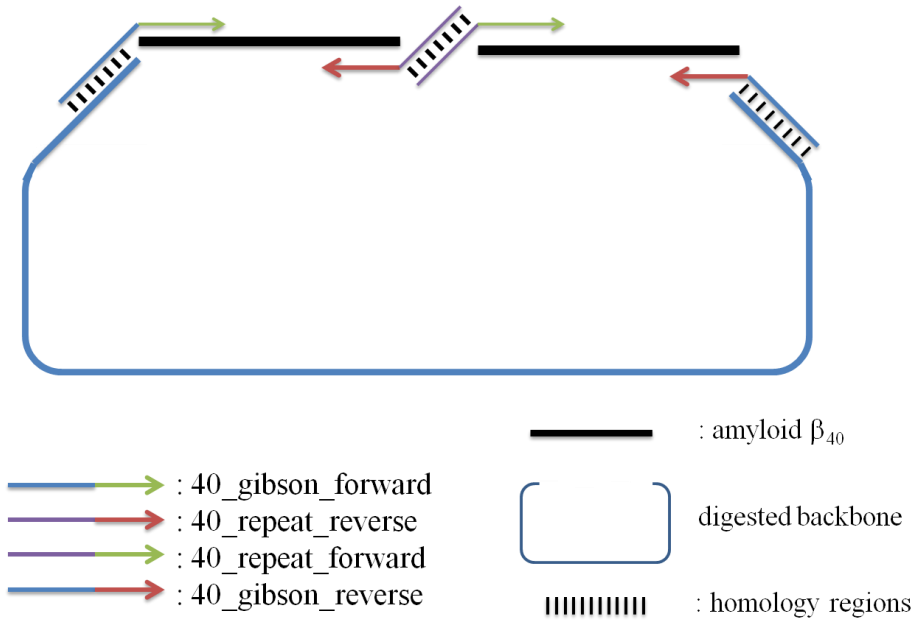

Figure 3.10: Schematic representation of how two amyloid β_{40} or amyloid β_{42} sequences joined together. One of the primers provided homology with pETcon backbone and the other primer provided a common region containing GS linker and MluI cut site.

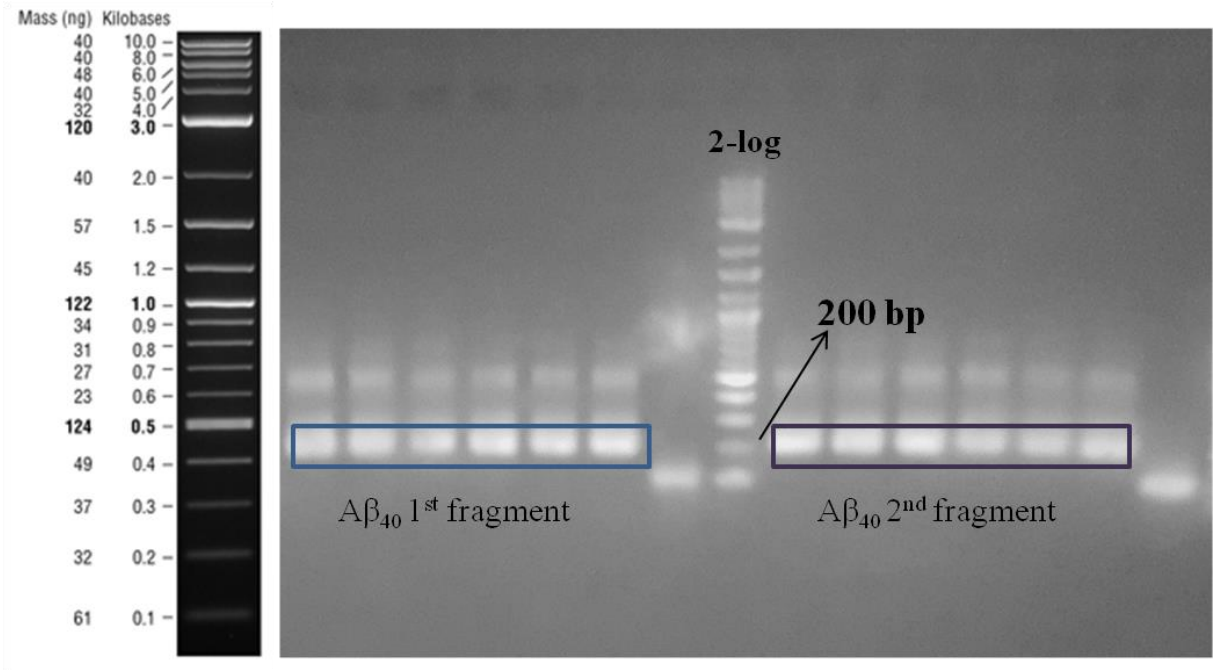

Figure 3.11: Agarose gel image showing the result of PCR to amplify amyloid β_{40} sequences with proper homology regions for Gibson assembly to join two amyloid β_{40} sequences successively. Lane 1-6: amyloid β_{40} first fragment, lane 7: negative control, lane 8: NEB 2-log ladder, lane 9-14: amyloid β_{40} second fragment, lane 15: negative control. Expected band length: ~200 bp.

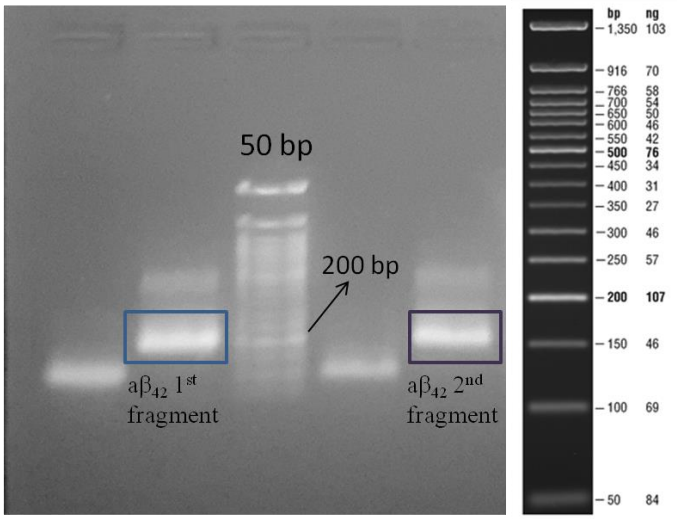

Figure 3.12: Agarose gel image showing the result of PCR to amplify amyloid β_{42} sequences with proper homology regions for Gibson assembly to join two amyloid β_{42} sequences successively. Lane 1: control, lane 2: amyloid β_{42} first fragment, lane 3: 50 bp ladder, lane 4: control, lane 5: amyloid β_{42} second fragment. Expected band length: ~200 bp.

3.1.6 Cloning of α-synuclein

α-synuclein sequence which is 420 base pairs and 140 amino acids in length was synthesized by Genewiz company with the addition of 40 nucleotide as homology regions for Gibson assembly to the each side. Five colonies were selected for further analysis. Plasmids isolated from those colonies were digested using two restriction enzymes: one was digesting plasmid at the backbone, the other was digesting at a site within α-synuclein sequence.

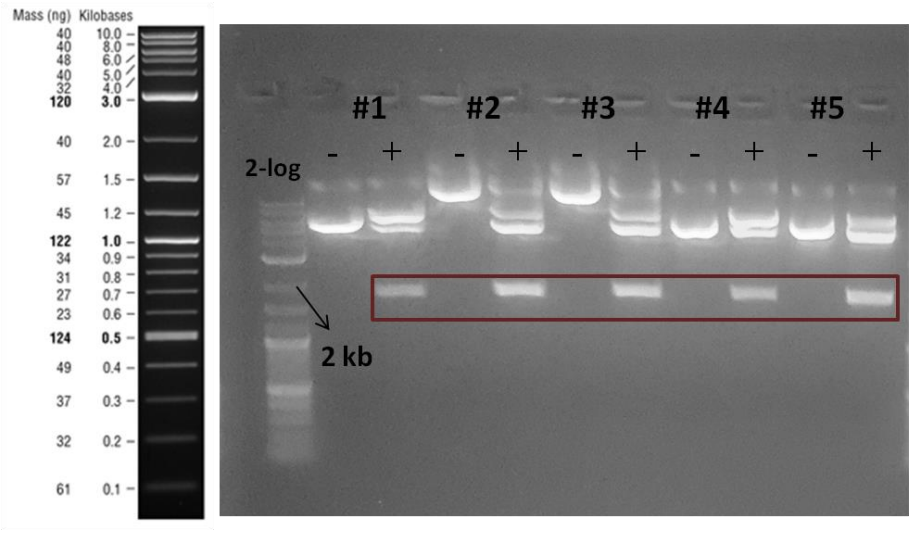

Figure 3.13: Agarose gel image showing the result of double restriction enzyme digestion reaction to verify the presence of α-synuclein sequence within pETcon backbone using one enzyme digesting α-synuclein sequence in the middle. Lane 1: NEB 2-log ladder, lane 2-3: colony #1, lane 4-5: colony #2, lane 6-7: colony #3, lane 8-9: colony #4, lane 10-11: colony #5. '-' stands for not digested, '+' stands for digested.

3.2 Transformation into Yeast Cells and Verifications regarding plasmid presence and protein production

Following transformation of plasmids into EBY100 cells, some verifications had been done in the DNA and protein level to demonstrate the presence of the proper plasmids and the production of proteins. To verify the plasmid presence, plasmids were isolated from yeast colonies. A region which included GAL1 promoter, Aga2 and the neurodegenerative protein of interest was amplified using universal primers, T3 and T7. Therefore, the length of amplicons was different depending on the length of the sequence of the neurodegenerative protein.

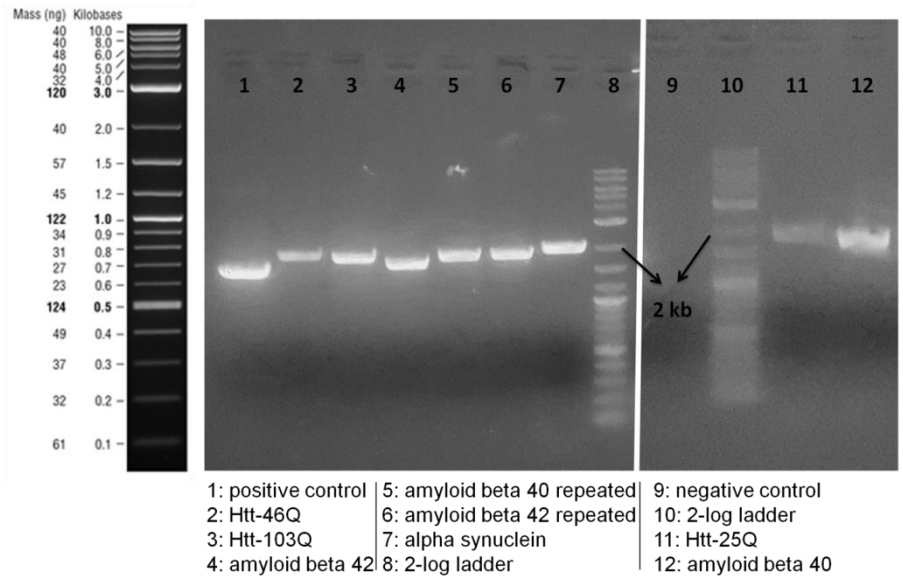

Figure 3.14: Agarose gel image showing the result of colony PCR on yeast colonies transformed with the indicated constructs above. Since two primers flanking Aga2p and gene of interest were used, amplicon lengths changed accordingly.

To do plasmid isolation to screen colonies obtained from each transformation was time consuming and expensive. Picking up a colony directly from the plate and use it in colony PCR mix resulted in mostly with low yields. This might be due to the fact that yeast cells have a dynamic and rigid cell wall structure composed of several molecules such as β-glucans, chitin, and mannoproteins [128,129]. To disrupt this structure for the applications like isolation of plasmid DNA, genomic DNA or proteins, special treatments should be done beforehand.

To find and optimize the most effective treatment, several conditions before running PCR were tried on the same colonies, amyloid β_{40} and amyloid β_{40} conjugated with sfGFP. Colonies were dissolved in sterile ddH_2O and distributed into the tubes for different conditions in the same volume to make sure that close amounts of DNA were treated in each condition. These conditions were

- 0.2 % SDS treatment and incubation at 95^{o}C for 5 minutes
- Incubation at 98^{o}C for 5 minutes
- Treatment with 20 mM NaOH and incubation at 98^{o}C for 10 minutes

- Without any treatment

Isolated plasmid DNA was used as a positive control to demonstrate PCR worked. Although there was a signal in the group of 'no treatment', the process of 0.2 % SDS treatment and incubation at 95^{o}C for 5 minutes was found to be more effective considering the yield. Next verifications via colony PCR was done in this way.

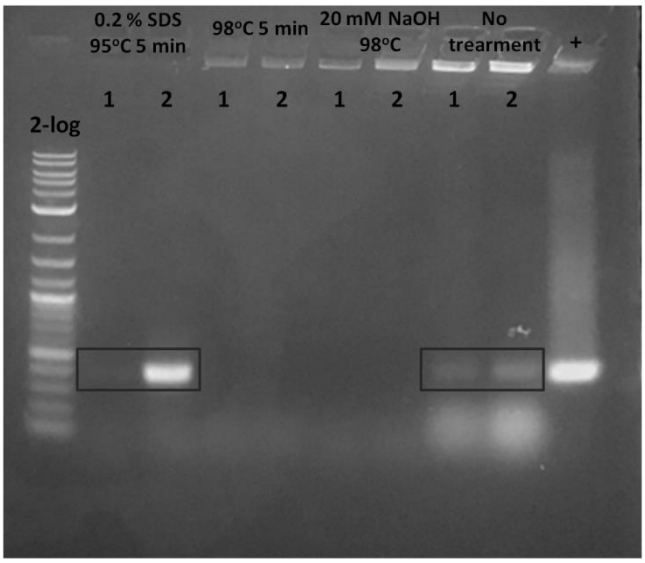

Figure 3.15: Agarose gel image showing the results of colony PCR experiments using colonies transformed with plasmids containing amyloid β_{40} and amyloid β_{40} conjugated with sfGFP followed by a series of different treatments.

Once the plasmid presence was verified, selected colonies were grown in growth medium and induced in induction medium with galactose. For the first trial, a construct with a neurodegenerative protein in conjugation with sfGFP was chosen to obtain a direct signal which was visible to the naked eye.

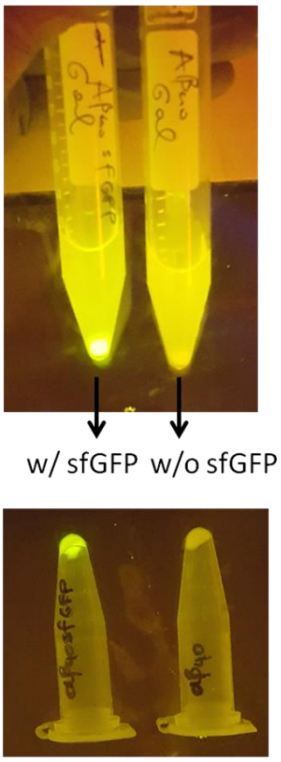

Figure 3.16: Pellets of *Saccharomyces cerevisiae* EBY100 cells transformed with amyloid β_{40} conjugated with sfGFP (left) and amyloid β_{40} (right) after induction with galactose.

Fluorescent signal in the pellets indicated that EBY100 cells synthesized proteins upon galactose induction. It was important to show that these signals were mainly coming from the surface of *Saccharomyces cerevisiae* cells. To do so, EBY100 cells that were transformed with amyloid β_{40} conjugated with sfGFP were grown, diluted and re-grown and induced. A small amount of cells induced overnight were spreaded onto positively charged slides uniformly. Slides were visualized under fluorescent microscope. The signal coming from inside of the cells might be fluorescent proteins stucked at endoplasmid reticulum or the other components of protein secretion mechanism.

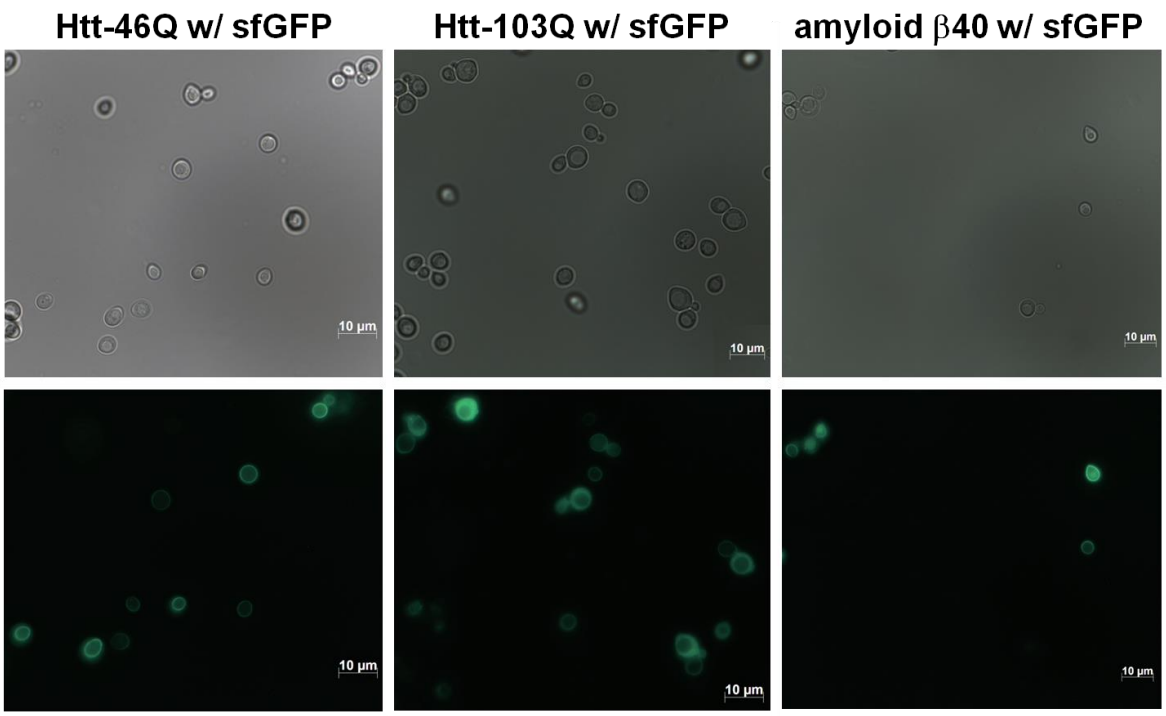

Figure 3.17: Fluorescent microscope images of Htt-46Q, Htt103-Q and amyloid β_{40} all conjugated with sfGFP. The ones on upper lane are bright field images.

It was important to check whether neurodegenerative proteins were forming clusters within yeast cells or in between yeast cells through the cell surface and leading to cell death. In case of an interaction between yeast cells which had neurodegenerative proteins on their surface, pellet formation was expected to be much more dramatic in Htt-103Q cells than in Htt46Q cells in comparison to Htt-25Q cells. To assess this possibility, OD660 values of induced cell cultures of EBY100 (in YPD), EBY100 cells transformed with empty pETcon without any neurodegenerative protein, and EBY100 cells transformed with Htt-25Q, Htt-46Q, Htt-103Q were equalized by the addition of fresh medium. Cell cultures were vortexed and waited on the bench. The formation of cell pellet was followed regularly. No significant difference between the amounts of cell pellet was observed.

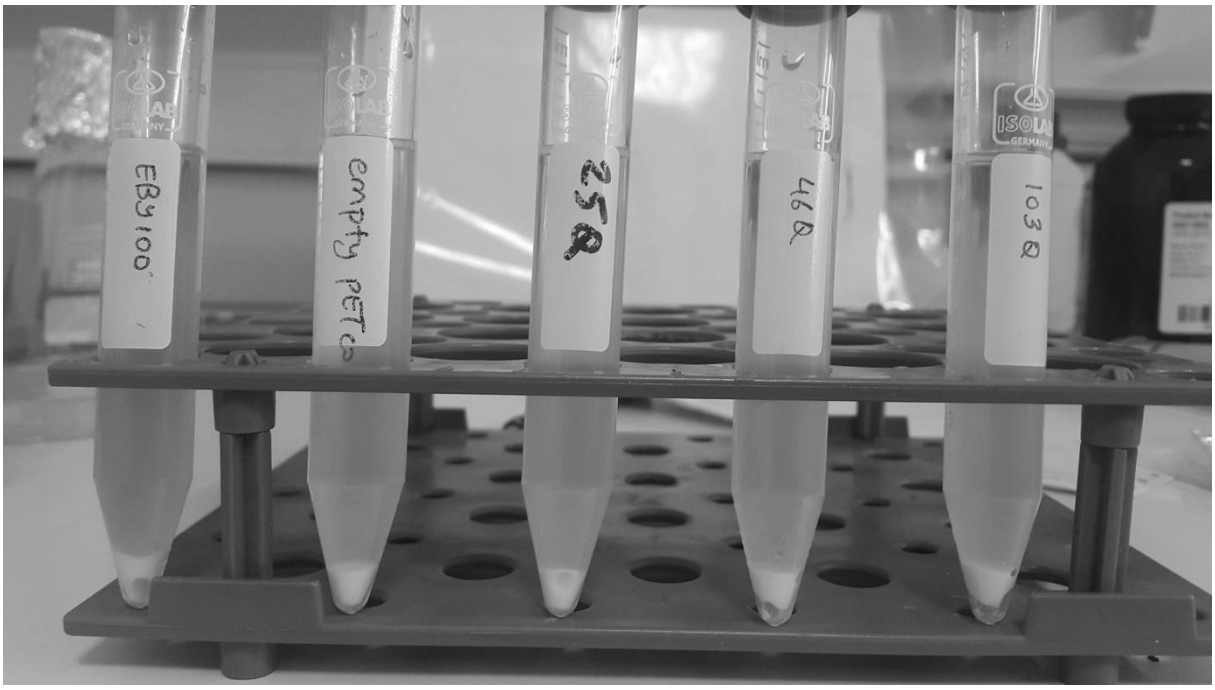

Figure 3.18: The result of the experiment to see whether proteins of interest were interacting within the cells or on the surface and leading to cell aggregation.

After appearance of sfGFP signal in response to galactose induction, other constructs with neurodegenerative proteins without sfGFP were induced. Presence of proteins within the induced cells was assessed through Western blot. The signal around ~12 kDa might be Aga2 protein produced due to a frame shift in empty pETcon backbone without any neurodegenerative protein.

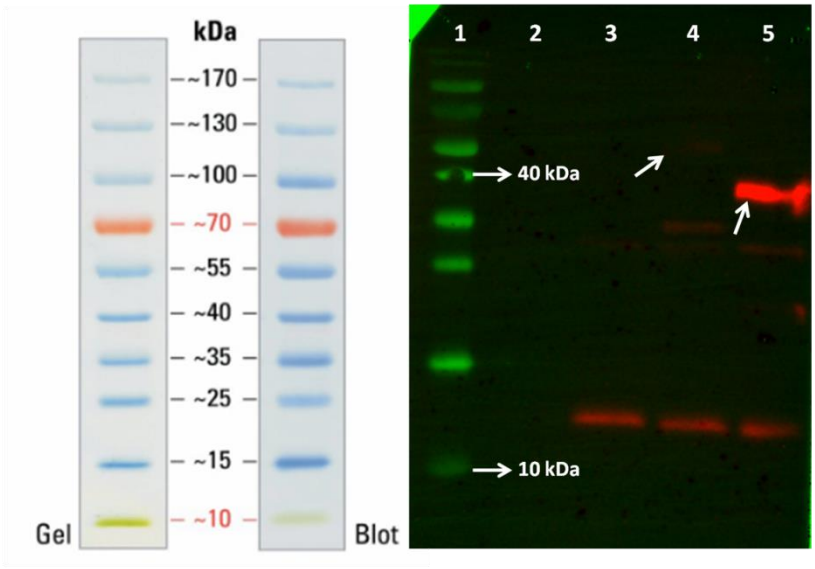

1: PageRuler Prestained 10-180kDa Protein Ladder
2: EBY100 (uninduced)
3: EBY100 with empty pETcon (induced)
4: EBY100 with pETcon- amyloid β_{40}–sfGFP (induced)
5: EBY100 with pETcon- α–synuclein (induced)

Expected bands:
46 kDa
31 kDa

Figure 3.19: Result of western blot analysis of proteins with c-myc tag produced by listed cells.

.

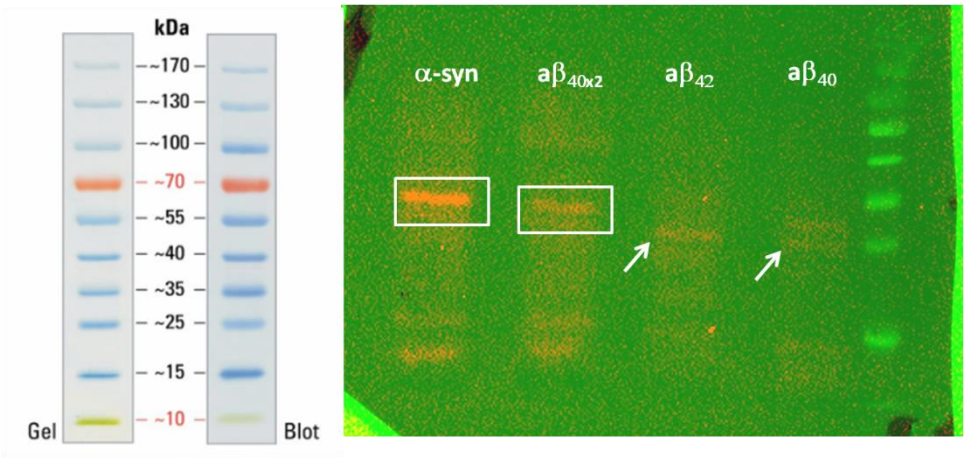

Figure 3.20: Result of western blot analysis of proteins with c-myc tag produced by cells transformed with pETcon with α-synuclein, repeated amyloid β40, amyloid β42, and amyloid β40 respectively.

3.3 Immunocytochemistry (ICC) Experiments

Following western blot analysis, immunocytochemisty protocol was applied on the induced cells to demonstrate the neurodegenerative protein presence on the cell surface. Since the proteins of interest were located on the surface, treatment with

detergents such as Tween-20, Triton X-100 was not applied to the cells. Cells were washed before spreading to remove the byproducts within the medium.

Antibody ratio, cell amount and incubation times were optimized considering four different protocols and results of the first trials. 1:300 dilution of primary antibody and 1:500 dilution of secondary antibody were found to be sufficient. To adjust optimal confluency on the slide, cull cultures induced overnight were diluted in PBS in the ratio of 1:1 or 1:2. Cells were spreaded onto the region surrounded by a parafilm frame. This parafilm frame had a capacity to hold 500 µl of liquid. Incubation at $+4^{o}C$ overnight resulted in better signals in comparison to the incubation at room temperature for 1 hour.

Use of mounting media on the slides, incubation with secondary antibody in the dark and storage at $+4^{o}C$ preserved fluorescent signal. To expose the slides to laser light for a long time caused a reduction in fluorescent signal, so the ideal position to get images was mostly determined using bright field mode.

Surface of *Saccharomyces cerevisiae* cells has a negative charge mostly contributed by the predominance of phosphate groups [130]. Therefore, EBY100 cells could easily stick to positively charged slides. Spending considerable time to spread yeast cells gently onto the positively charged slides prevented not only disruption of the cells but also overlapping cells. Spreading cells near flame provided both an aseptic environment and acceleration of air-dry of the cell suspension.

3.3.1 ICC analysis of Htt-25Q

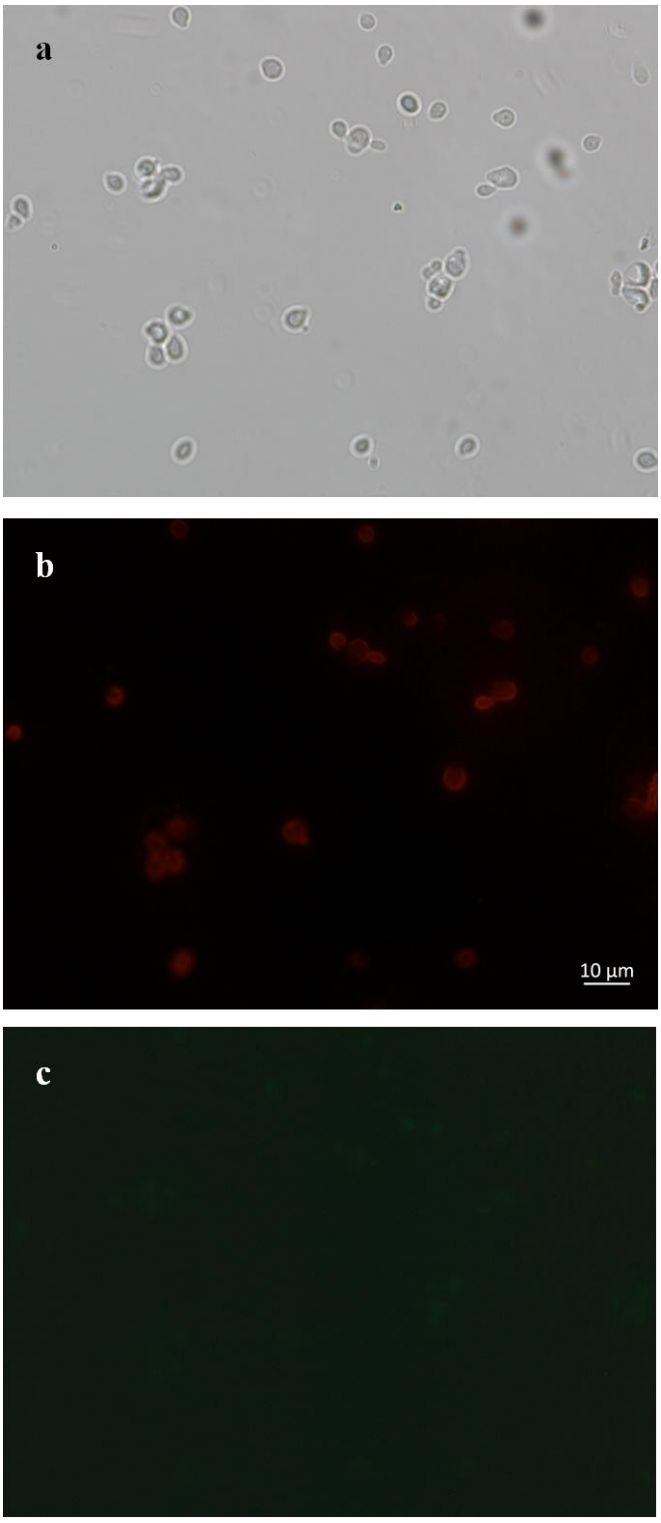

Figure 3.21: Bright field (a) and fluorescence microscopy (b,c) images of EBY100 cells transformed with pETcon plasmid expressing Htt-25Q upon galactose induction.

Green signal in part c that was coming from the whole cell structure was probably caused by autofluorescence of yeast cells as a response to tryptophan metabolism [131].

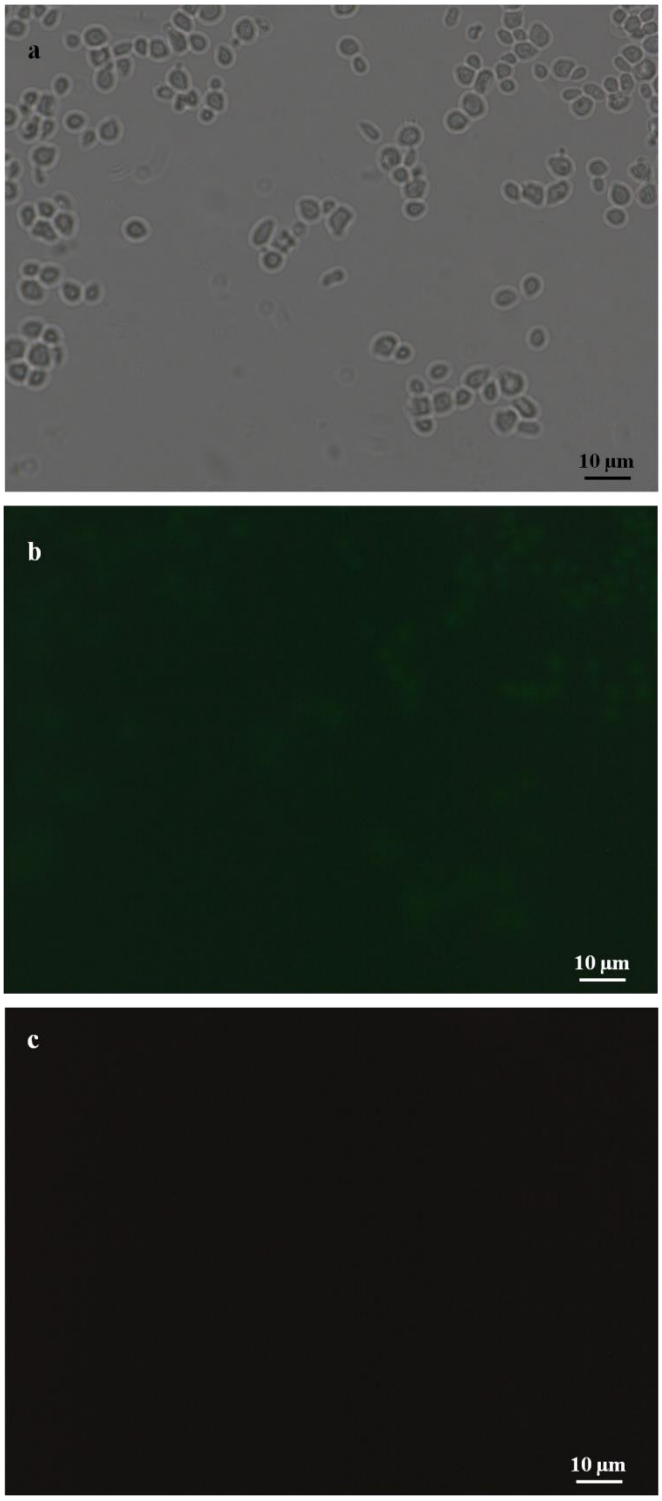

Figure 3.22: Bright field (a) and fluorescence microscopy with green filter (b) and red filter (c) images of control cells which were EBY100 cells transformed with pETcon plasmid expressing Htt-25Q upon galactose induction but not treated with primary antibody, anti c-myc antibody

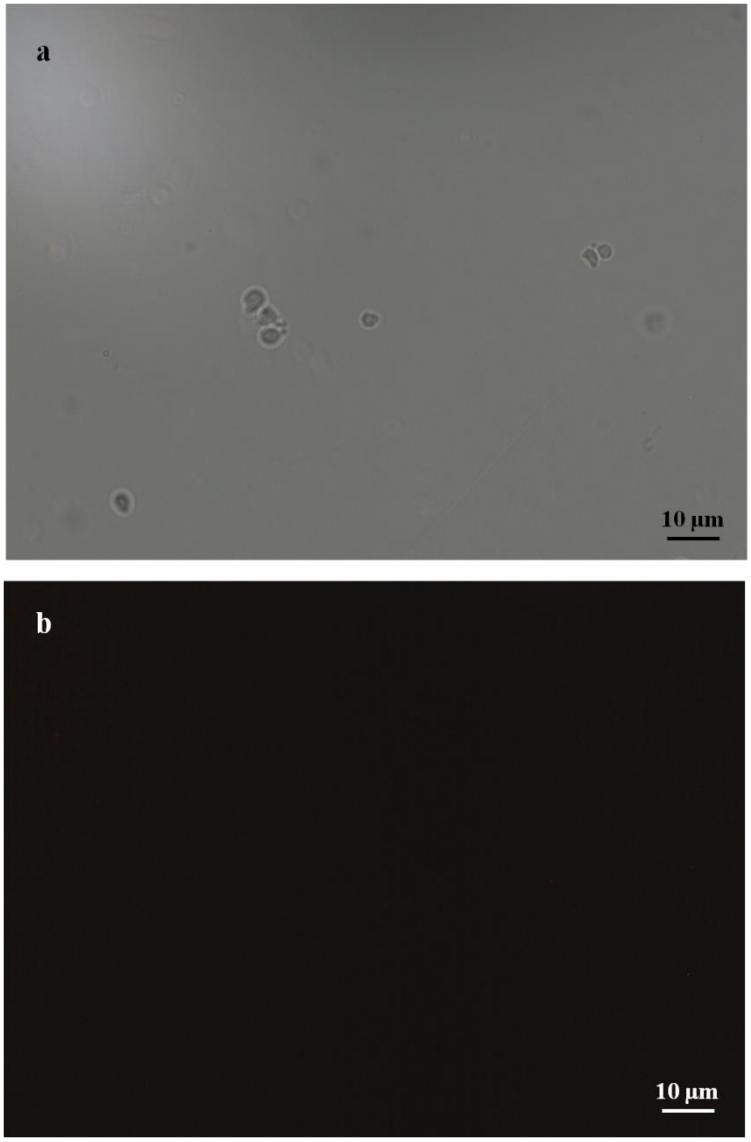

Figure 3.23: Bright field (a) and fluorescence microscopy with red filter (b) images of control cells which were control EBY100 without pETcon plasmid upon galactose induction.

3.3.2 ICC analysis of Htt-46Q

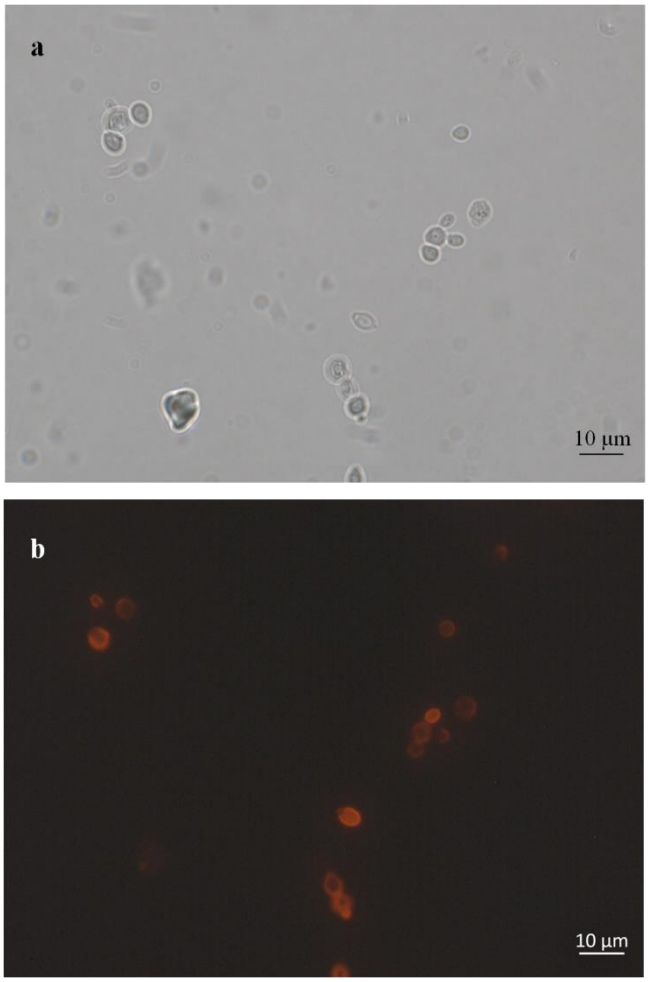

Figure 3.24: Bright field (a) and fluorescence microscopy (b) images of EBY100 cells transformed with pETcon plasmid expressing Htt-46Q upon galactose induction.

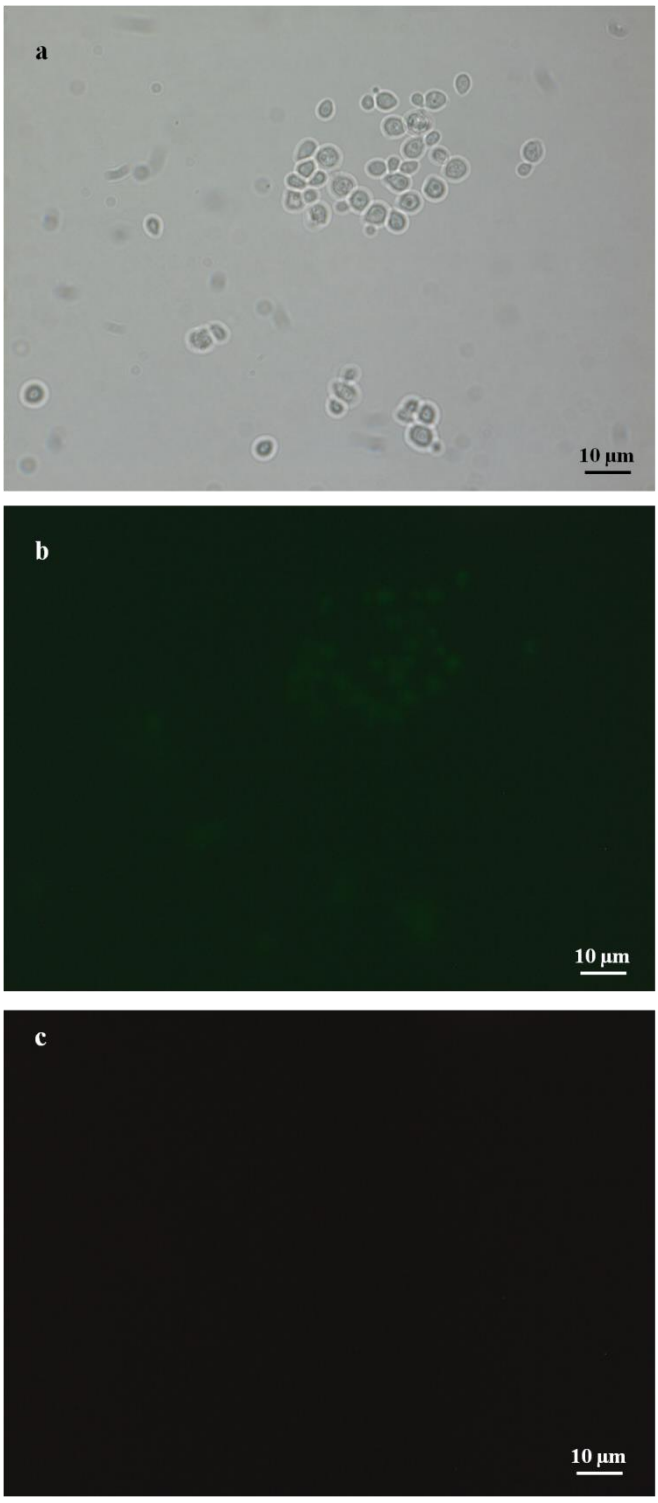

Figure 3.25: Bright field (a) and fluorescence microscopy with green filter (b) and red filter (c) images of control cells which were EBY100 cells transformed with pETcon plasmid expressing Htt-46Q upon galactose induction but not treated with primary antibody, anti c-myc antibody.

3.3.3 ICC analysis of Htt-103Q

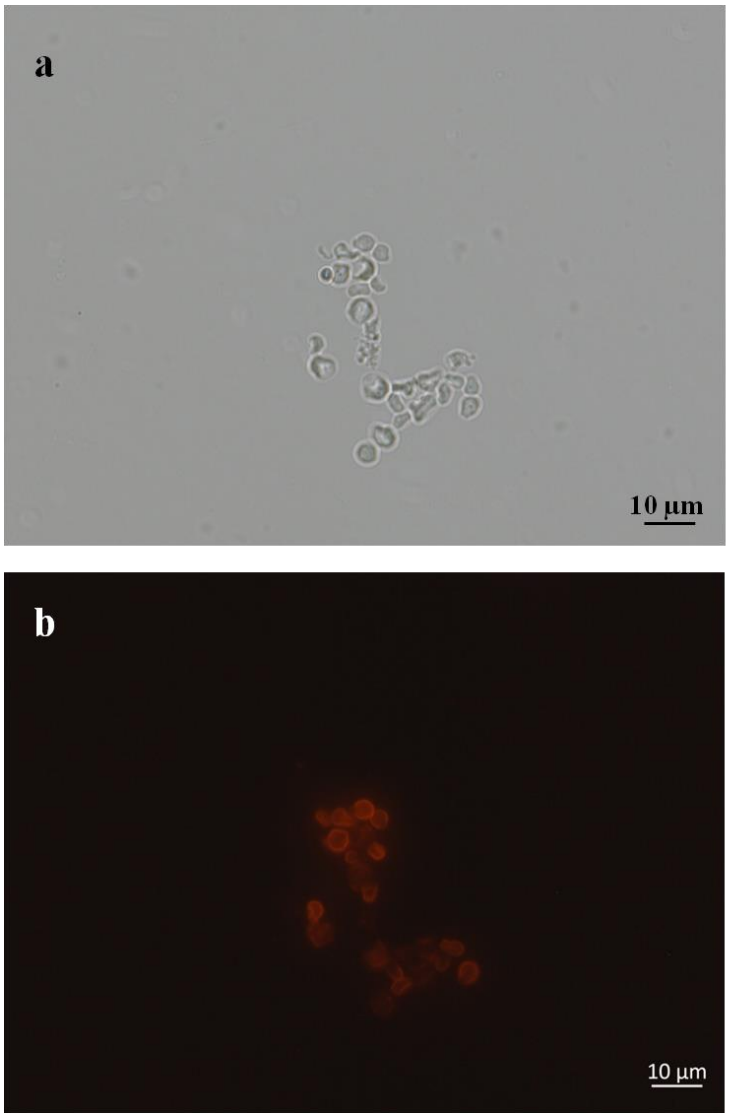

Figure 3.26: Bright field (a) and fluorescence microscopy (b) images of EBY100 cells transformed with pETcon plasmid expressing Htt-103Q upon galactose induction.

3.3.4 ICC analysis of amyloid β_{40}

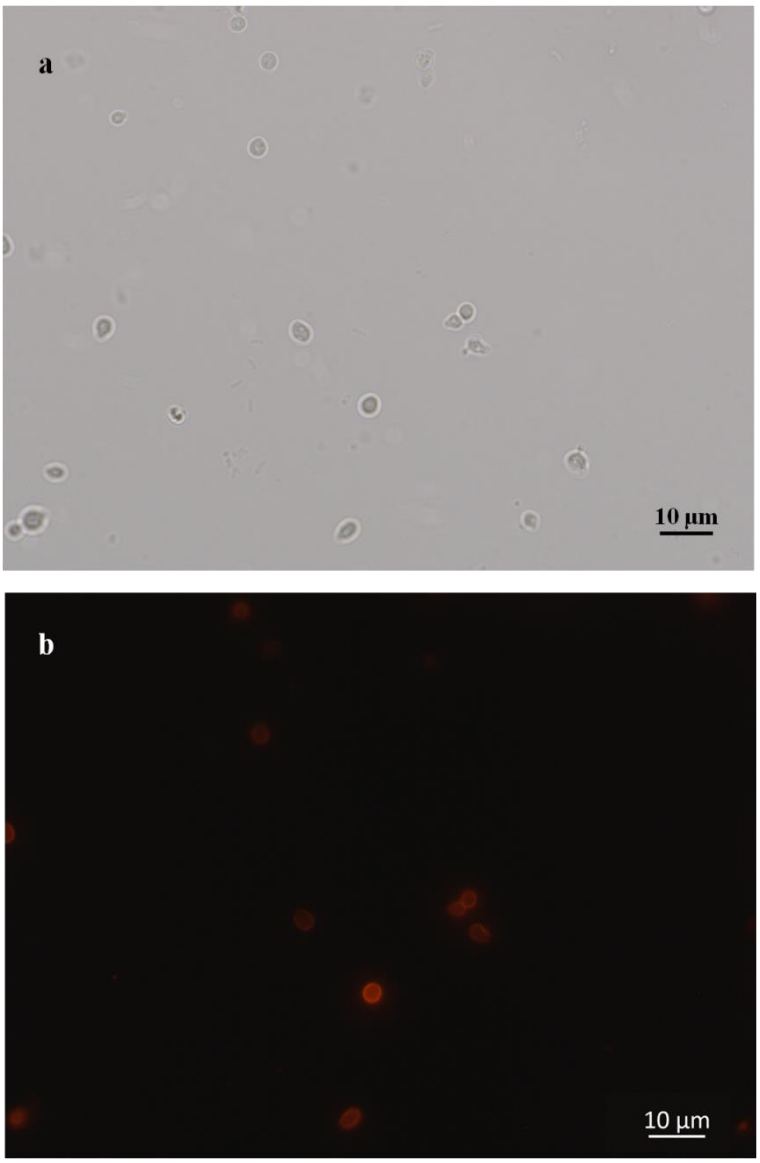

Figure 3.27: Bright field (a) and fluorescence microscopy (b) images of EBY100 cells transformed with pETcon plasmid expressing amyloid β_{40} upon galactose induction.

3.3.5 ICC analysis of amyloid β_{42}

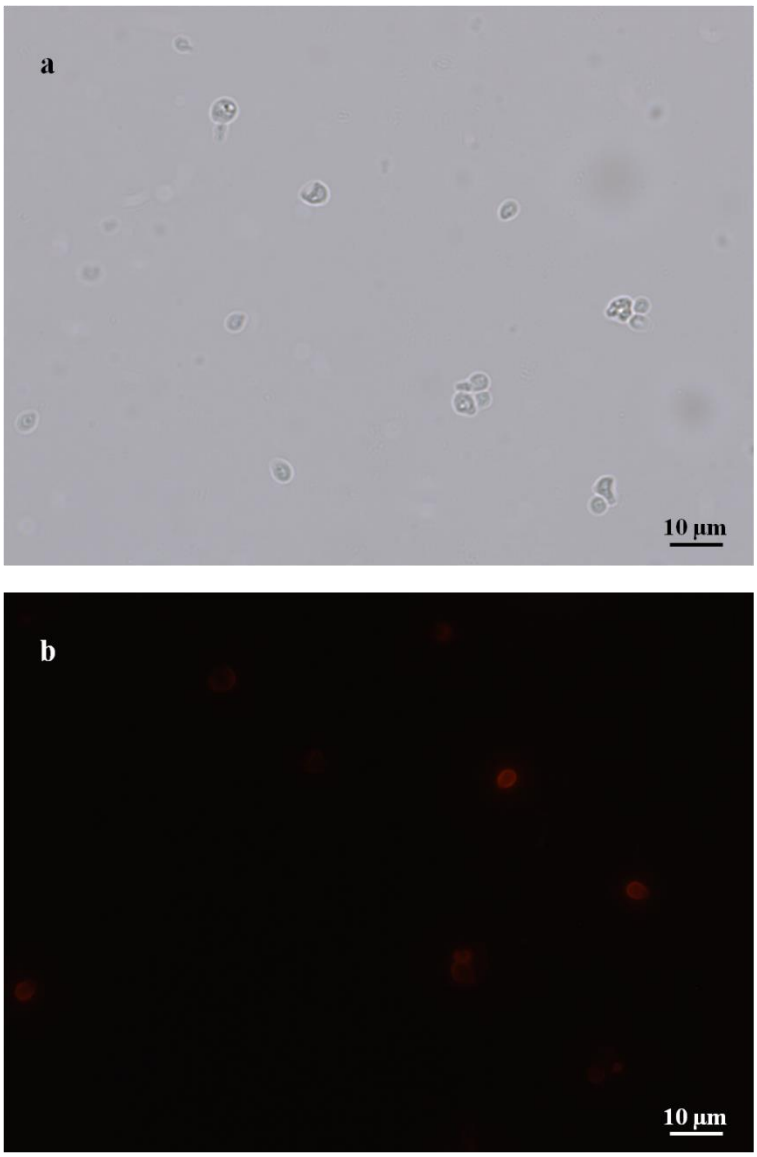

Figure 3.28: Bright field (a) and fluorescence microscopy (b) images of EBY100 cells transformed with pETcon plasmid expressing amyloid β_{42} upon galactose induction.

3.3.6 ICC analysis of amyloid β_{40x2}

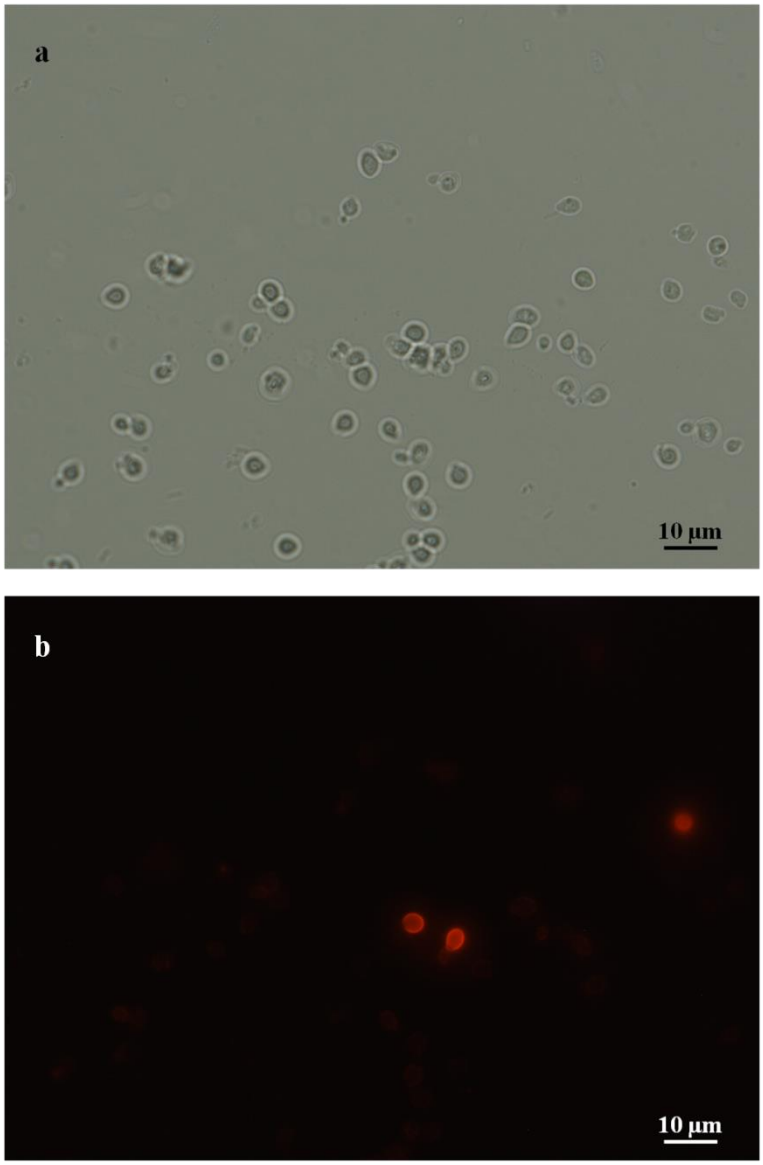

Figure 3.29: Bright field (a) and fluorescence microscopy (b) images of EBY100 cells transformed with pETcon plasmid expressing amyloid β_{40x2} upon galactose induction.

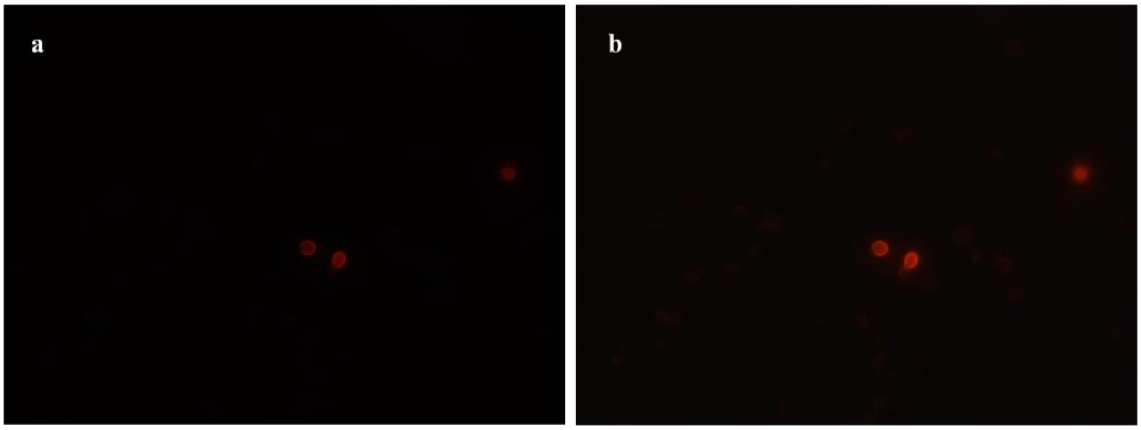

Figure 3.30: The image showing the difference coming from the EBY100 cells transformed with pETcon plasmid expressing amyloid β_{40x2} upon galactose induction depending on the low (a) or high (b) exposure.

3.3.7 ICC analysis of amyloid β_{42x2}

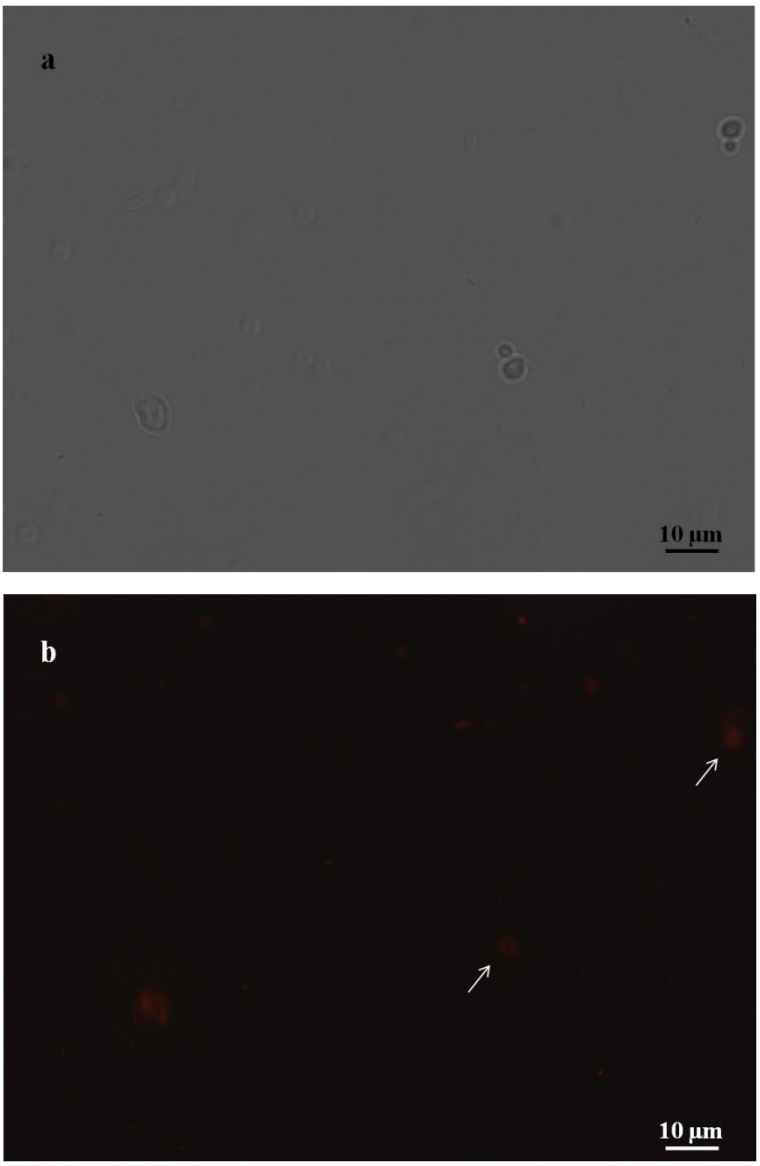

Figure 3.31: Bright field (a) and fluorescence microscopy (b) images of EBY100 cells transformed with pETcon plasmid expressing amyloid β_{42x2} upon galactose induction.

3.3.8 ICC analysis of α-synuclein

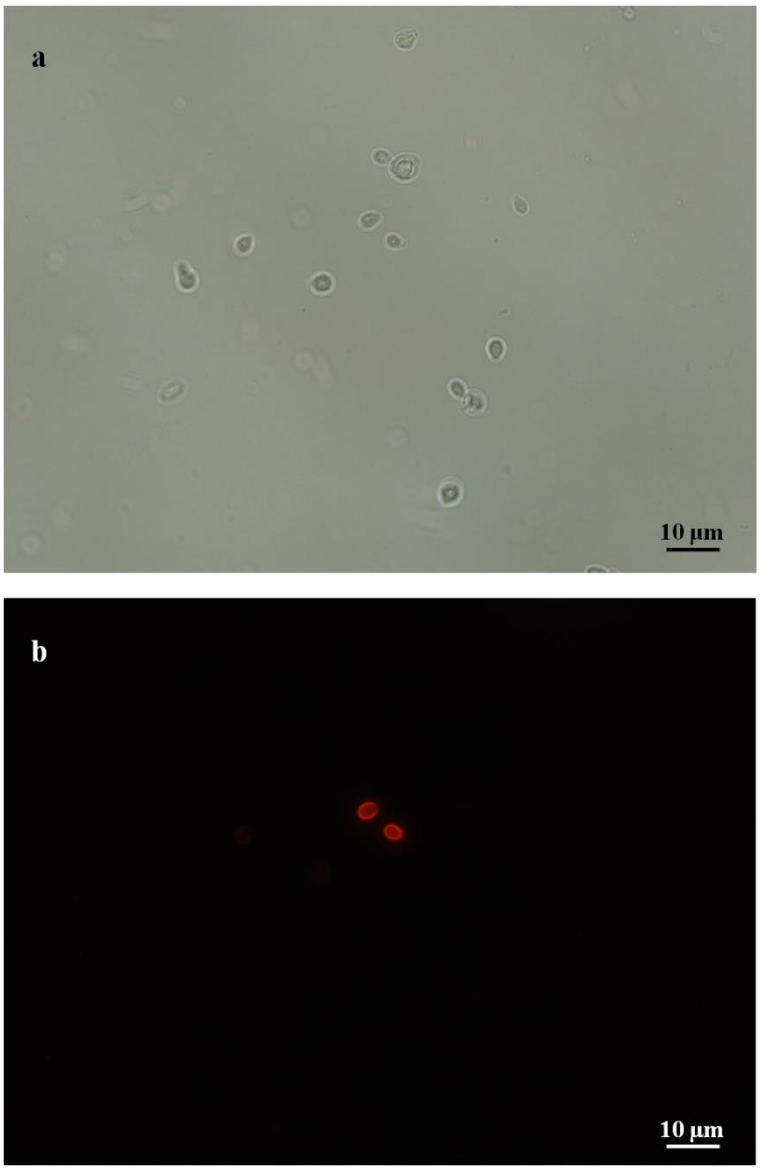

Figure 3.32: Bright field (a) and fluorescence microscopy (b) images of EBY100 cells transformed with pETcon plasmid expressing α-synuclein upon galactose induction.

3.4 Fluorescent Profiles

Fluorescent profiles were formed by using the profile section of Zeiss ZEN microscope software. It measures the fluorescence values through a line between two selected data points.

3.4.1 Fluorescent profile of Htt-25Q

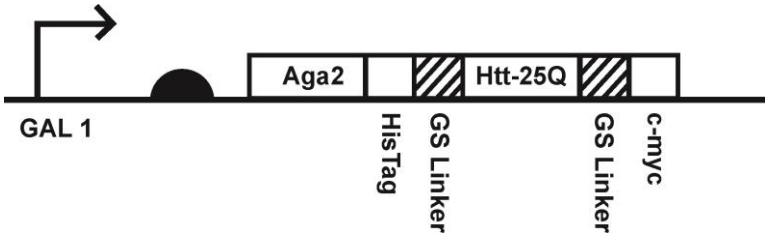

3.33: Linear map demonstrating the parts for the expression of Htt-25Q protein within *Saccharomyces cerevisiae* cells

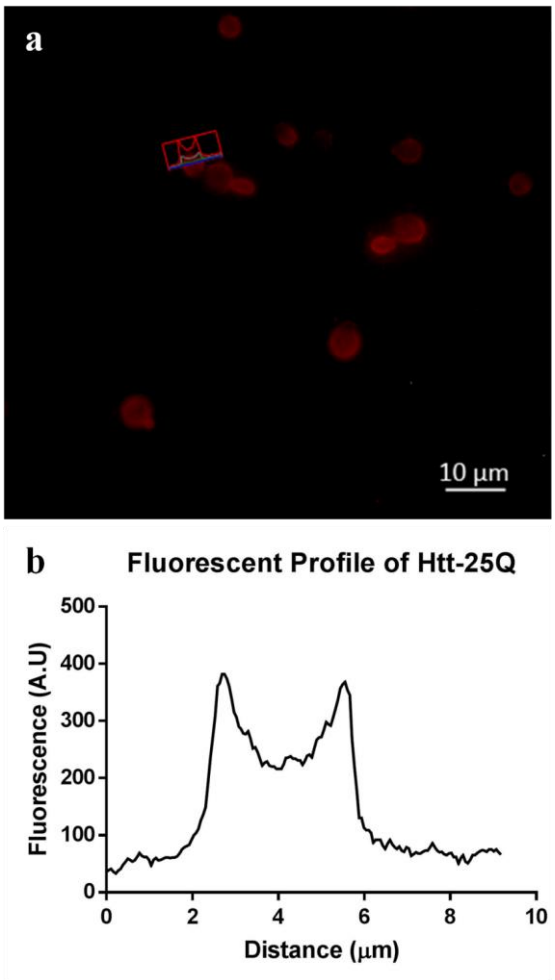

Figure 3.34: Fluorescent profile of EBY100 cells transformed with pETcon plasmid expressing Htt-25Q upon galactose induction. Using the data points on the line indicated (a), graph of the fluorescent profile of data points (b) was drawn.

3.4.2 Fluorescent profile of Htt-46Q

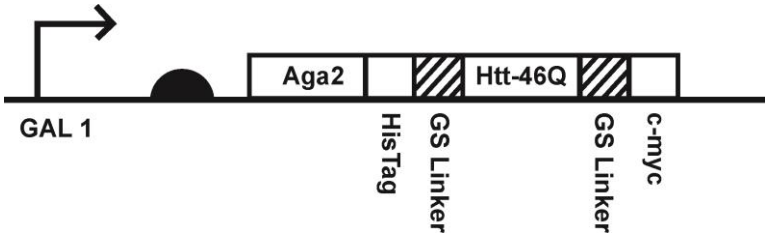

3.35: Linear map demonstrating the parts for the expression of Htt-46Q protein within *Saccharomyces cerevisiae* cells

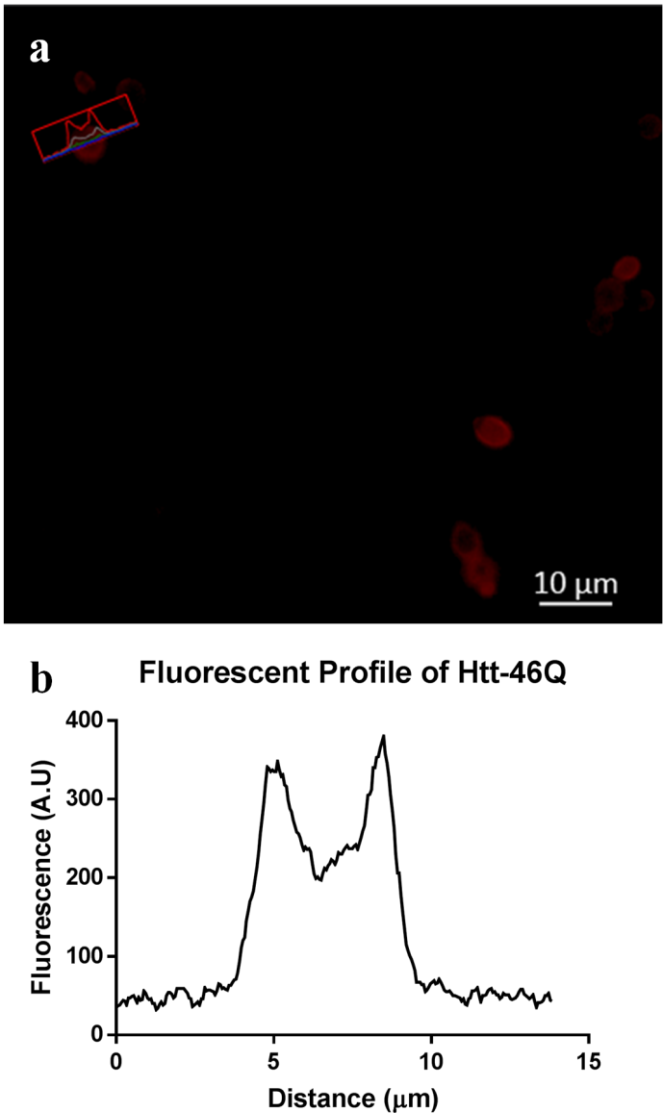

Figure 3.36: Fluorescent profile of EBY100 cells transformed with pETcon plasmid expressing Htt-46Q upon galactose induction. Using the data points on the line indicated (a), graph of the fluorescent profile of data points (b) was drawn.

3.4.3 Fluorescent profile of Htt-103Q

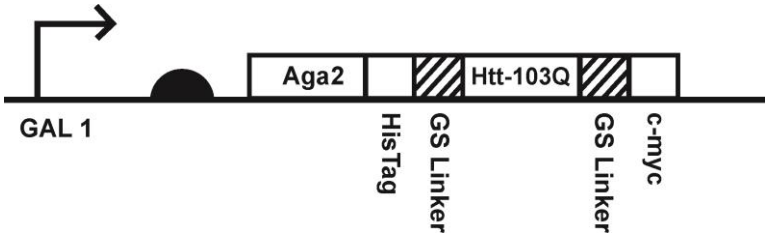

3.37: Linear map demonstrating the parts for the expression of Htt-46Q protein within *Saccharomyces cerevisiae* cells

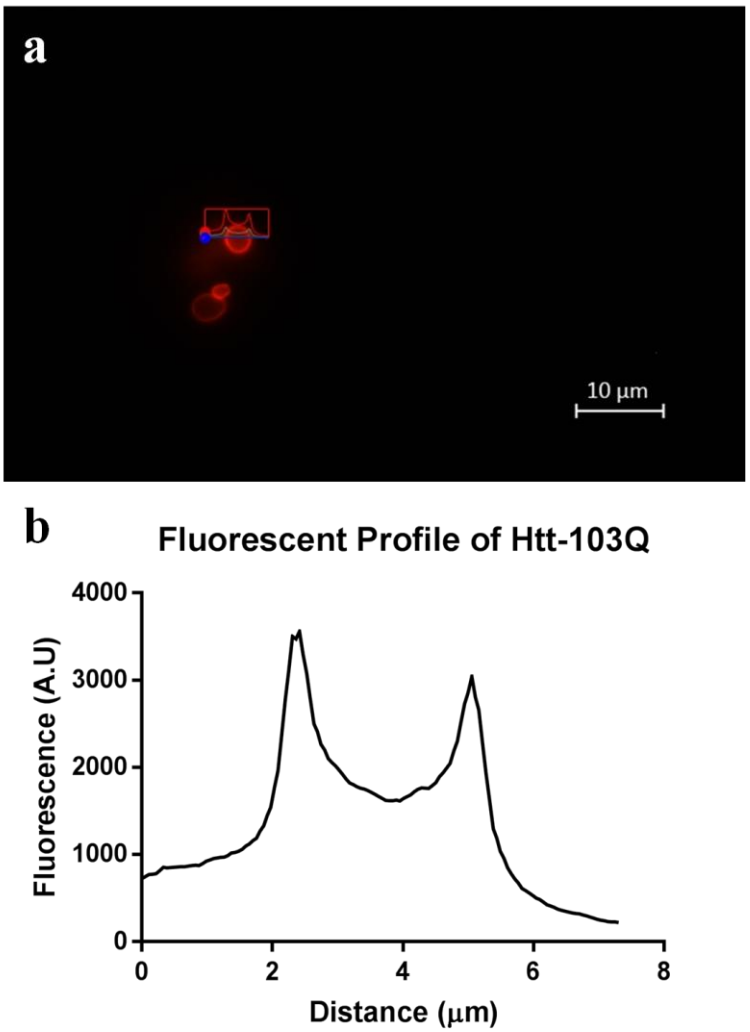

Figure 3.38: Fluorescent profile of EBY100 cells transformed with pETcon plasmid expressing Htt-103Q upon galactose induction. Using the data points on the line indicated (a), graph of the fluorescent profile of data points (b) was drawn

3.4.4 Fluorescent profile of amyloid β 40

3.39: Linear map demonstrating the parts for the expression of $a\beta_{40}$ protein within *Saccharomyces cerevisiae* cells

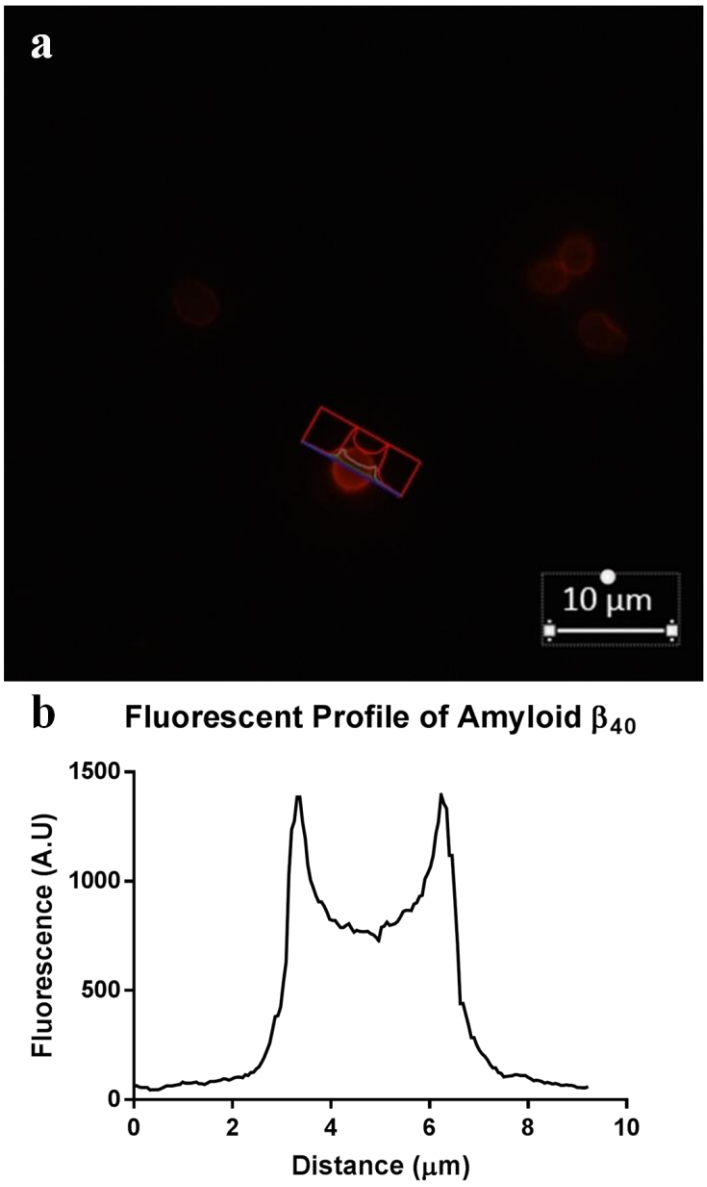

Figure 3.40: Fluorescent profile of EBY100 cells transformed with pETcon plasmid expressing amyloid β_{40} upon galactose induction. Using the data points on the line indicated (a), graph of the fluorescent profile of data points (b) was drawn.

3.4.5 Fluorescent profile of amyloid β 42

3.41: Linear map demonstrating the parts for the expression of aβ$_{42}$ protein within *Saccharomyces cerevisiae* cells

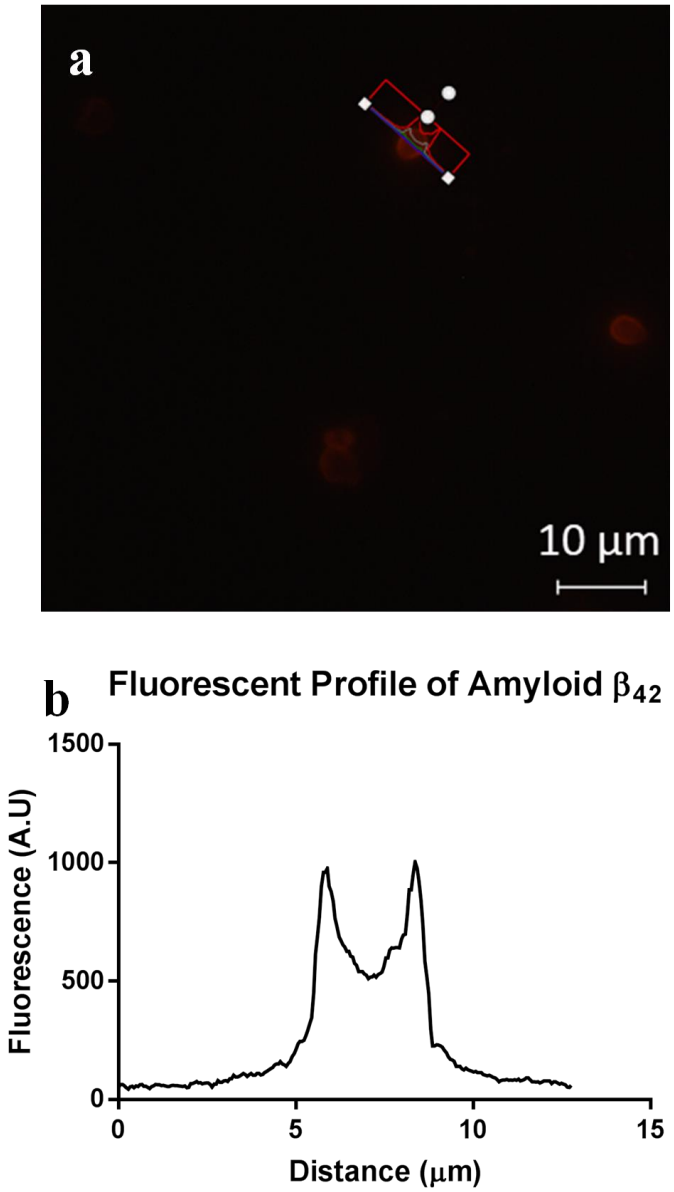

Figure 3.42: Fluorescent profile of EBY100 cells transformed with pETcon plasmid expressing amyloidβ$_{42}$ upon galactose induction. Using the data points on the line indicated (a), graph of the fluorescent profile of data points (b) was drawn.

3.4.6 Fluorescent profile of amyloid β $_{40x2}$

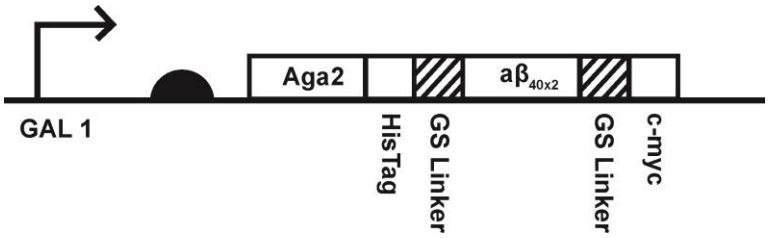

3.43: Linear map demonstrating the parts for the expression of aβ$_{40x2}$ protein within *Saccharomyces cerevisiae* cells

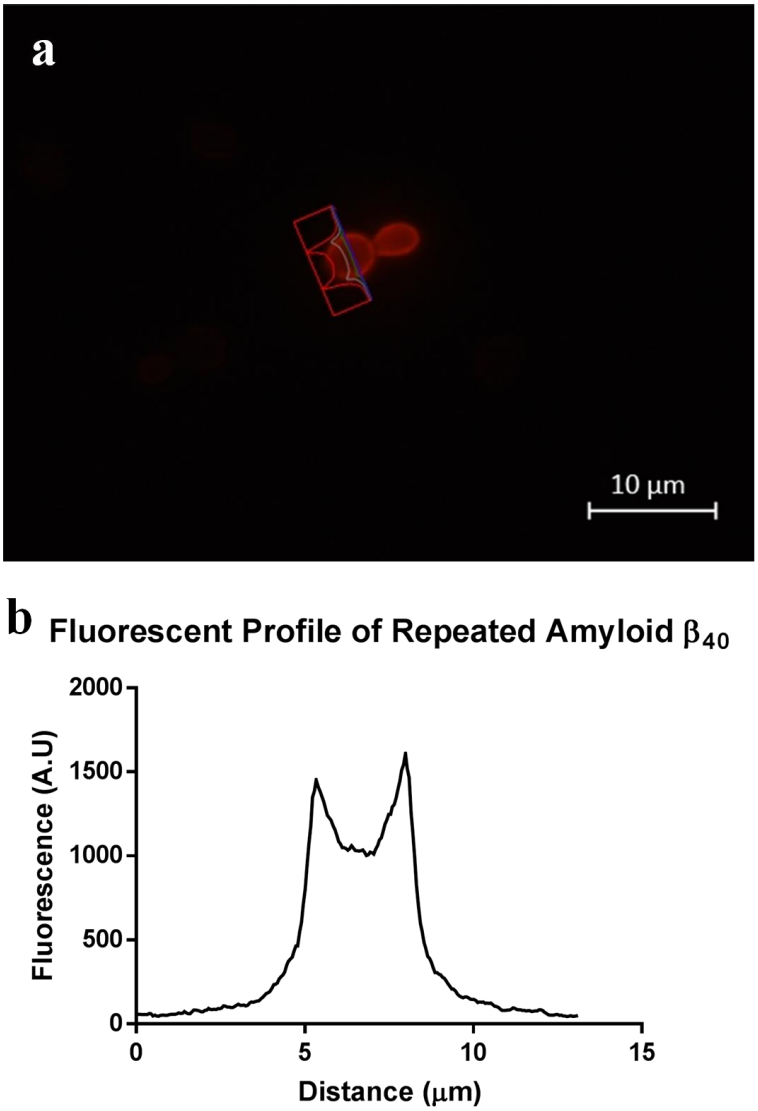

Figure 3.44: Fluorescent profile of EBY100 cells transformed with pETcon plasmid expressing repeated amyloid β40 upon galactose induction. Using the data points on the line indicated (a), graph of the fluorescent profile of data points (b) was drawn.

3.4.7 Fluorescent profile of α-synuclein

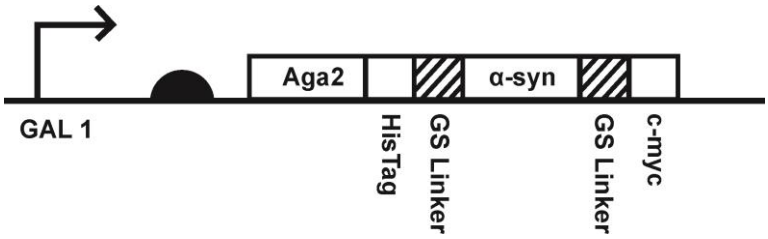

3.45: Linear map demonstrating the parts for the expression of α-synuclein protein within *Saccharomyces cerevisiae* cells

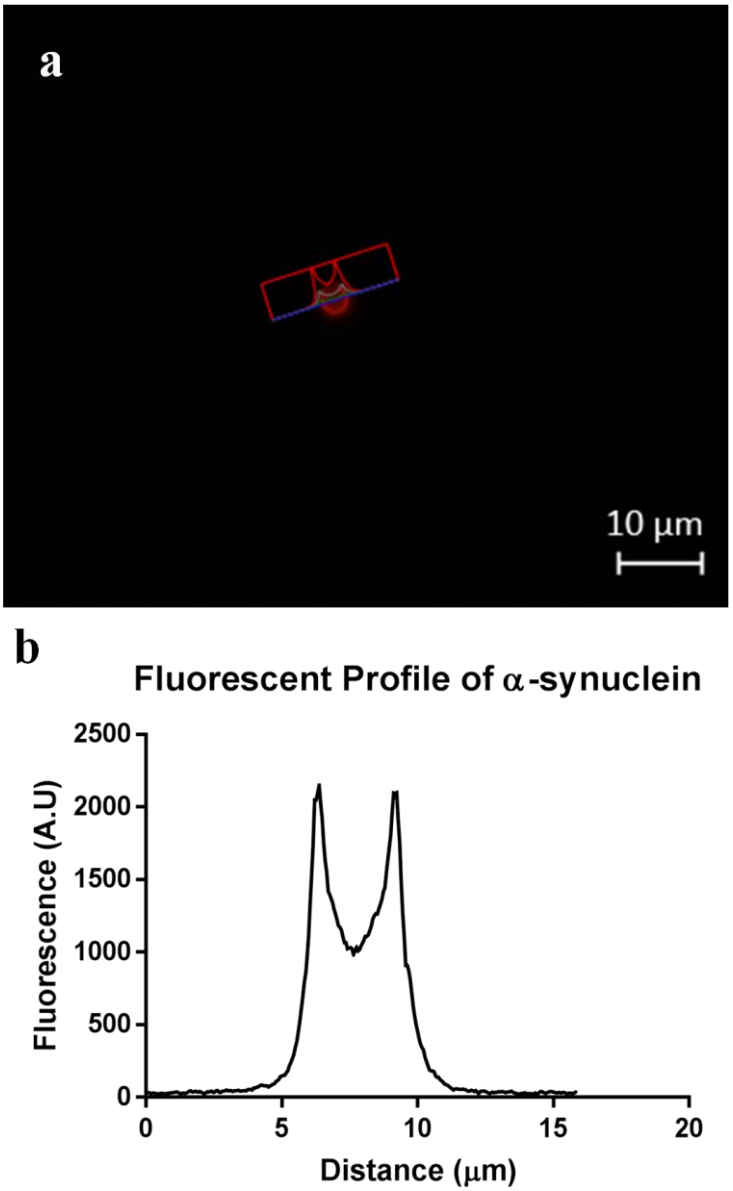

Figure 3.46: Fluorescent profile of EBY100 cells transformed with pETcon plasmid expressing α-synuclein upon galactose induction. Using the data points on the line indicated (a), graph of the fluorescent profile of data points (b) was drawn.

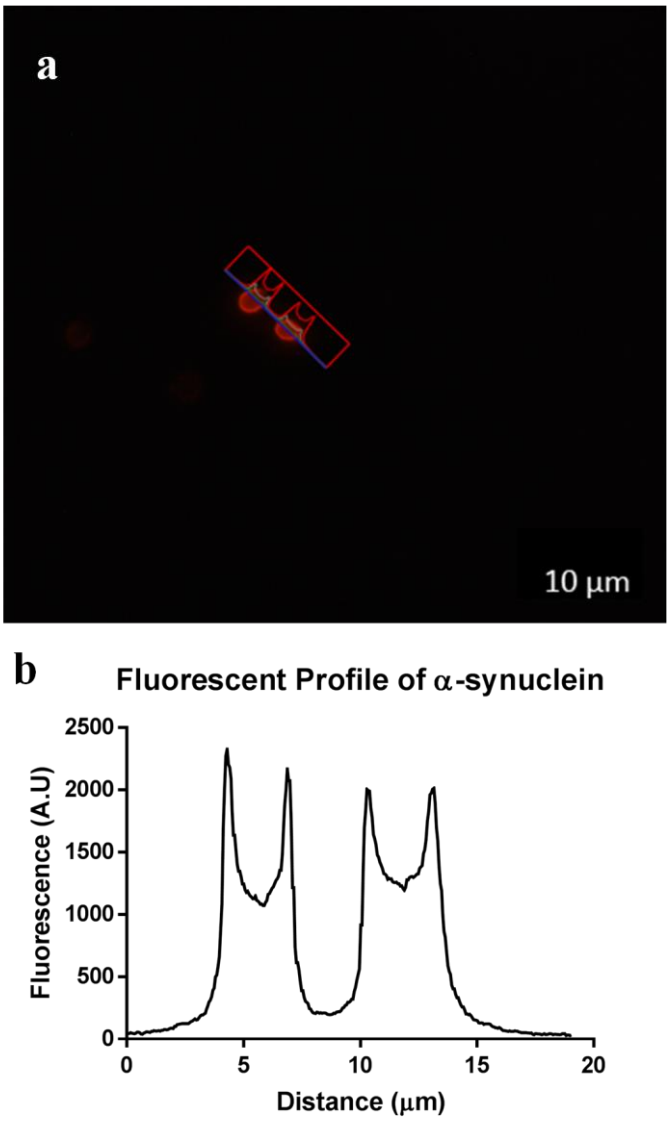

Figure 3.47: Fluorescent profile of EBY100 cells transformed with pETcon plasmid expressing α-synuclein upon galactose induction. Using the data points on the line indicated (a), graph of the fluorescent profile of data points (b) was drawn.

A phage library has been screened against the neurodegenerative proteins on the surface of yeast cells. The purpose is to select the peptides which bind to each neurodegenerative proteins with high affinity. Those peptides are promising drug candidates that can potentially block the neurodegenerative proteins in their monomeric forms and prevent their aggregation. Peptides against Htt-25Q, Htt-46Q and amyloid β_{40} have been selected by Cemile Elif Özçelik as a part of her project.

Peptide against	Amino acid sequence	3D model
25Q-HTT	HSWLGEVLVQNT	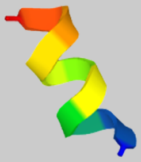
46Q-HTT	DMHGRYMMTTRE	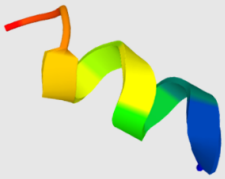
amyloid β_{40}	HLNLNIYITQKH	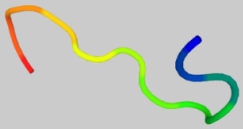

Figure 3.48: The sequences and 3D models of peptides against Htt-25Q, Htt-46Q and amyloid β_{40}.

The sequences encoding these peptides were fused to super folder GFP (sfGFP) sequence with the addition of poly-histidine tag (6xHisTag) and GS linkers in between. sfGFP is a reporter protein to track the surface localization of the selected peptides after incubation with the yeast cells expressing the neurodegenerative proteins on their surfaces. GS linkers lead to proper exposure of the peptide and 6x HisTag. Exposure is crucial since the fusion protein is purified using HisTrap HP histidine-tagged protein purification columns. Also, for the binding assays that are conducted to assess the binding of selected peptides to protein of interest, the peptide sequence should be properly folded and exposed to provide an optimal interaction.

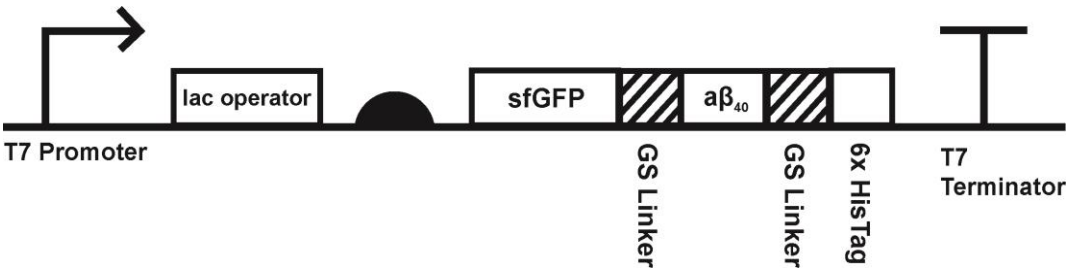

Figure 3.49: Linear map demonstrating the parts for the expression of the selected peptide as a fusion with sfGFP protein on pET22b expression vector and within BL21 cells.

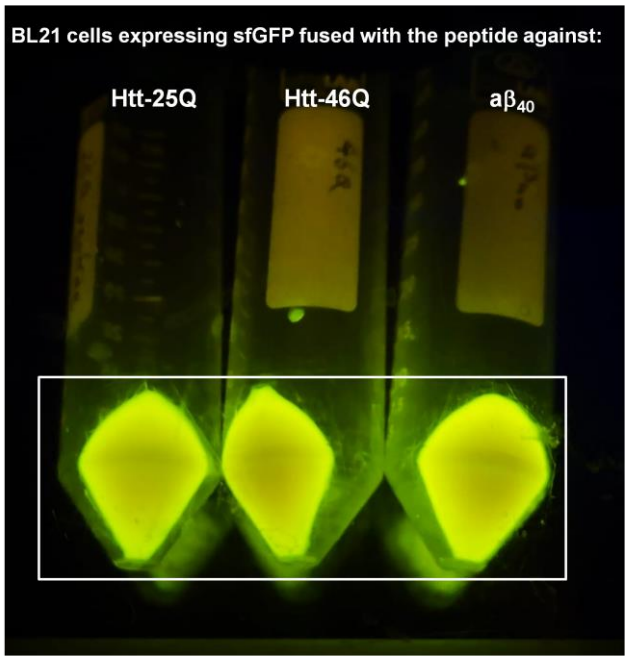

Figure 3.50: Fluorescent signals of the BL21 cell pellets expressing sfGFP fused with the selected peptides against Htt-25Q, Htt-46Q and $a\beta_{40}$ on pET22b vector.

Sequences of peptides against Htt-25Q, Htt-46Q and $a\beta_{40}$ were added to the C-terminal of sfGFP sequence with the addition of GS linker and HisTag. sfGFP with added sequences and pET22b backbone digested with XbaI and XhoI were joined via Gibson assembly reaction at 50^{o}C for 1 hour. Assembly product is transformed into DH5α cells for cloning applications. Eight colonies from each of three clonings were screened via colony PCR using pfu polymerase. 23 colonies out of 24 colonies were successfully transformed. Two colonies that had been successfully transformed were selected for each of three constructs and sent for sequence analysis. Sequences encoding sfGFP-peptide fusion were verified. The peptide against $a\beta_{40}$ was selected for binding experiments.

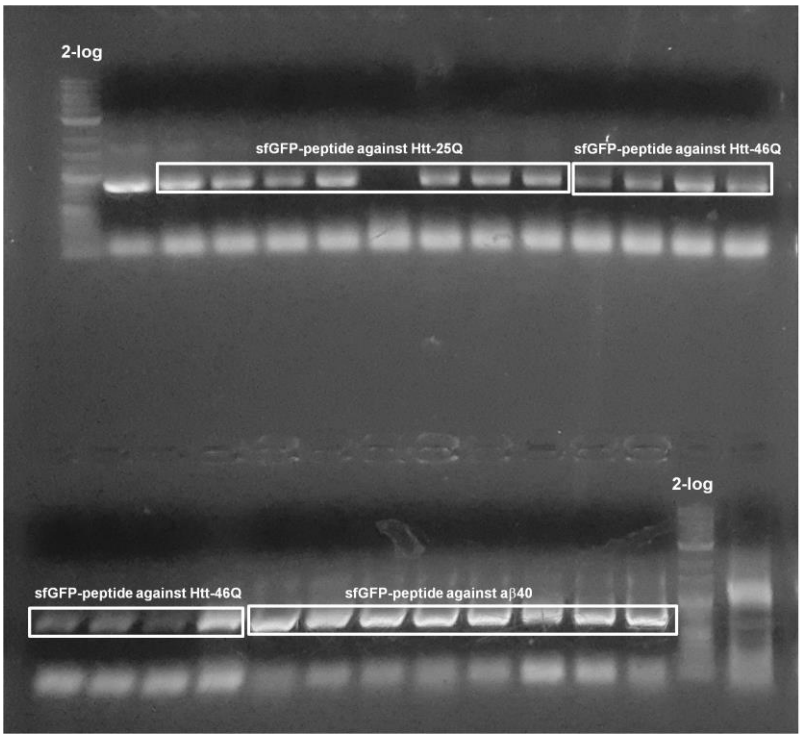

Figure 3.51: Agarose gel showing the result of colony PCR to screen the presence of sfGFP within the transformants.

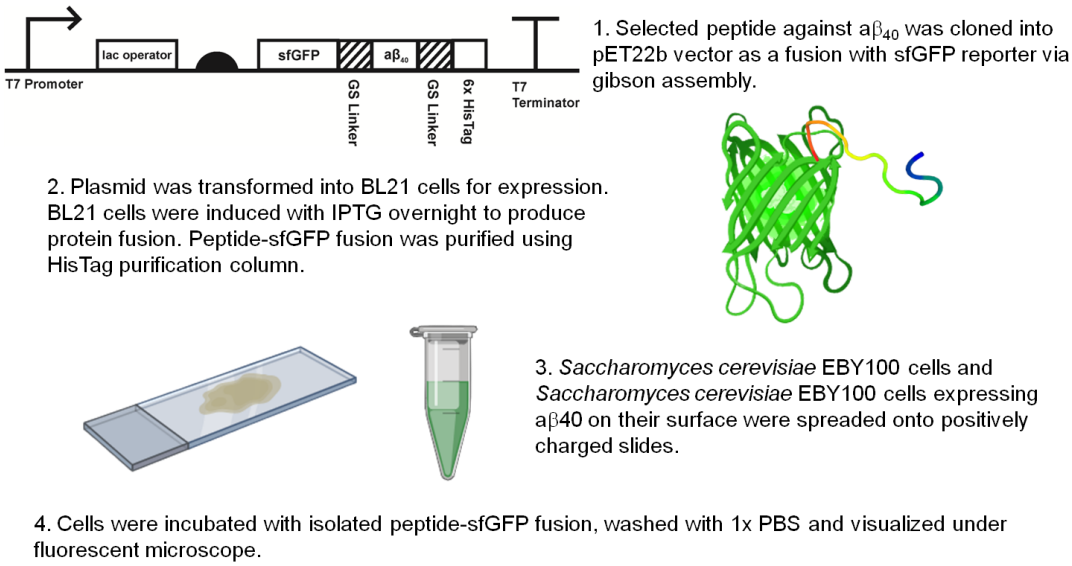

Figure 3.52: A workflow showing the steps of binding assay.

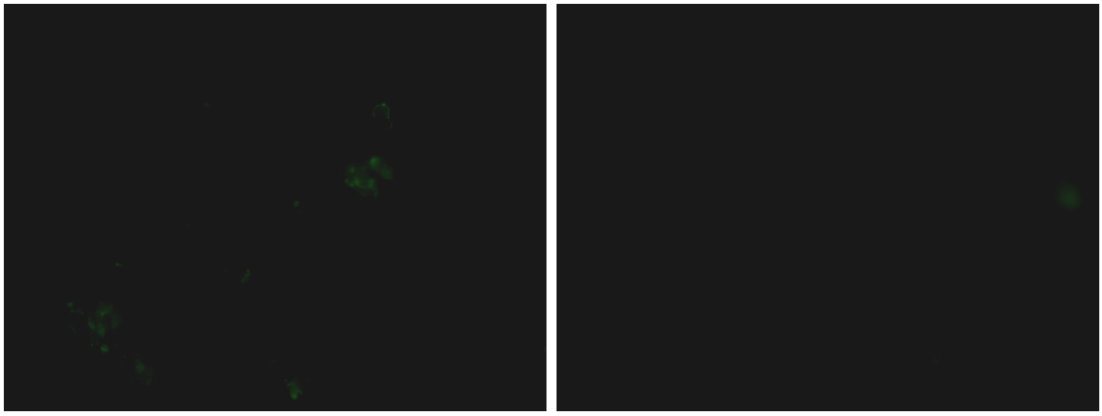

Figure 3.53: The fluorescent microscope images of the slides containing EBY100 cells expressing amyloid β_{40} (sample) and empty EBY100 cells (negative control) both treated with purified fusion protein composed of sfGFP and the peptide against amyloid β_{40}.

Binding assay was performed by incubating *Saccharomyces cerevisiae* EBY100 cells expressing aβ_{40} on their surface and purified sfGFP-peptide against aβ_{40} at room temperature for 2 hours. Skipping the blocking step due to the concern of limiting the interaction might result in some nonspecific bindings and the sfGFP signal in the background. Therefore the assay will be repeated with blocking step prior to the incubation with purified fusion. Proper controls such as isolated sfGFP without peptide will be included in that trial. Incubation time, concentration of purified fusion protein and blocking solution, cell fluency on the slide, blocking time should be optimized carefully. In addition to the trials using yeast cells, purified neurodegenerative proteins can be used in the quartz crystal microbalance (QCM) analysis conducted with the purified selected peptide-sfGFP fusion. More than one peptide can be included for the same neurodegenerative protein to select the one with the highest affinity.

The peptides being discovered after several selection processes and binding assays will be promising drug candidates for neurodegenerative diseases. They can be delivered to the brain via viral mediated delivery using AAV9 because of its safe profile and the ability to cross blood brain barrier. Peptides against more toxic forms of the proteins such as Htt-46Q, Htt-103Q and aβ_{42} can be incubated with cells expressing less toxic or non-toxic forms such as Htt-25Q and aβ_{42}. Using the ones that bind to more toxic form rather than less toxic form is feasible since the effect of blocking the less toxic or non-toxic forms within the cell is not clear and might result

in adverse effects due to the known and unknown functions of the proteins within the cells. In addition to the possible therapeutic effects, these peptides may also display some neuroprotective features before the disease is developed. Additionally, they can be applied in the early phases of the disease to prevent aggregation. Since aggregation is mostly a rapid process, some neuroprotective and neurorestorative precautions coupled with the peptides will be effective. Biomolecules such as neurotrophic factors and growth factors that support neurogenesis and growth of neurons might be efficient interventions.

The effect of neurodegenerative proteins on the aggregation can be monitored under microscope by tracking inclusion bodies or using scanning electron microscope to track fibrous structures. By doing so, the effect of the peptides can also be assessed to understand whether they prevent aggregation or contribute to accumulation of neurodegenerative proteins by acting as a linker. Additionally, binding assays might fail not because the peptides do not bind to the neurodegenerative proteins, but they are not exposed enough to interact with them. As a solution for this problem, GS linker regions can be expanded.

3.5 Genome Integration Cassette

Tablo 3.1: A table indicating the presence or absence of the restriction sites within yeast parts. '-' stands for the absence, and the numbers indicating the number of the restriction sites within corresponding part. '*' shows that the restriction site is absent in the sequence the part, but it is present within the 100 bp flanking regions of that part.

	LEU2	HIS3	TRP1	URA3	eGFP	ADH1	pTDH3	mOrange
AatII	-	-	-	-	-	-	-	-
BamHI	-	-	-	-	-	-	-	-
BglII	-	2	1*	-	-	-	-	-
EcoRI	-	-	1*	-	-	-	-	-
HindIII	-	2	1	-	-	-	-	-
KpnI	-	1	-	-	-	-	-	-
MluI	-	-	-	-	-	-	-	-
NcoI	-	-	-	1	1	-	-	-
NotI	-	-	-	-	-	-	-	-
PstI	-	-	1*	-	-	-	-	-
SpeI	-	-	-	-	-	-	-	-
XbaI	-	-	-	1	-	-	-	-
XhoI	-	-	-	-	-	-	-	-

To standardise genome manipulation experiments, it has been aimed to construct a cassette that can be used for integration and deletion. Based on the study in which

Lee and colleagues have assembled several yeast parts from a collection using golden gate assembly technique [132], the purpose of this part of the thesis is to construct a cassette with yeast parts that are available in our laboratory. The favorable side of the cassette that is cloned into a plasmid is that each part can be replaced with another by digesting the vector with the enzymes flanking that part. To do so, restriction enzymes should be carefully chosen to not digest the sequences of the parts. Therefore, a table was formed to see the presence of restriction sites within the parts that were available. LEU2, HIS3, TRP1 and URA3 are auxotrophic markers that can be obtained from shuttle vectors such as pETcon and pML107 and from the genome of *Saccharomyces cerevisiae* strains such as BY4742, BY4743 and EBY100. eGFP and mOrange are fluorescent reporters. pTDH3 is a strong promoter and ADH1 is a terminator.

To target a genomic locus, integration cassette can be amplified by adding homologous regions to the target site. Once they find sufficient homology, yeast cells are capable of using homologous recombination mechanism. It has been showed that 40-50 bp homology is enough; however, longer homology provides more precise targeting.

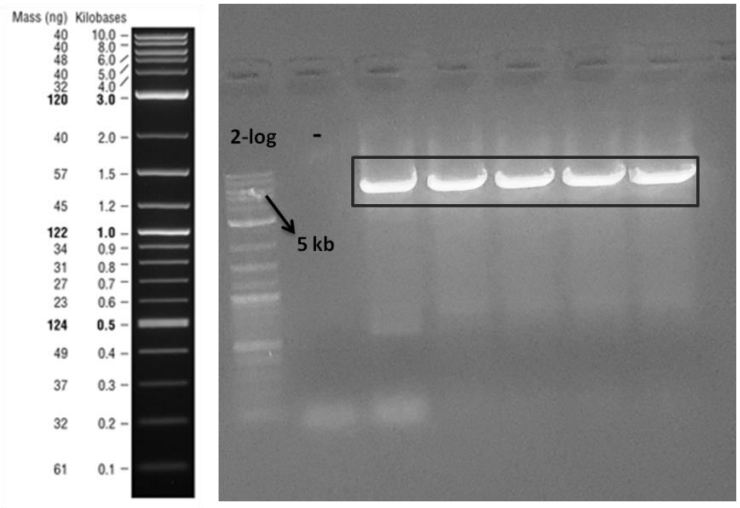

Figure 3.54: Agarose gel image of the result of PCR to obtain a backbone without any yeast marker to clone gene integration cassette. Expected band length: 5.2 kb

lane 1: NEB 2-log ladder; lane 2: negative control, lane 3-7: PCR products

TRP1 marker has been removed from the backbone since TRP1 could be a target to delete or marker to be integrated in the next trials. To delete TRP1 gene, backbone was amplified from both sides of the gene with the addition of AflII restriction site. Following amplification, the PCR product was digested with AflII and ligated on itself.

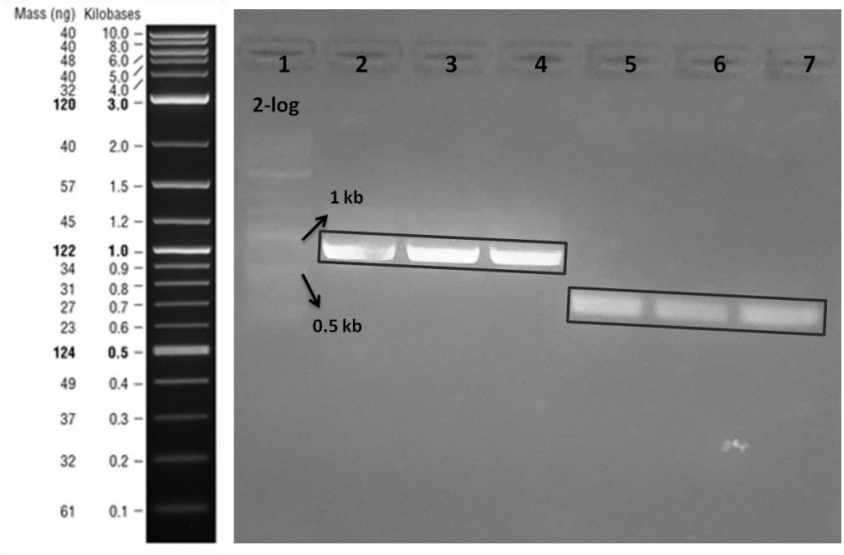

Figure 3.55: Agarose gel image showing the results of PCR amplifying pTDH3 promoter (lane 2-4) and ADH1 terminator (lane 5-7). Expected band length for pTDH3 is 750 bp, for ADH1 is 250 bp.

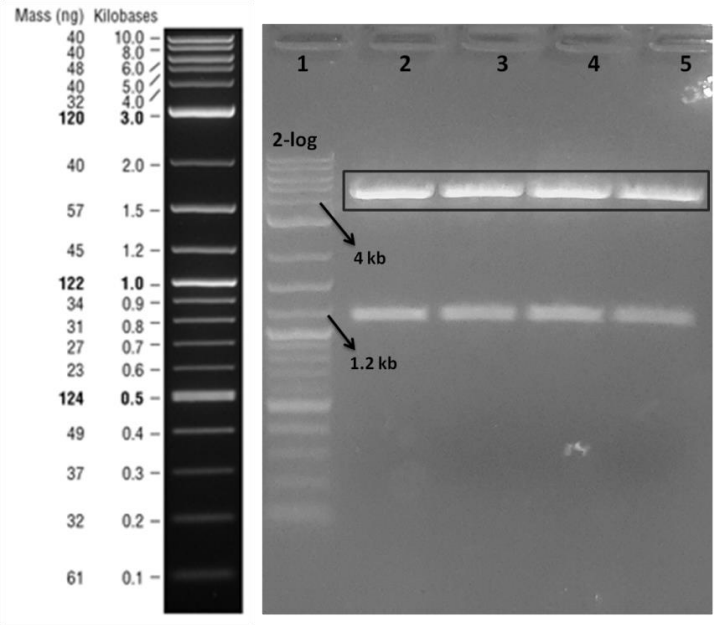

Figure 3.56:Agarose gel image showing the result of restriction enzyme digestion reaction with Acc65I and XhoI to clone pTDH3 and LEU2 marker after the successful cloning of ADH1 terminator. Expected band lengths: 4.1 kb and 1.1 kb.

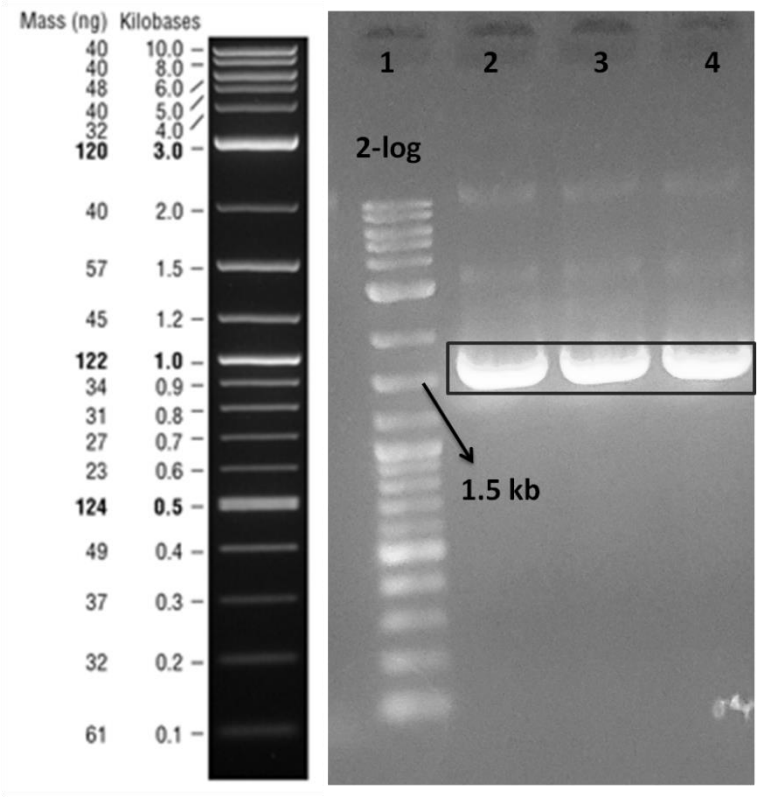

Figure 3.57:Agarose gel image showing the result of polymerase chain reaction that amplify LEU2 marker from pML107 plasmid to be cloned into genome integration cassette. Expected band length: 1.6 kb.

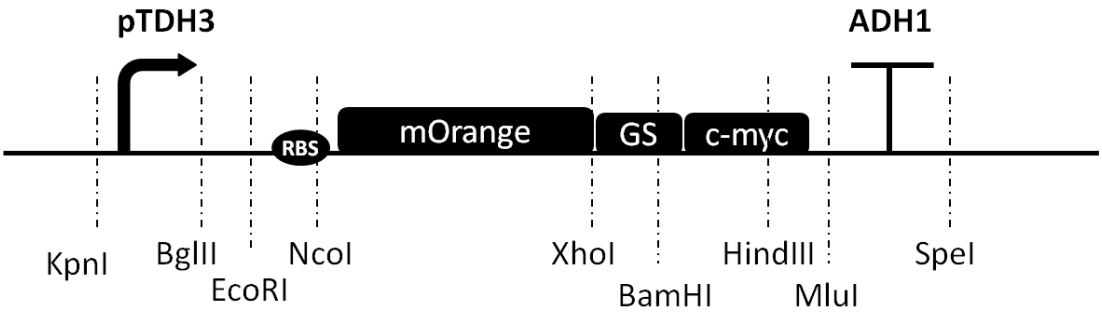

Figure 3.58: Schematic representation of genome integration cassette containing mOrange as the selection marker with the other parts and restriction sites.

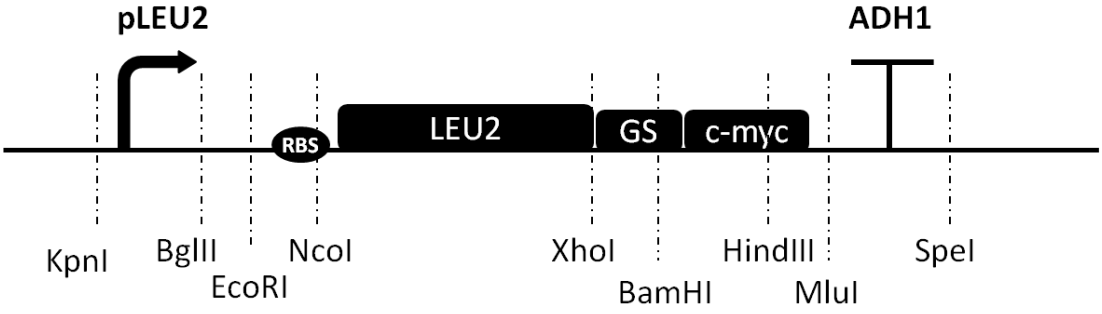

Figure 3.59: Schematic representation of genome integration cassette containing LEU2 as the selection marker with the other parts and restriction sites.

4 CONCLUSION AND FUTURE PERSPECTIVES

The purpose of this study to discover ligands that can potentially block the monomeric forms of neurodegenerative proteins before the aggregation takes place. The protein targets in this study are amyloid β, α-synuclein and mutant huntingtin that are found in toxic accumulations causing neurodegeneration in Alzheirmer's Disease, Parkinson's Disease and Huntington's Disease. To assess the differences in propensity to form aggregates, some variations of the proteins are also included such as repeated amyloid β40, repeated amyloid β42, and mutant huntingtin protein with varying polyglutamine repeat size.

Most of the current therapeutic interventions target the toxic accumulations and focus on their clearance after aggregation takes place. Additionally, another concern of the existing therapies is to support the healthy neurons in the diseased region. Although these approaches slow down the neurodegeneration, result in symptomatic relief and provide neuroprotection and neurorestoration, they are insufficient to solve the underlying factors of the aggregation. This study possesses novel characteristics considering the targeting of the monomeric and small oligomeric structures that are involved in the propagation of aggregates.

To study neurodegenerative proteins as monomeric structures, yeast surface display has been used. Yeast cells are convenient organisms to study human proteins since they have eukaryotic protein translation and secretion systems and quality check mechanisms. Fusing neurodegenerative proteins to the Aga2 which is a surface protein involved in cell adhesion during yeast mating result in display of immobile and exposed proteins on the surface of *Saccharomyces cerevisiae* cells.

The hypothesis is based on the potential of peptides that bind to the monomeric forms of neurodegenerative proteins with high affinity to prevent aggregation. To select the binding peptides, a phage display library has been screened against neurodegenerative proteins displayed on the yeast surface. Due to the large library size, phage display is a suitable tool to discover novel peptides.

Following selection of peptides against neurodegenerative proteins, in vitro binding assays will be conducted. Binding kinetics will be studied using quartz crystal microbalance (QCM). The blocking capacity of selected peptides will be observed within neural cell line in vitro. In vivo animal experiments can be conducted with peptides that bind to the neurodegenerative proteins with high affinity. Moreover, selected peptide-neurodegenerative protein interactions enable the development of a biosensor system. As drug candidates and recognition units of a biosensor, selected peptides are highly promising for the diagnosis and the treatment of the neurodegenerative diseases.

5 BIBLIOGRAPHY

1. Gao, H.M. and J.S. Hong, *Why neurodegenerative diseases are progressive: uncontrolled inflammation drives disease progression.* Trends Immunol, 2008. **29**(8): p. 357-65.
2. Metcalfe, S.M., S. Bickerton, and T. Fahmy, *Neurodegenerative Disease: A Perspective on Cell-Based Therapy in the New Era of Cell-Free Nano-Therapy.* Curr Pharm Des, 2017. **23**(5): p. 776-783.
3. Josephs, K.A., et al., *Rapidly progressive neurodegenerative dementias.* Archives of neurology, 2009. **66**(2): p. 201-207.
4. Halliwell, B., *Role of Free Radicals in the Neurodegenerative Diseases.* Drugs & Aging, 2001. **18**(9): p. 685-716.
5. Wyss-Coray, T. and L. Mucke, *Inflammation in neurodegenerative disease—a double-edged sword.* Neuron, 2002. **35**(3): p. 419-432.
6. Lin, M.T. and M.F. Beal, *Mitochondrial dysfunction and oxidative stress in neurodegenerative diseases.* Nature, 2006. **443**(7113): p. 787.
7. Hetz, C. and B. Mollereau, *Disturbance of endoplasmic reticulum proteostasis in neurodegenerative diseases.* Nature Reviews Neuroscience, 2014. **15**(4): p. 233.
8. Sudhakar, V. and R.M. Richardson, *Gene Therapy for Neurodegenerative Diseases.* Neurotherapeutics, 2019. **16**(1): p. 166-175.
9. Soto, C. and S. Pritzkow, *Protein misfolding, aggregation, and conformational strains in neurodegenerative diseases.* Nature neuroscience, 2018: p. 1.
10. Katsnelson, A., B. De Strooper, and H.Y. Zoghbi, *Neurodegeneration: From cellular concepts to clinical applications.* Sci Transl Med, 2016. **8**(364): p. 364ps18.
11. Agustín- Pavón, C. and M. Isalan, *Synthetic biology and therapeutic strategies for the degenerating brain: Synthetic biology approaches can transform classical cell and gene therapies, to provide new cures for neurodegenerative diseases.* Bioessays, 2014. **36**(10): p. 979-990.
12. Brundin, P., R. Melki, and R. Kopito, *Prion-like transmission of protein aggregates in neurodegenerative diseases.* Nature reviews Molecular cell biology, 2010. **11**(4): p. 301.
13. Soto, C. and S. Pritzkow, *Protein misfolding, aggregation, and conformational strains in neurodegenerative diseases.* Nat Neurosci, 2018. **21**(10): p. 1332-1340.
14. Esler, W.P., et al., *Alzheimer's disease amyloid propagation by a template-dependent dock-lock mechanism.* Biochemistry, 2000. **39**(21): p. 6288-6295.
15. Reddy, G., J.E. Straub, and D. Thirumalai, *Dynamics of locking of peptides onto growing amyloid fibrils.* Proceedings of the National Academy of Sciences, 2009. **106**(29): p. 11948-11953.
16. Jarrett, J.T. and P.T. Lansbury Jr, *Seeding "one-dimensional crystallization" of amyloid: a pathogenic mechanism in Alzheimer's disease and scrapie?* Cell, 1993. **73**(6): p. 1055-1058.
17. Soto, C., L. Estrada, and J. Castilla, *Amyloids, prions and the inherent infectious nature of misfolded protein aggregates.* Trends in biochemical sciences, 2006. **31**(3): p. 150-155.
18. Abounit, S., et al., *Tunneling nanotubes: A possible highway in the spreading of tau and other prion-like proteins in neurodegenerative diseases.* Prion, 2016. **10**(5): p. 344-351.
19. Mohamed, N.V., et al., *Spreading of tau pathology in A lzheimer's disease by cell- to- cell transmission.* European Journal of Neuroscience, 2013. **37**(12): p. 1939-1948.

20. Costanzo, M. and C. Zurzolo, *The cell biology of prion-like spread of protein aggregates: mechanisms and implication in neurodegeneration.* Biochemical Journal, 2013. **452**(1): p. 1-17.
21. Danzer, K.M., et al., *Exosomal cell-to-cell transmission of alpha synuclein oligomers.* Molecular neurodegeneration, 2012. **7**(1): p. 42.
22. Chung, S., et al., *Genetic engineering of mouse embryonic stem cells by Nurr1 enhances differentiation and maturation into dopaminergic neurons.* European Journal of Neuroscience, 2002. **16**(10): p. 1829-1838.
23. Podlesniy, P. and R. Trullas, *Biomarkers in Cerebrospinal Fluid: Analysis of Cell-Free Circulating Mitochondrial DNA by Digital PCR,* in *Digital PCR: Methods and Protocols,* G. Karlin-Neumann and F. Bizouarn, Editors. 2018, Springer New York: New York, NY. p. 111-126.
24. Pollitt, S.K., et al., *A rapid cellular FRET assay of polyglutamine aggregation identifies a novel inhibitor.* Neuron, 2003. **40**(4): p. 685-94.
25. Holmes, B.B. and M.I. Diamond, *Cellular Models for the Study of Prions.* Cold Spring Harb Perspect Med, 2017. **7**(2).
26. Holmes, B.B., et al., *Proteopathic tau seeding predicts tauopathy in vivo.* Proceedings of the National Academy of Sciences, 2014. **111**(41): p. E4376-E4385.
27. Newby, G.A., et al., *A Genetic Tool to Track Protein Aggregates and Control Prion Inheritance.* Cell, 2017. **171**(4): p. 966-979.e18.
28. Bobo, R.H., et al., *Convection-enhanced delivery of macromolecules in the brain.* Proceedings of the National Academy of Sciences, 1994. **91**(6): p. 2076-2080.
29. Richardson, R.M., et al., *Novel platform for MRI-guided convection-enhanced delivery of therapeutics: preclinical validation in nonhuman primate brain.* Stereotact Funct Neurosurg, 2011. **89**(3): p. 141-51.
30. Mittermeyer, G., et al., *Long-term evaluation of a phase 1 study of AADC gene therapy for Parkinson's disease.* Hum Gene Ther, 2012. **23**(4): p. 377-81.
31. O'Connor, D.M. and N.M. Boulis, *Gene therapy for neurodegenerative diseases.* Trends Mol Med, 2015. **21**(8): p. 504-12.
32. Wang, L., et al., *In vivo delivery systems for therapeutic genome editing.* International journal of molecular sciences, 2016. **17**(5): p. 626.
33. Davis, M.E., *Non-viral gene delivery systems.* Current opinion in biotechnology, 2002. **13**(2): p. 128-131.
34. Yin, H., et al., *Non-viral vectors for gene-based therapy.* Nature Reviews Genetics, 2014. **15**(8): p. 541.
35. Graham, F.L. and L. Prevec, *Methods for construction of adenovirus vectors.* Molecular biotechnology, 1995. **3**(3): p. 207-220.
36. Liu, J. and S.-l. Shui, *Delivery methods for site-specific nucleases: Achieving the full potential of therapeutic gene editing.* Journal of Controlled Release, 2016. **244**: p. 83-97.
37. Howe, S.J., et al., *Insertional mutagenesis combined with acquired somatic mutations causes leukemogenesis following gene therapy of SCID-X1 patients.* The Journal of clinical investigation, 2008. **118**(9).
38. Kreppel, F. and S. Kochanek, *Modification of adenovirus gene transfer vectors with synthetic polymers: a scientific review and technical guide.* Molecular Therapy, 2008. **16**(1): p. 16-29.
39. Hardee, C., et al., *Advances in non-viral DNA vectors for gene therapy.* Genes, 2017. **8**(2): p. 65.
40. Duque, S., et al., *Intravenous administration of self-complementary AAV9 enables transgene delivery to adult motor neurons.* Molecular Therapy, 2009. **17**(7): p. 1187-1196.
41. Fjord-Larsen, L., et al., *Increased encapsulated cell biodelivery of nerve growth factor in the brain by transposon-mediated gene transfer.* Gene therapy, 2012. **19**(10): p. 1010.

42. Wahlberg, L.U., et al., *Targeted delivery of nerve growth factor via encapsulated cell biodelivery in Alzheimer disease: a technology platform for restorative neurosurgery.* Journal of neurosurgery, 2012. **117**(2): p. 340-347.
43. Kim, S.U. and J. de Vellis, *Stem cell-based cell therapy in neurological diseases: a review.* J Neurosci Res, 2009. **87**(10): p. 2183-200.
44. Dunn, K., et al., *ARPE-19, a human retinal pigment epithelial cell line with differentiated properties.* Experimental eye research, 1996. **62**(2): p. 155-170.
45. Renfranz, P.J., M.G. Cunningham, and R.D. McKay, *Region-specific differentiation of the hippocampal stem cell line HiB5 upon implantation into the developing mammalian brain.* Cell, 1991. **66**(4): p. 713-729.
46. Flax, J.D., et al., *Engraftable human neural stem cells respond to development cues, replace neurons, and express foreign genes.* Nature biotechnology, 1998. **16**(11): p. 1033.
47. Kim, S.U., *Human neural stem cells genetically modified for brain repair in neurological disorders.* Neuropathology, 2004. **24**(3): p. 159-171.
48. Hwang, D., et al., *Intrathecal transplantation of human neural stem cells overexpressing VEGF provide behavioral improvement, disease onset delay and survival extension in transgenic ALS mice.* Gene therapy, 2009. **16**(10): p. 1234.
49. Biffi, A., et al., *Lentiviral hematopoietic stem cell gene therapy benefits metachromatic leukodystrophy.* Science, 2013. **341**(6148): p. 1233158.
50. Gatz, M., et al., *Role of genes and environments for explaining Alzheimer disease.* Archives of general psychiatry, 2006. **63**(2): p. 168-174.
51. Piaceri, I., B. Nacmias, and S. Sorbi, *Genetics of familial and sporadic Alzheimer's disease.* Front Biosci (Elite Ed), 2013. **5**: p. 167-77.
52. Rafii, M.S., et al., *Adeno-Associated Viral Vector (Serotype 2)-Nerve Growth Factor for Patients With Alzheimer Disease: A Randomized Clinical Trial.* JAMA Neurol, 2018. **75**(7): p. 834-841.
53. Rafii, M.S., et al., *A phase1 study of stereotactic gene delivery of AAV2-NGF for Alzheimer's disease.* Alzheimer's & Dementia, 2014. **10**(5): p. 571-581.
54. Saadoun, D., et al., *Regulatory T-cell responses to low-dose interleukin-2 in HCV-induced vasculitis.* N Engl J Med, 2011. **365**(22): p. 2067-77.
55. Alves, S., et al., *Interleukin-2 improves amyloid pathology, synaptic failure and memory in Alzheimer's disease mice.* Brain, 2017. **140**(3): p. 826-842.
56. Sud, R., E.T. Geller, and G.D. Schellenberg, *Antisense-mediated exon skipping decreases tau protein expression: a potential therapy for tauopathies.* Molecular Therapy-Nucleic Acids, 2014. **3**: p. e180.
57. Oddo, S., et al., *Triple-transgenic model of Alzheimer's disease with plaques and tangles: intracellular Abeta and synaptic dysfunction.* Neuron, 2003. **39**(3): p. 409-21.
58. Murphy, S.R., et al., *Acat1 knockdown gene therapy decreases amyloid-beta in a mouse model of Alzheimer's disease.* Mol Ther, 2013. **21**(8): p. 1497-506.
59. Carty, N., et al., *Intracranial injection of AAV expressing NEP but not IDE reduces amyloid pathology in APP+PS1 transgenic mice.* PLoS One, 2013. **8**(3): p. e59626.
60. Iwata, N., et al., *Global brain delivery of neprilysin gene by intravascular administration of AAV vector in mice.* Scientific reports, 2013. **3**: p. 1472.
61. Pascual- Lucas, M., et al., *Insulin- like growth factor 2 reverses memory and synaptic deficits in APP transgenic mice.* EMBO molecular medicine, 2014. **6**(10): p. 1246-1262.
62. Revilla, S., et al., *Lenti- GDNF gene therapy protects against Alzheimer's disease- like neuropathology in 3xTg- AD mice and MC65 cells.* CNS neuroscience & therapeutics, 2014. **20**(11): p. 961-972.
63. Perry, T. and N.H. Greig, *The glucagon-like peptides: a new genre in therapeutic targets for intervention in Alzheimer's disease.* Journal of Alzheimer's Disease, 2002. **4**(6): p. 487-496.

64. Perry, T., et al., *Glucagon‐like peptide‐1 decreases endogenous amyloid‐β peptide (Aβ) levels and protects hippocampal neurons from death induced by Aβ and iron.* Journal of neuroscience research, 2003. **72**(5): p. 603-612.
65. Perry, T., et al., *Protection and reversal of excitotoxic neuronal damage by glucagon-like peptide-1 and exendin-4.* Journal of Pharmacology and Experimental Therapeutics, 2002. **302**(3): p. 881-888.
66. Klinge, P.M., et al., *Encapsulated native and glucagon-like peptide-1 transfected human mesenchymal stem cells in a transgenic mouse model of Alzheimer's disease.* Neuroscience letters, 2011. **497**(1): p. 6-10.
67. Spuch, C., et al., *The effect of encapsulated VEGF-secreting cells on brain amyloid load and behavioral impairment in a mouse model of Alzheimer's disease.* Biomaterials, 2010. **31**(21): p. 5608-5618.
68. Garcia, P., et al., *Ciliary neurotrophic factor cell-based delivery prevents synaptic impairment and improves memory in mouse models of Alzheimer's disease.* Journal of Neuroscience, 2010. **30**(22): p. 7516-7527.
69. Dauer, W. and S. Przedborski, *Parkinson's disease: mechanisms and models.* neuron, 2003. **39**(6): p. 889-909.
70. Spillantini, M.G., et al., *α-Synuclein in filamentous inclusions of Lewy bodies from Parkinson's disease and dementia with Lewy bodies.* Proceedings of the National Academy of Sciences, 1998. **95**(11): p. 6469-6473.
71. Fasano, A., et al., *Axial disability and deep brain stimulation in patients with Parkinson disease.* Nat Rev Neurol, 2015. **11**(2): p. 98-110.
72. Bankiewicz, K.S., et al., *Long-term clinical improvement in MPTP-lesioned primates after gene therapy with AAV-hAADC.* Molecular Therapy, 2006. **14**(4): p. 564-570.
73. Hadaczek, P., et al., *Eight years of clinical improvement in MPTP-lesioned primates after gene therapy with AAV2-hAADC.* Molecular Therapy, 2010. **18**(8): p. 1458-1461.
74. Forsayeth, J.R., et al., *A dose-ranging study of AAV-hAADC therapy in Parkinsonian monkeys.* Molecular Therapy, 2006. **14**(4): p. 571-577.
75. San Sebastian, W., et al., *Safety and tolerability of magnetic resonance imaging-guided convection-enhanced delivery of AAV2-hAADC with a novel delivery platform in nonhuman primate striatum.* Human gene therapy, 2011. **23**(2): p. 210-217.
76. Bankiewicz, K.S., et al., *Convection-enhanced delivery of AAV vector in parkinsonian monkeys; in vivo detection of gene expression and restoration of dopaminergic function using pro-drug approach.* Experimental neurology, 2000. **164**(1): p. 2-14.
77. Richardson, R.M., et al., *Interventional MRI-guided putaminal delivery of AAV2-GDNF for a planned clinical trial in Parkinson's disease.* Molecular Therapy, 2011. **19**(6): p. 1048-1057.
78. Tresco, P., S. Winn, and P. Aebischer, *Polymer encapsulated neurotransmitter secreting cells. Potential treatment for Parkinson's disease.* ASAIO journal (American Society for Artificial Internal Organs: 1992), 1992. **38**(1): p. 17-23.
79. Tresco, P.A., et al., *Polymer-encapsulated PC12 cells: long-term survival and associated reduction in lesion-induced rotational behavior.* Cell transplantation, 1992. **1**(2-3): p. 255-264.
80. Aebischer, P., et al., *Functional recovery in hemiparkinsonian primates transplanted with polymer-encapsulated PC12 cells.* Experimental neurology, 1994. **126**(2): p. 151-158.
81. Lindner, M.D. and D.F. Emerich, *Therapeutic potential of a polymer-encapsulated L-DOPA and dopamine-producing cell line in rodent and primate models of Parkinson's disease.* Cell transplantation, 1998. **7**(2): p. 165-174.
82. Emerich, D.F., et al., *Encapsulated cell therapy for neurodegenerative diseases: from promise to product.* Adv Drug Deliv Rev, 2014. **67-68**: p. 131-41.

83. Tseng, J.L., et al., *GDNF reduces drug-induced rotational behavior after medial forebrain bundle transection by a mechanism not involving striatal dopamine.* Journal of Neuroscience, 1997. **17**(1): p. 325-333.
84. Ross, C.A. and S.J. Tabrizi, *Huntington's disease: from molecular pathogenesis to clinical treatment.* The Lancet Neurology, 2011. **10**(1): p. 83-98.
85. Agustin-Pavon, C. and M. Isalan, *Synthetic biology and therapeutic strategies for the degenerating brain: Synthetic biology approaches can transform classical cell and gene therapies, to provide new cures for neurodegenerative diseases.* Bioessays, 2014. **36**(10): p. 979-90.
86. MacDonald, M.E., et al., *A novel gene containing a trinucleotide repeat that is expanded and unstable on Huntington's disease chromosomes.* Cell, 1993. **72**(6): p. 971-983.
87. Zühike, C., et al., *Expansion of the (CAG) n repeat causing Huntington's disease in 352 patients of German origin.* Human molecular genetics, 1993. **2**(9): p. 1467-1469.
88. Ross, C.A. and S.J. Tabrizi, *Huntington's disease: from molecular pathogenesis to clinical treatment.* Lancet Neurol, 2011. **10**(1): p. 83-98.
89. Walker, F.O., *Huntington's disease.* The Lancet, 2007. **369**(9557): p. 218-228.
90. Pfister, E.L., et al., *Artificial miRNAs reduce human mutant huntingtin throughout the striatum in a transgenic sheep model of Huntington's disease.* Human gene therapy, 2018. **29**(6): p. 663-673.
91. Cheng, A., et al., *Mitochondrial SIRT3 mediates adaptive responses of neurons to exercise and metabolic and excitatory challenges.* Cell metabolism, 2016. **23**(1): p. 128-142.
92. Evers, M.M., et al., *AAV5-miHTT gene therapy demonstrates broad distribution and strong human mutant huntingtin lowering in a Huntington's disease minipig model.* Molecular Therapy, 2018. **26**(9): p. 2163-2177.
93. Boudreau, R.L., et al., *Nonallele-specific silencing of mutant and wild-type huntingtin demonstrates therapeutic efficacy in Huntington's disease mice.* Molecular Therapy, 2009. **17**(6): p. 1053-1063.
94. Drouet, V., et al., *Sustained effects of nonallele- specific Huntingtin silencing.* Annals of Neurology: Official Journal of the American Neurological Association and the Child Neurology Society, 2009. **65**(3): p. 276-285.
95. Wang, G., et al., *Ablation of huntingtin in adult neurons is nondeleterious but its depletion in young mice causes acute pancreatitis.* Proceedings of the National Academy of Sciences, 2016. **113**(12): p. 3359-3364.
96. Shin, J.W., et al., *Permanent inactivation of Huntington's disease mutation by personalized allele-specific CRISPR/Cas9.* Human molecular genetics, 2016. **25**(20): p. 4566-4576.
97. Monteys, A.M., et al., *CRISPR/Cas9 editing of the mutant huntingtin allele in vitro and in vivo.* Molecular Therapy, 2017. **25**(1): p. 12-23.
98. Vachey, G. and N. Déglon, *CRISPR/Cas9-Mediated Genome Editing for Huntington's Disease*, in *Huntington's Disease*. 2018, Springer. p. 463-481.
99. Emerich, D.F., et al., *Implantation of polymer-encapsulated human nerve growth factor-secreting fibroblasts attenuates the behavioral and neuropathological consequences of quinolinic acid injections into rodent striatum.* Experimental neurology, 1994. **130**(1): p. 141-150.
100. Emerich, D.F., et al., *Implants of encapsulated human CNTF-producing fibroblasts prevent behavioral deficits and striatal degeneration in a rodent model of Huntington's disease.* Journal of neuroscience, 1996. **16**(16): p. 5168-5181.
101. Emerich, D.F., et al., *Cellular delivery of human CNTF prevents motor and cognitive dysfunction in a rodent model of Huntington's disease.* Cell transplantation, 1997. **6**(3): p. 249-266.

102. Emerich, D.F., et al., *Protective effect of encapsulated cells producing neurotrophic factor CNTF in a monkey model of Huntington's disease.* Nature, 1997. **386**(6623): p. 395.
103. Mittoux, V., et al., *Restoration of cognitive and motor functions by ciliary neurotrophic factor in a primate model of Huntington's disease.* Human gene therapy, 2000. **11**(8): p. 1177-1188.
104. Feldhaus, M.J. and R.W. Siegel, *Yeast display of antibody fragments: a discovery and characterization platform.* Journal of immunological methods, 2004. **290**(1-2): p. 69-80.
105. Gai, S.A. and K.D. Wittrup, *Yeast surface display for protein engineering and characterization.* Current opinion in structural biology, 2007. **17**(4): p. 467-473.
106. Shusta, E.V., et al., *A decade of yeast surface display technology: where are we now?* Combinatorial chemistry & high throughput screening, 2008. **11**(2): p. 127-134.
107. Boder, E.T. and K.D. Wittrup, *Yeast surface display for screening combinatorial polypeptide libraries.* Nature biotechnology, 1997. **15**(6): p. 553.
108. Kondo, A. and M. Ueda, *Yeast cell-surface display--applications of molecular display.* Appl Microbiol Biotechnol, 2004. **64**(1): p. 28-40.
109. Phizicky, E.M. and S. Fields, *Protein-protein interactions: methods for detection and analysis.* Microbiol. Mol. Biol. Rev., 1995. **59**(1): p. 94-123.
110. Gardner, J.M. and S.L. Jaspersen, *Manipulating the yeast genome: deletion, mutation, and tagging by PCR*, in *Yeast Genetics*. 2014, Springer. p. 45-78.
111. Brachmann, C.B., et al., *Designer deletion strains derived from Saccharomyces cerevisiae S288C: a useful set of strains and plasmids for PCR- mediated gene disruption and other applications.* Yeast, 1998. **14**(2): p. 115-132.
112. Nevoigt, E., *Progress in metabolic engineering of Saccharomyces cerevisiae.* Microbiol Mol Biol Rev, 2008. **72**(3): p. 379-412.
113. Mann, J.K. and S. Park, *Epitope-Specific Binder Design by Yeast Surface Display.* Methods Mol Biol, 2015. **1319**: p. 143-54.
114. Angelini, A., et al., *Protein Engineering and Selection Using Yeast Surface Display.* Methods Mol Biol, 2015. **1319**: p. 3-36.
115. Gera, N., M. Hussain, and B.M. Rao, *Protein selection using yeast surface display.* Methods, 2013. **60**(1): p. 15-26.
116. Lipke, P.N. and J. Kurjan, *Sexual agglutination in budding yeasts: structure, function, and regulation of adhesion glycoproteins.* Microbiology and Molecular Biology Reviews, 1992. **56**(1): p. 180-194.
117. Zhao, H., et al., *Interaction of α-agglutinin and a-agglutinin, Saccharomyces cerevisiae sexual cell adhesion molecules.* Journal of bacteriology, 2001. **183**(9): p. 2874-2880.
118. Smith, G.P. and V.A. Petrenko, *Phage display.* Chemical reviews, 1997. **97**(2): p. 391-410.
119. Aghebati-Maleki, L., et al., *Phage display as a promising approach for vaccine development.* Journal of biomedical science, 2016. **23**(1): p. 66.
120. Smith, G.P., *Filamentous fusion phage: novel expression vectors that display cloned antigens on the virion surface.* Science, 1985. **228**(4705): p. 1315-1317.
121. Smith, G.P. and J.K. Scott, *[15] Libraries of peptides and proteins displayed on filamentous phage*, in *Methods in enzymology*. 1993, Elsevier. p. 228-257.
122. Noren, K.A. and C.J. Noren, *Construction of high-complexity combinatorial phage display peptide libraries.* Methods, 2001. **23**(2): p. 169-178.
123. Pande, J., M.M. Szewczyk, and A.K. Grover, *Phage display: concept, innovations, applications and future.* Biotechnology advances, 2010. **28**(6): p. 849-858.
124. Lõoke, M., K. Kristjuhan, and A. Kristjuhan, *Extraction of genomic DNA from yeasts for PCR-based applications.* Biotechniques, 2011. **50**(5): p. 325-328.

125. Suga, M. and T. Hatakeyama, *High-efficiency electroporation by freezing intact yeast cells with addition of calcium.* Current genetics, 2003. **43**(3): p. 206-211.
126. Burke, D., D. Dawson, and T. Stearns, *Methods in Yeast Genetics: A Cold Spring Harbor Laboratory Course Manual (2000 Edition)*. 2000: Cold Spring Harbor Laboratory Press, Cold Spring Harbor, NY.
127. Labbadia, J. and R.I. Morimoto, *Huntington's disease: underlying molecular mechanisms and emerging concepts.* Trends in biochemical sciences, 2013. **38**(8): p. 378-385.
128. Bonnet, C., et al., *PCR on yeast colonies: an improved method for glyco-engineered Saccharomyces cerevisiae.* BMC research notes, 2013. **6**(1): p. 201.
129. Lesage, G. and H. Bussey, *Cell wall assembly in Saccharomyces cerevisiae.* Microbiol. Mol. Biol. Rev., 2006. **70**(2): p. 317-343.
130. Amory, D.E. and P.G. Rouxhet, *Surface properties of Saccharomyces cerevisiae and Saccharomyces carlbergensis: chemical composition, electrostatic charge and hydrophobicity.* Biochimica et Biophysica Acta (BBA)-Biomembranes, 1988. **938**(1): p. 61-70.
131. Maslanka, R., M. Kwolek-Mirek, and R. Zadrag-Tecza, *Autofluorescence of yeast Saccharomyces cerevisiae cells caused by glucose metabolism products and its methodological implications.* Journal of microbiological methods, 2018. **146**: p. 55-60.
132. Lee, M.E., et al., *A highly characterized yeast toolkit for modular, multipart assembly.* ACS synthetic biology, 2015. **4**(9): p. 975-986.

APPENDIX A

DNA sequences of the proteins and parts that have been used in this study

Tablo A.1: The DNA sequences of the neurodegenerative proteins and the parts of integration cassette that have been used in this study in 5' to 3' orientation

Gene Fragment	Sequence (5'- 3')
Htt-25Q	ATGGCGACCCTGGAAAAGCTGATGAAGGCCTTCGAG TCCCTCAAAAGCTTCCAACAGCAGCAACAGCAACAA CAGCAGCAACAGCAACAACAGCAGCAACAGCAACA ACAGCAGCAACAGCAACAACCGCCACCACCTCCCCC TCCACCCCCACCTCCTCAACTTCCTCAACCTCCTCCA CAGGCACAGCCTCTGCTGCCTCAGCCACAACCTCCTC CACCTCCACCTCCACCTCCTCCAGGCCCAGCTGTGGC TGAGGAGCCTCTGCACCGACCT
Htt-46Q	ATGGCGACCCTGGAAAAGCTGATGAAGGCCTTCGAG TCCCTCAAAAGCTTCCAACAGCAGCAACAGCAACAA CAGCAGCAACAGCAACAACAGCAGCAACAGCAACA ACAGCAGCAACAGCAGCAACAGCAACAACAGCAGC AACAGCAACAACAGCAGCAACAGCAACAACAGCAG CAACAGCAACAACCGCCACCACCTCCCCCTCCACCC CCACCTCCTCAACTTCCTCAACCTCCTCCACAGGCAC AGCCTCTGCTGCCTCAGCCACAACCTCCTCCACCTCC ACCTCCACCTCCTCCAGGCCCAGCTGTGGCTGAGGA GCCTCTGCACCGACCT
Htt-103Q	ATGAAGGCCTTCGAGTCCCTCAAAAGCTTCCAACAG CAGCAACAGCAACAACAGCAGCAACAGCAACAACA GCAGCAACAGCAACAACAGCAGCAACAGCAACAAC AGCAGCAACAGCAACAACAGCAGCAACAGCAACAA CAGCAGCAACAGCAACAACAGCAGCAACAGCAACA ACAGCAGCAACAGCAACAACAGCAGCAACAGCAAC AACAGCAGCAACAGCAACAACAGCAGCAACAGCAA CAACAGCAGCAACAGCAACAACAGCAGCAACAGCA ACAACAGCAGCAACAGCAACAACAGCAGCAACAGC AACAACCGCCACCACCTCCCCCTCCACCCCCACCTCC TCAACTTCCTCAACCTCCTCCACAGGCACAGCCTCTG CTGCCTCAGCCACAACCTCCTCCACCTCCACCTCCAC CTCCTCCAGGCCCAGCTGTGGCTGAGGAG
Amyloid β_{40}	ATGGACGCGGAGTTTCGTCACGATAGTGGATATGAG GTTCATCATCAAAAGCTAGTCTTCTTTGCGGAGGATG TAGGTTCTAATAAAGGTGCCATAATCGGACTAATGG TCGGCGGAGTTGTG
Amyloid β_{42}	ATGGACGCGGAGTTTCGTCACGATAGTGGATATGAG GTTCATCATCAAAAGCTAGTCTTCTTTGCGGAGGATG

	TAGGTTCTAATAAAGGTGCCATAATCGGACTAATGG TCGGCGGAGTTGTGATAGCT
Repeated Amyloid β_{40}	ATGGACGCGGAGTTTCGTCACGATAGTGGATATGAG GTTCATCATCAAAAGCTAGTCTTCTTTGCGGAGGATG TAGGTTCTAATAAAGGTGCCATAATCGGACTAATGG TCGGCGGAGTTGTGACGCGTGGGGGCGGATCCGGTA CCGGGGGCGGATCCACGCGTATGGACGCGGAGTTTC GTCACGATAGTGGATATGAGGTTCATCATCAAAAGC TAGTCTTCTTTGCGGAGGATGTAGGTTCTAATAAAGG TGCCATAATCGGACTAATGGTCGGCGGAGTTGTG
Repeated Amyloid β_{42}	ATGGACGCGGAGTTTCGTCACGATAGTGGATATGAG GTTCATCATCAAAAGCTAGTCTTCTTTGCGGAGGATG TAGGTTCTAATAAAGGTGCCATAATCGGACTAATGG TCGGCGGAGTTGTGATAGCTACGCGTGGGGGCGGAT CCGGTACCGGGGGCGGATCCACGCGTATGGACGCGG AGTTTCGTCACGATAGTGGATATGAGGTTCATCATCA AAAGCTAGTCTTCTTTGCGGAGGATGTAGGTTCTAAT AAAGGTGCCATAATCGGACTAATGGTCGGCGGAGTT GTGATAGCT
α-synuclein	ATGGACGTTTTCATGAAGGGTCTTTCTAAAGCGAAA GAGGGCGTGGTAGCTGCGGCCGAAAAAACTAAACA AGGGGTGGCCGAGGCTGCTGGGAAAACGAAGGAAG GTGTATTGTACGTTGGTTCAAAGACCAAAGAGGGAG TAGTTCACGGAGTCGCCACAGTTGCCGAGAAGACCA AGGAACAGGTAACGAATGTGGGAGGTGCAGTGGTG ACTGGTGTCACTGCGGTCGCCCAAAAAACAGTTGAA GGAGCGGGATCAATAGCCGCAGCAACGGGATTTGTT AAGAAGGACCAATTAGGAAAAAATGAAGAGGGAGC ACCTCAAGAAGGTATTCTAGAGGATATGCCAGTCGA CCCCGATAACGAGGCTTATGAGATGCCGTCAGAGGA AGGGTATCAGGACTATGAGCCAGAAGCC
Amyloid β_{40} fused with sfGFP (written in green)	ATGGACGCGGAGTTTCGTCACGATAGTGGATATGAG GTTCATCATCAAAAGCTAGTCTTCTTTGCGGAGGATG TAGGTTCTAATAAAGGTGCCATAATCGGACTAATGG TCGGCGGAGTTGTGGGGGGCGGATCCATGCGTAAAG GCGAAGAGCTGTTCACTGGTGTCGTCCCTATTCTGGT GGAACTGGATGGTGATGTCAACGGTCATAAGTTTTC CGTGCGTGGCGAGGGTGAAGGTGACGCAACTAATGG TAAACTGACGCTGAAGTTCATCTGTACTACTGGTAA ACTGCCGGTACCTTGGCCGACTCTGGTAACGACGCT GACTTATGGTGTTCAGTGCTTTGCTCGTTATCCGGAC CATATGAAGCAGCATGACTTCTTCAAGTCCGCCATG CCGGAAGGCTATGTGCAGGAACGCACGATTTCCTTT AAGGATGACGGCACGTACAAAACGCGTGCGGAAGT GAAATTTGAAGGCGATACCCTGGTAAACCGCATTGA GCTGAAAGGCATTGACTTTAAAGAAGACGGCAATAT CCTGGGCCATAAGCTGGAATACAATTTTAACAGCCA CAATGTTTACATCACCGCCGATAAACAAAAAAATGG CATTAAAGCGAATTTTAAAATTCGCCACAACGTGGA GGATGGCAGCGTGCAGCTGGCTGATCACTACCAGCA

	AAACACTCCAATCGGTGATGGTCCTGTTCTGCTGCCA GACAATCACTATCTGAGCACGCAAAGCGTTCTGTCT AAAGATCCGAACGAGAAACGCGATCATATGGTTCTG CTGGAGTTCGTAACCGCAGCGGGCATCACGCATGGT ATGGATGAACTGTACAAA
pTDH3 promoter	TCAGTTCGAGTTTATCATTATCAATACTGCCATTTCA AAGAATACGTAAATAATTAATAGTAGTGATTTTCCT AACTTTATTTAGTCAAAAAATTAGCCTTTTAATTCTG CTGTAACCCGTACATGCCCAAAATAGGGGGCGGGTT ACACAGAATATATAACATCGTAGGTGTCTGGGTGAA CAGTTTATTCCTGGCATCCACTAAATATAATGGAGCC CGCTTTTTTAAGCTGGCATCCAGAAAAAAAAAGAATC CCAGCACCAAAATATTGTTTTCTTCACCAACCATCAG TTCATAGGTCCATTCTCTTAGCGCAACTACAGAGAAC AGGGGCACAAACAGGCAAAAAACGGGCACAACCTC AATGGAGTGATGCAACCTGCCTGGAGTAAATGATGA CACAAGGCAATTGACCCACGCATGTATCTATCTCATT TTCTTACACCTTCTATTACCTTCTGCTCTCTCTGATTT GGAAAAAGCTGAAAAAAAAGGTTGAAACCAGTTCC CTGAAATTATTCCCCTACTTGACTAATAAGTATATAA AGACGGTAGGTATTGATTGTAATTCTGTAAATCTATT TCTTAAACTTCTTAAATTCTACTTTTATAGTTAGTCTT TTTTTTAGTTTTAAAACACCAAGAACTTAGTTTCGAA TAAACACACATAAACAAACAAA
ADH1 terminator	GCGAATTTCTTATGATTTATGATTTTTATTATTAAAT AAGTTATAAAAAAAATAAGTGTATACAAATTTTAAA GTGACTCTTAGGTTTTAAAACGAAAATTCTTATTCTT GAGTAACTCTTTCCTGTAGGTCAGGTTGCTTTCTCAG GTATAGCATGAGGTCGCTCTTATTGACCACACCTCTA CCGGCATGC
pLEU2	AACTGTGGGAATACTCAGGTATCGTAAGATGCAAGA GTTCGAATCTCTTAGCAACCATTATTTTTTTCCTCAA CATAACGAGAACACACAGGGGCGCTATCGCACAGA ATCAAATTCGATGACTGGAAATTTTTTGTTAATTTCA GAGGTCGCCTGACGCATATACCTTTTTCAACTGAAA AATTGGGAGAAAAAGGAAAGGTGAGAGCGCCGGAA CCGGCTTTTCATATAGAATAGAGAAGCGTTCATGAC TAAATGCTTGCATCACAATACTTGAAGTTGACAATAT TATTTAAGGACCTATTGTTTTTTCCAATAGGTGGTTA GCAATCGTCTTACTTTCTAACTTTTCTTACCTTTTACA TTTCAGCAATATATATATATATATTTCAAGGATATAC CATTCTA
LEU2	ATGTCTGCCCCTAAGAAGATCGTCGTTTTGCCAGGTG ACCACGTTGGTCAAGAAATCACAGCCGAAGCCATTA AGGTTCTTAAAGCTATTTCTGATGTTCGTTCCAATGT CAAGTTCGATTTCGAAAATCATTTAATTGGTGGTGCT GCTATAGATGCTACAGGTGTTCCACTTCCAGATGAG GCGCTGGAAGCCTCCAAGAAGGCTGATGCCGTTTTG TTAGGTGCTGTGGGTGGTCCTAAATGGGGTACAGGT AGTGTTAGACCTGAACAAGGTTTACTAAAAATCCGT

	AAAGAACTTCAATTGTACGCCAACTTAAGACCATGT AACTTTGCATCCGACTCTCTTTTAGACTTATCTCCAA TCAAGCCACAATTTGCTAAAGGTACTGACTTCGTTGT TGTCAGAGAATTAGTGGGAGGTATTTACTTTGGTAA GAGAAAGGAAGACGATGGTGATGGTGTCGCTTGGGA TAGTGAACAATACACCGTTCCAGAAGTGCAAAGAAT CACAAGAATGGCCGCTTTCATGGCCCTACAACATGA GCCACCATTGCCTATTTGGTCCTTGGATAAAGCTAAT GTTTTGGCCTCTTCAAGATTATGGAGAAAAACTGTG GAGGAAACCATCAAGAACGAATTTCCTACATTGAAG GTTCAACATCAATTGATTGATTCTGCCGCCATGATCC TAGTTAAGAACCCAACCCACCTAAATGGTATTATAA TCACCAGCAACATGTTTGGTGATATCATCTCCGATGA AGCCTCCGTTATCCCAGGTTCCTTGGGTTTGTTGCCA TCTGCGTCCTTGGCCTCTTTGCCAGACAAGAACACCG CATTTGGTTTGTACGAACCATGCCACGGTTCTGCTCC AGATTTGCCAAAGAATAAGGTCAACCCTATCGCCAC TATCTTGTCTGCTGCAATGATGTTGAAATTGTCATTG AACTTGCCTGAAGAAGGTAAGGCCATTGAAGATGCA GTTAAAAAGGTTTTGGATGCAGGTATCAGAACTGGT GATTTAGGTGGTTCCAACAGTACCACCGAAGTCGGT GATGCTGTCGCCGAAGAAGTTAAGAAAATCCTTGCT TAA
mOrange	ATGGTTAGTAAAGGAGAAGAAAACAATATGGCAATC ATAAAAGAATTTATGAGATTCAAAGTCAGAATGGAA GGTTCTGTAAATGGTCACGAGTTCGAAATAGAAGGG GAAGGTGAAGGTAGACCCTATGAAGGCTTTCAAACG GCTAAATTAAAAGTTACCAAGGGTGGACCATTGCCC TTTGCTTGGGATATCCTGTCTCCTCAGTTCACTTATG GTAGTAAAGCCTATGTTAAGCATCCTGCTGATATTCC TGATTACTTCAAGTTGAGTTTTCCAGAAGGTTTCAAA TGGGAGAGAGTTATGAATTTTGAAGATGGCGGAGTT GTGACAGTGACACAAGACTCCTCACTTCAAGACGGT GAGTTTATTTACAAGGTAAAACTACGTGGCACTAAC TTTCCGTCGGATGGACCAGTCATGCAAAAAAAGACG ATGGGTTGGGAGGCTTCATCTGAGCGAATGTATCCA GAAGATGGGGCACTAAAGGGCGAAATTAAGATGAG GCTCAAATTAAAGGATGGTGGACATTATACCTCGGA AGTGAAAACTACCTATAAAGCCAAAAAGCCAGTTCA ATTACCTGGTGCATACATTGTTGGCATTAAGTTGGAC ATCACAAGCCACAATGAAGATTATACAATAGTAGAG CAGTACGAACGCGCGGAAGGTAGGCATTCTACTGGA GGCATGGATGAACTATACAAA
Integration cassete with mOrange	TCAGTTCGAGTTTATCATTATCAATACTGCCATTTCA AAGAATACGTAAATAATTAATAGTAGTGATTTTCCT AACTTTATTTAGTCAAAAAATTAGCCTTTTAATTCTG CTGTAACCCGTACATGCCCAAAATAGGGGGCGGGTT ACACAGAATATATAACATCGTAGGTGTCTGGGTGAA CAGTTTATTCCTGGCATCCACTAAATATAATGGAGCC CGCTTTTTAAGCTGGCATCCAGAAAAAAAAAGAATC

	CCAGCACCAAAATATTGTTTTCTTCACCAACCATCAG TTCATAGGTCCATTCTCTTAGCGCAACTACAGAGAAC AGGGGCACAAACAGGCAAAAAACGGGCACAACCTC AATGGAGTGATGCAACCTGCCTGGAGTAAATGATGA CACAAGGCAATTGACCCACGCATGTATCTATCTCATT TTCTTACACCTTCTATTACCTTCTGCTCTCTCTGATTT GGAAAAAGCTGAAAAAAAAGGTTGAAACCAGTTCC CTGAAATTATTCCCCTACTTGACTAATAAGTATATAA AGACGGTAGGTATTGATTGTAATTCTGTAAATCTATT TCTTAAACTTCTTAAATTCTACTTTTATAGTTAGTCTT TTTTTTAGTTTTAAAACACCAAGAACTTAGTTTCGAA TAAACACACATAAACAAACAAAAGATCTGATATGGA TCGAATTAGAATTCGCCACCATGGTTAGTAAAGGAG AAGAAAACAATATGGCAATCATAAAAGAATTTATGA GATTCAAAGTCAGAATGGAAGGTTCTGTAAATGGTC ACGAGTTCGAAATAGAAGGGGAAGGTGAAGGTAGA CCCTATGAAGGCTTTCAAACGGCTAAATTAAAAGTT ACCAAGGGTGGACCATTGCCCTTTGCTTGGGATATCC TGTCTCCTCAGTTCACTTATGGTAGTAAAGCCTATGT TAAGCATCCTGCTGATATTCCTGATTACTTCAAGTTG AGTTTTCCAGAAGGTTTCAAATGGGAGAGAGTTATG AATTTTGAAGATGGCGGAGTTGTGACAGTGACACAA GACTCCTCACTTCAAGACGGTGAGTTTATTTACAAGG TAAAACTACGTGGCACTAACTTTCCGTCGGATGGAC CAGTCATGCAAAAAAAGACGATGGGTTGGGAGGCTT CATCTGAGCGAATGTATCCAGAAGATGGGGCACTAA AGGGCGAAATTAAGATGAGGCTCAAATTAAAGGATG GTGGACATTATACCTCGGAAGTGAAAACTACCTATA AAGCCAAAAAGCCAGTTCAATTACCTGGTGCATACA TTGTTGGCATTAAGTTGGACATCACAAGCCACAATG AAGATTATACAATAGTAGAGCAGTACGAACGCGCGG AAGGTAGGCATTCTACTGGAGGCATGGATGAACTAT ACAAACTCGAGGGGGGCGGATCCGAACAAAAGCTT ATTTCTGAAGAGGACTTGTAATAGAACGCGTGCGAA TTTCTTATGATTTATGATTTTTATTATTAAATAAGTTA TAAAAAAAATAAGTGTATACAAATTTTAAAGTGACT CTTAGGTTTTAAAACGAAAATTCTTATTCTTGAGTAA CTCTTTCCTGTAGGTCAGGTTGCTTTCTCAGGTATAG CATGAGGTCGCTCTTATTGACCACACCTCTACCGGCA TGC
Integration cassette with LEU2	AACTGTGGGAATACTCAGGTATCGTAAGATGCAAGA GTTCGAATCTCTTAGCAACCATTATTTTTTTCCTCAA CATAACGAGAACACACAGGGGCGCTATCGCACAGA ATCAAATTCGATGACTGGAAATTTTTTGTTAATTTCA GAGGTCGCCTGACGCATATACCTTTTTCAACTGAAA AATTGGGAGAAAAAGGAAAGGTGAGAGCGCCGGAA CCGGCTTTTCATATAGAATAGAGAAGCGTTCATGAC TAAATGCTTGCATCACAATACTTGAAGTTGACAATAT TATTTAAGGACCTATTGTTTTTTCCAATAGGTGGTTA GCAATCGTCTTACTTTCTAACTTTTCTTACCTTTTACA

	TTTCAGCAATATATATATATATATTTCAAGGATATAC CATTCTAATGTCTGCCCCTAAGAAGATCGTCGTTTTG CCAGGTGACCACGTTGGTCAAGAAATCACAGCCGAA GCCATTAAGGTTCTTAAAGCTATTTCTGATGTTCGTT CCAATGTCAAGTTCGATTTCGAAAATCATTTAATTGG TGGTGCTGCTATAGATGCTACAGGTGTTCCACTTCCA GATGAGGCGCTGGAAGCCTCCAAGAAGGCTGATGCC GTTTTGTTAGGTGCTGTGGGTGGTCCTAAATGGGGTA CAGGTAGTGTTAGACCTGAACAAGGTTTACTAAAAA TCCGTAAAGAACTTCAATTGTACGCCAACTTAAGAC CATGTAACTTTGCATCCGACTCTCTTTTAGACTTATC TCCAATCAAGCCACAATTTGCTAAAGGTACTGACTTC GTTGTTGTCAGAGAATTAGTGGGAGGTATTTACTTTG GTAAGAGAAAGGAAGACGATGGTGATGGTGTCGCTT GGGATAGTGAACAATACACCGTTCCAGAAGTGCAAA GAATCACAAGAATGGCCGCTTTCATGGCCCTACAAC ATGAGCCACCATTGCCTATTTGGTCCTTGGATAAAGC TAATGTTTTGGCCTCTTCAAGATTATGGAGAAAAACT GTGGAGGAAACCATCAAGAACGAATTTCCTACATTG AAGGTTCAACATCAATTGATTGATTCTGCCGCCATGA TCCTAGTTAAGAACCCAACCCACCTAAATGGTATTAT AATCACCAGCAACATGTTTGGTGATATCATCTCCGAT GAAGCCTCCGTTATCCCAGGTTCCTTGGGTTTGTTGC CATCTGCGTCCTTGGCCTCTTTGCCAGACAAGAACAC CGCATTTGGTTTGTACGAACCATGCCACGGTTCTGCT CCAGATTTGCCAAAGAATAAGGTCAACCCTATCGCC ACTATCTTGTCTGCTGCAATGATGTTGAAATTGTCAT TGAACTTGCCTGAAGAAGGTAAGGCCATTGAAGATG CAGTTAAAAAGGTTTTGGATGCAGGTATCAGAACTG GTGATTTAGGTGGTTCCAACAGTACCACCGAAGTCG GTGATGCTGTCGCCGAAGAAGTTAAGAAAATCCTTG CTCTCGAGGGGGGCGGATCCGAACAAAAGCTTATTT CTGAAGAGGACTTG

APPENDIX B

List of the primers that have been used in this study

Tablo B.1: The sequences of primers that have been used in cloning experiments of neurodegenerative proteins and genome integration cassette

Htt-25Q cloning	OB01 (25Q_forward_1)	GGCGGTAGCGGAGGCGGAGGGTCG ACTAGTATGGCGACCCTGGAAAAGC T
	OB02 (25Q_forward_2)	CTACGCTCTGCAGGCTAGTGGTGGA GGAGGCTCTGGTGGAGGCGGTAGCG GAGG
	OB03 (25Q_reverse)	ATATATCTCGAGAGGTCGGTGCAGA GGCTCCTC
Htt-46Q cloning	OB04 (46Q_forward)	CAGAAGACTAGTATGGCGACCCTGG AAAAGCTGATGAAG
	OB03 (25Q_reverse)	ATATATCTCGAGAGGTCGGTGCAGA GGCTCCTC
Htt-103Q cloning	OB05 (103Q_forward)	AGGTGAACTAGTATGGCGACCCTGG AAAAGCTGATGA
	OB03 (25Q_reverse)	ATATATCTCGAGAGGTCGGTGCAGA GGCTCCTC
Amyloid β_{40} and amyloid β_{42} clonings	OB06 (top)	AGGTTCATCATCAAAAGCTAGTCTT CTTTGCGGAGGATGTAGGTTCTAAT AAAGGTGCCA
	OB07 (bottom)	TGGCACCTTTATTAGAACCTACATC CTCCGCAAAGAAGACTAGCTTTTGA TGATGAACCT
	OB08 (forward_ab40-42)	ACTAGTATGGACGCGGAGTTTCGTC ACGATAGTGGATATGAGGTTCATCA TCAAAAGCTA
	OB09 (reverse_ab40)	CTCGAGCACAACTCCGCCGACCATT AGTCCGATTATGGCACCTTTATTAG AACC
	OB10 (reverse_ab42)	CTCGAGAGCTATCACAACTCCGCCG ACCATTAGTCCGATTATGGCACCTTT ATTAGAACC
	OB11 (gibson_ab40_forward)	TCTGGTGGAGGCGGTAGCGGAGGCG GAGGGTCGACTAGTATGGACGCGGA GTTTCGTCAC
	OB12 (gibson_ab40_reverse)	AGTCCTCTTCAGAAATAAGCTTTTGT TCGGATCCGCCCCCCTCGAGCACAA CTCCGCCGA

	OB13 (gibson_ab42_forward)	CTCTGGTGGAGGCGGTAGCGGAGGC GGAGGGTCGACTAGTATGGACGCGG AGTTTCGTCA
	OB14 (gibson_ab42_reverse)	CTTCAGAAATAAGCTTTTGTTCGGA TCCGCCCCCCTCGAGAGCTATCACA ACTCCGCCGA
Repeated amyloid β_{40} and amyloid β_{42} clonings	OB15 (AB40_repeat_reverse)	GCGTGGATCCGCCCCCGGTACCGGA TCCGCCCCCACGCGTCACAACTCCG CCGACCATTA
	OB16 (AB40_repeat_forward)	GCGTGGGGGCGGATCCGGTACCGGG GGCGGATCCACGCGTATGGACGCGG AGTTTCGTCACG
	OB17 (AB42_repeat_reverse)	GCGTGGATCCGCCCCCGGTACCGGA TCCGCCCCCACGCGTAGCTATCACA ACTCCGCCGA
	OB18 (Ab42_repeat_forward)	GCGTGGGGGCGGATCCGGTACCGGG GGCGGATCCACGCGTATGGACGCGG AGTTTCGTCA
Integration cassettes	OB70 (pTDH3_fwd)	CGAAATTAACCCTCACTAAAGGGAA CAAAAGCTGGTACCAATTTCAGTTC GAGTTTATCATTATCAATAC
	OB81 (Ptdh3_rev_dc)	ATGGTGGCGAATTCTAATTCGATCC ATATCAGATCTTTTGTTTGTTTATGT GTGTTTATTC
	OB82 (mOrange_fwd_dc)	GATATAGATCGAATTAGAATTCGCC ACCATGGTTAGTAAAGGAGAAGAA AACAATATGG
	OB83 (mOrange_rev_dc)	TAAGCTTTTGTTCGGATCCGCCCCCC TCGAGTTTGTATAGTTCATCCATGCC TCC
	OB84 (ADH1_fwd_dc)	GAACAAAAGCTTATTTCTGAAGAGG ACTTGTAATAGACGCGTGCGAATTT CTTATGATTTATG
	OB85 (ADH1_rev_dc)	AAGTCGATTTTGTTACATCTACACTG TTGTTATCACTGCAGGCATGCCGGT AGAGGTG
	OB86 (noTRP_fwd)	ATATGAACTTAAGTCTGCTCTGATG CCGCATAGTTAAG
	OB87 (NO_trp_rev)	GAATCATCTTAAGGAAATACCGCAC AGATGCGTAAGG
	OB74 (fwd_dc(pETcon))	CTCGAAATTAACCCTCACTAAAGGG AACAAAAGCTGGTACCAACTGTGGG AATACTCAGG
	OB75 (rev_dc(pETcon))	AGAAATAAGCTTTTGTTCGGATCCG CCCCCCTCGAGAGCAAGGATTTTCT TAACTTCTTCG
Colony PCR and sequencing	T3	ATTAACCCTCACTAAAGGGA
	T7	TAATACGACTCACTATAGGG
Fusion of selected	OB104 (sfGFP_peptide-	TGTGAGCGGATAACAATTCCCCTCT AGATTAACTTTAAGAAGGAGGGTAC

peptides with sfGFP and cloning into the expression vector	cloning_r1)	CATGCGTAAAGGCGAAGAG
	OB105 (sfGFP_peptide-cloning_r2)	GGATCGAGATCTCGATCCCGCGAAATTAATACGACTCACTATAGGGGAATTGTGAGCGGATAACAATTCC
	OB106 (25Q_peptide_f1)	TCTGAACCAACACCTCACCAAGCCAAGAATGCATGGATCCGCCCCCTTTGTACAGTTCATCCATACCATG
	OB107 (25Q_peptide_f2)	ATCTCAGTGGTGGTGGTGGTGGTGCTCGAGGGATCCGCCCCCAGTATTCTGAACCAACACCTCAC
	OB108 (46Q_peptide_f1)	CTCCCTAGTAGTCATCATATACCGCCCATGCATATCCATGGATCCGCCCCCTTTGTACAGTTCATCCATACCATG
	OB109 (46Q_peptide_f2)	ATCTCAGTGGTGGTGGTGGTGGTGCTCGAGGGATCCGCCCCCCTCCCTAGTAGTCATCATATACCG
	OB110 (ab40_peptide_f1)	CCATGCTTCTGCGTAATATAAATATTCAAATTCAGATGCATGGATCCGCCCCCTTTGTACAGTTCATCCATACCATG
	OB111 (ab40_peptide_f2)	GGATCTCAGTGGTGGTGGTGGTGGTGCTCGAGGGATCCGCCCCCATGCTTCTGCGTAATATAAATATTC

APPENDIX C

Maps of the plasmids that have been used in this study

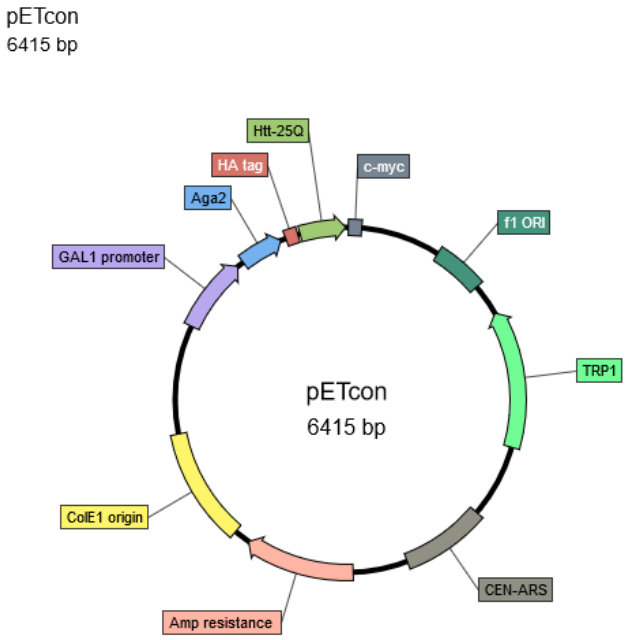

Figure C.1: Plasmid map of pETcon vector in which Aga2 gene is fused with Htt-25Q

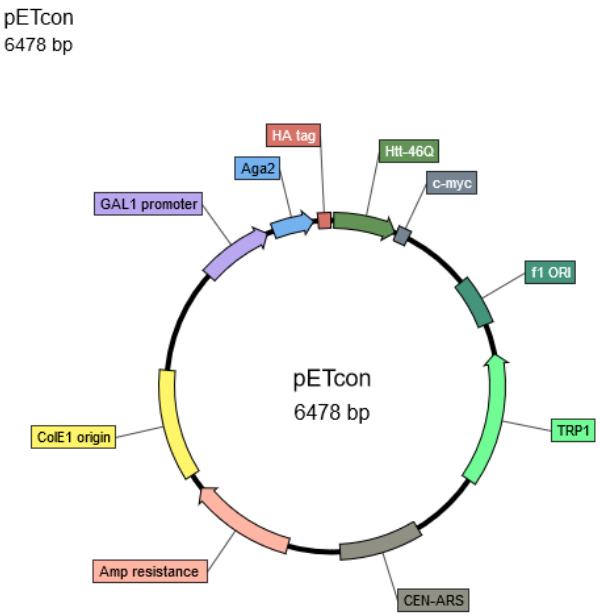

Figure C.2: Plasmid map of pETcon vector in which Aga2 gene is fused with Htt-46Q

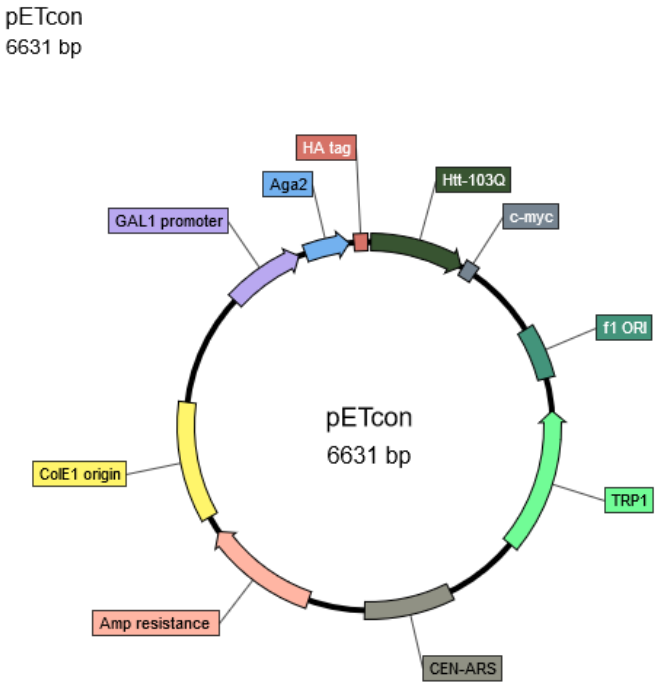

Figure C.3: Plasmid map of pETcon vector in which Aga2 gene is fused with Htt-103Q

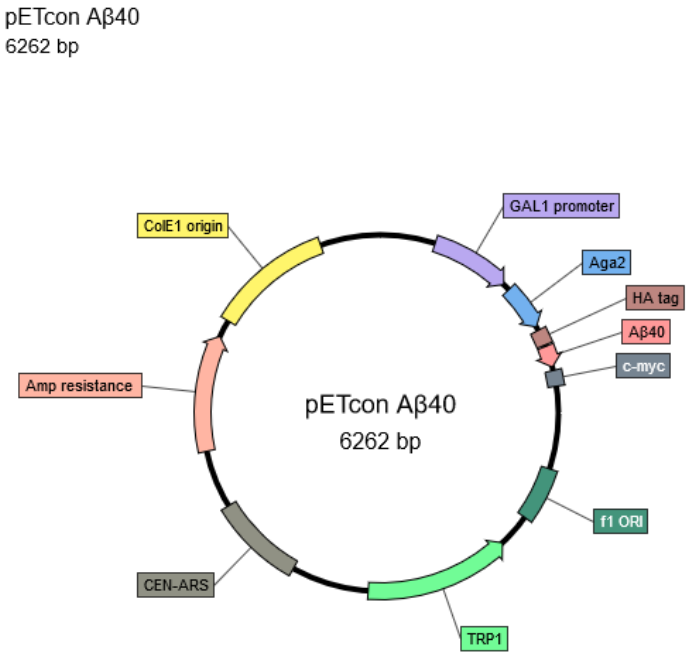

Figure C.4: Plasmid map of pETcon vector in which Aga2 gene is fused with amyloid β40

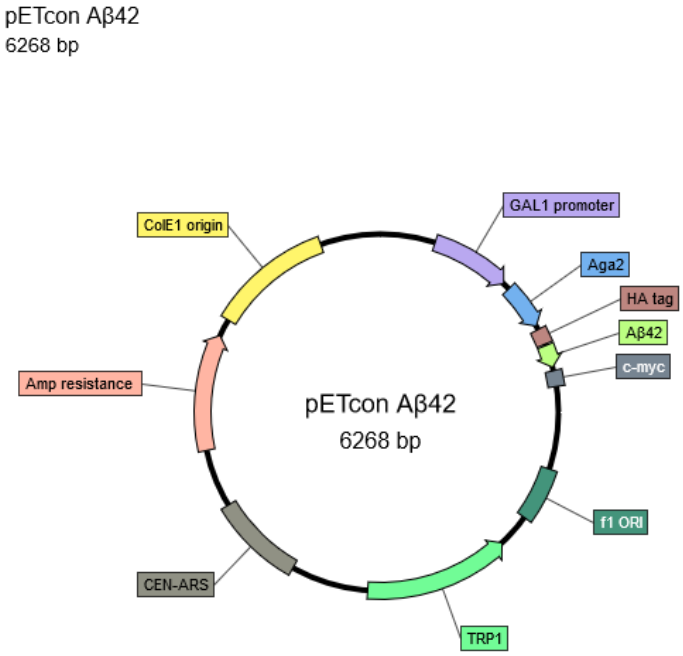

Figure C.5: Plasmid map of pETcon vector in which Aga2 gene is fused with amyloid β42

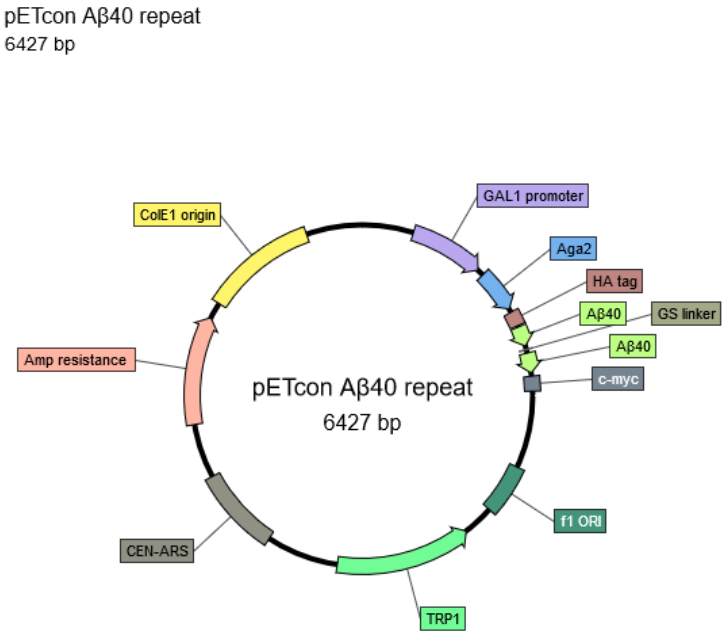

Figure C.6: Plasmid map of pETcon vector in which Aga2 gene is fused with repeated amyloid β40

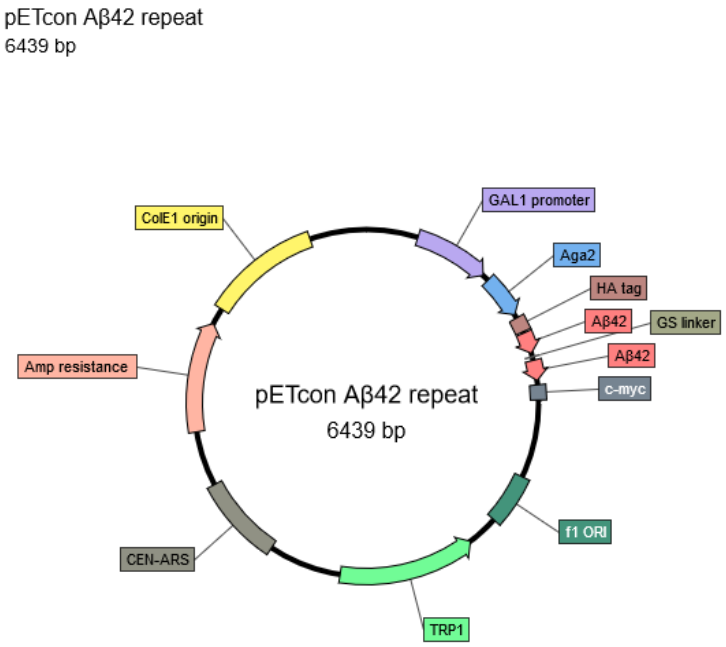

Figure C.7: Plasmid map of pETcon vector in which Aga2 gene is fused with repeated amyloid β42

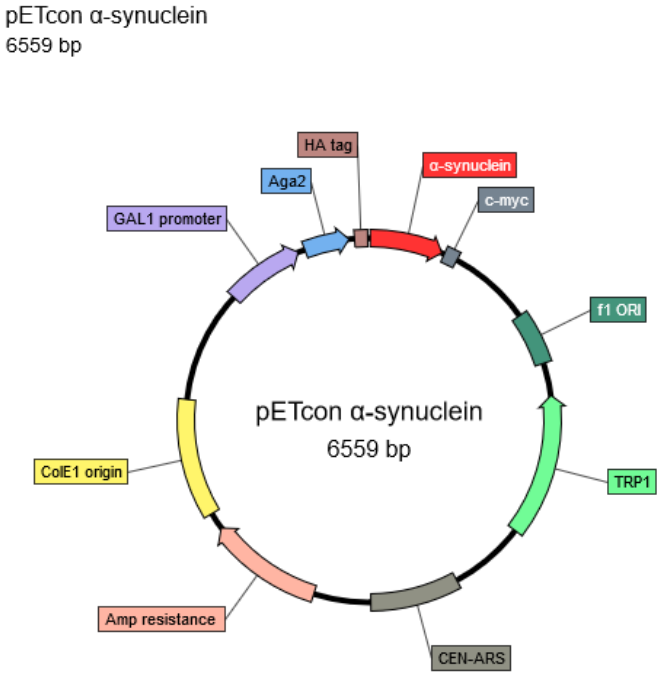

Figure C.8: Plasmid map of pETcon vector in which Aga2 gene is fused with α-synuclein

APPENDIX D

Sequencing results of the clonings

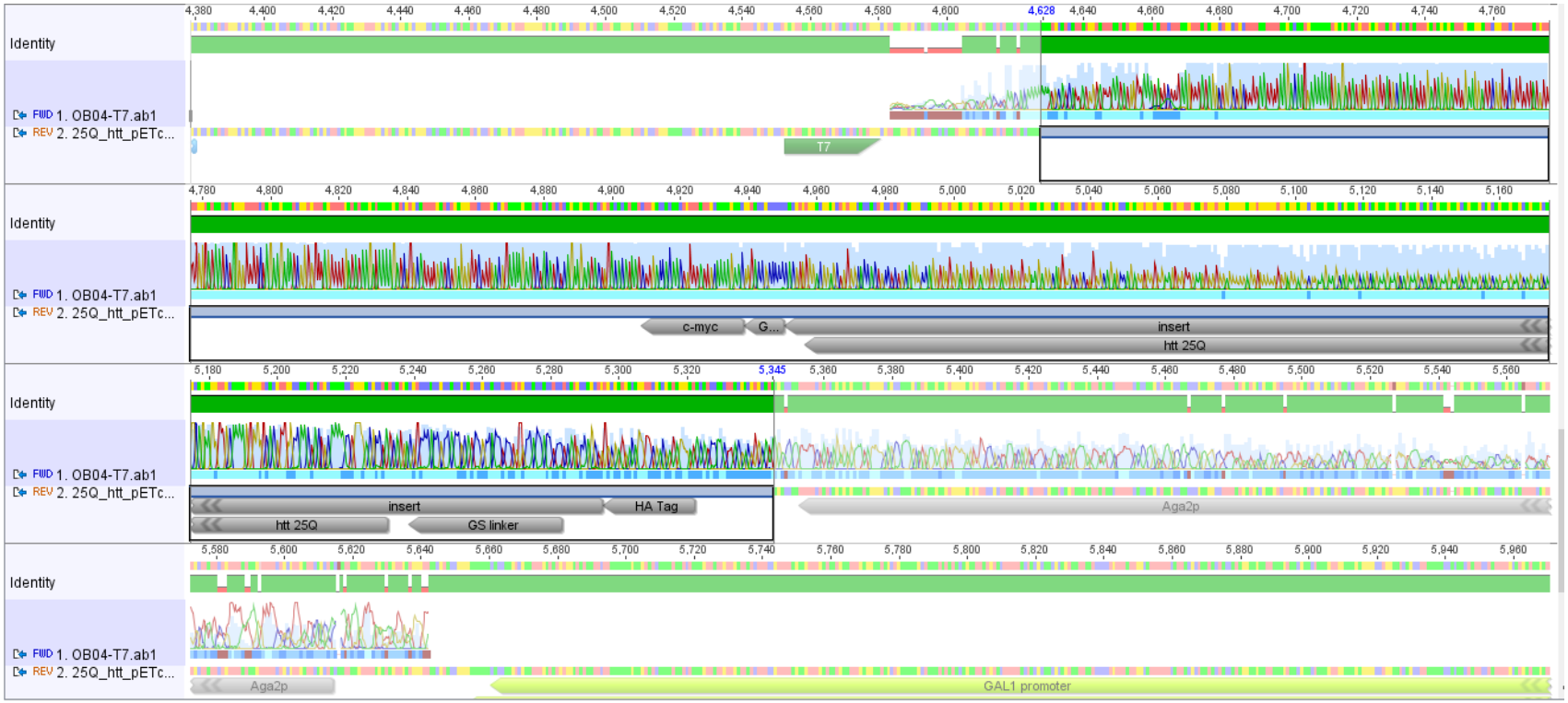

Figure D.1:The result indicating the sequence analysis of Htt-25Q being cloned into pETcon backbone. 'G...' Stands for GS linker.

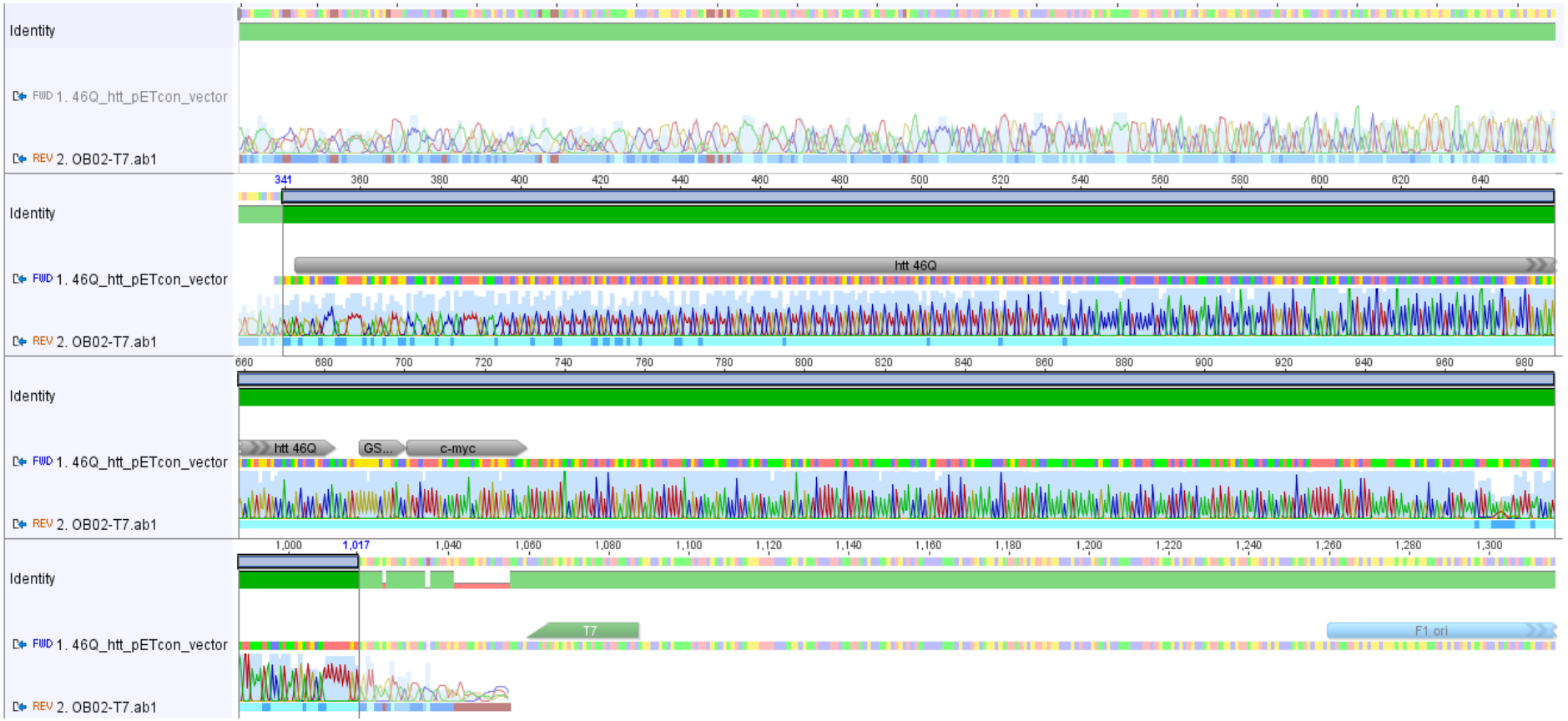

Figure D.2: The result indicating the sequence analysis of Htt-46Q being cloned into pETcon backbone. ‘GS...’ Stands for GS linker.

Figure D.3: The result indicating the sequence analysis of Htt-103Q being cloned into pETcon backbone. ‘G...’ Stands for GS linker.

Figure D.4: The result indicating the sequence analysis of amyloid β_{40} being cloned into pETcon backbone. 'G...' Stands for GS linker.

Figure D.5: The result indicating the sequence analysis of amyloid β_{42} being cloned into pETcon backbone.

Figure D.6: The result indicating the sequence analysis of repeated amyloid β_{40} being cloned into pETcon backbone. 'G...' stands for GS linker.

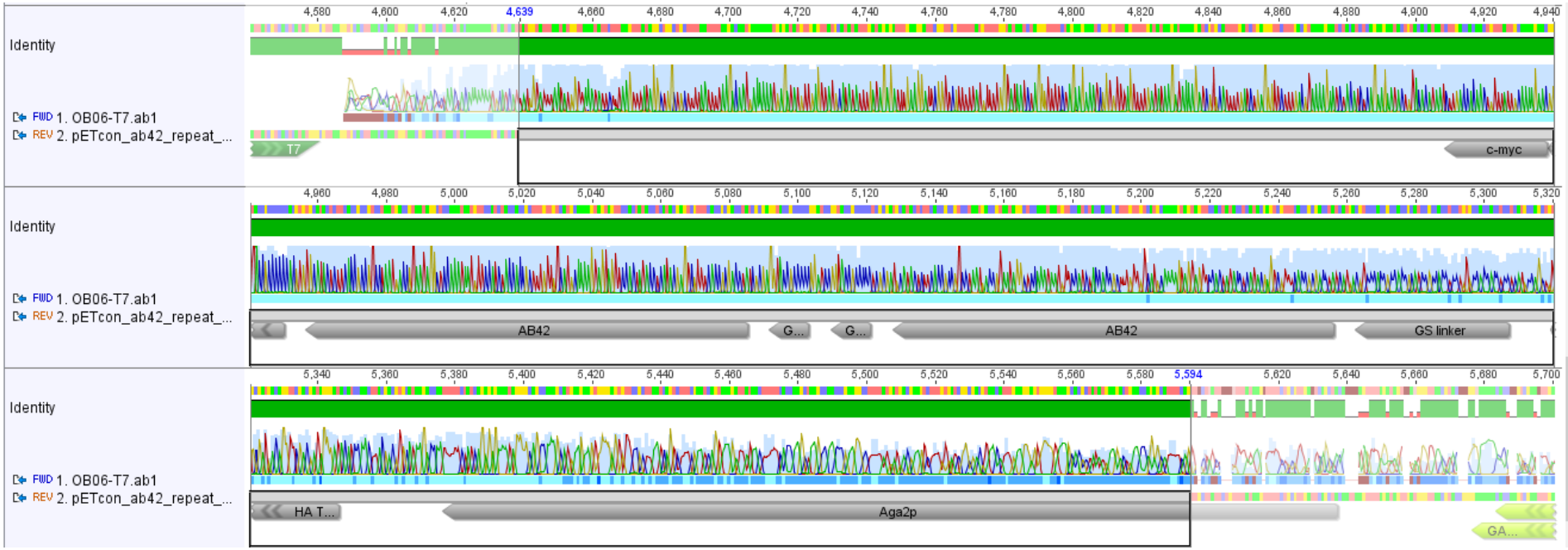

Figure D.7: The result indicating the sequence analysis of repeated amyloid β_{42} being cloned into pETcon backbone. 'G...' stands for GS linker.

Figure D.8: The result indicating the sequence analysis of repeated α-synuclein being cloned into pETcon backbone. ‘G...’ stands for GS linker.

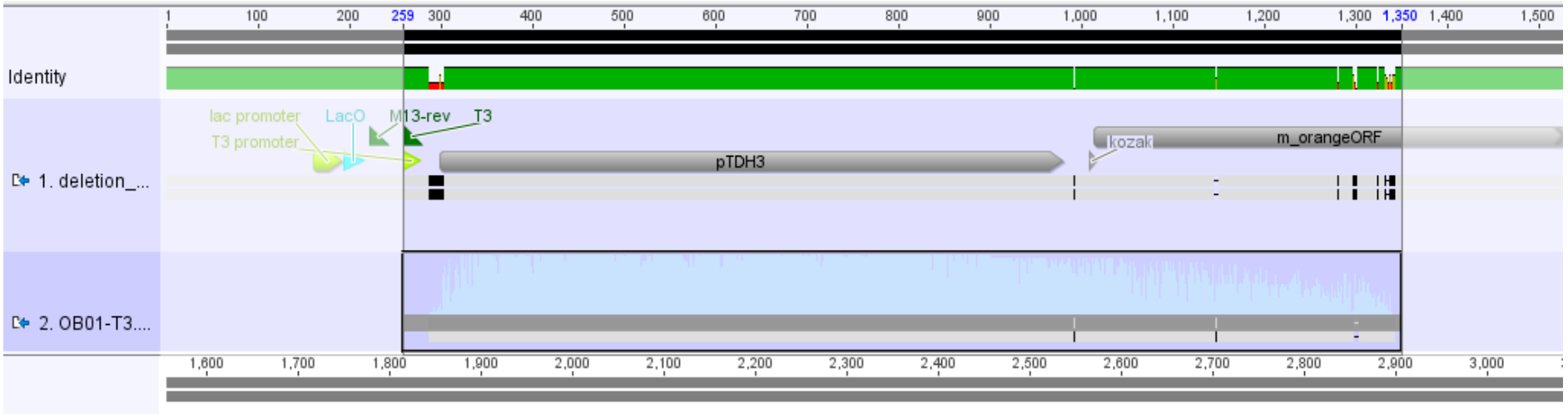

Figure D.9: The result indicating the sequence analysis of integration cassette being cloned into pETcon backbone with a forward primer.

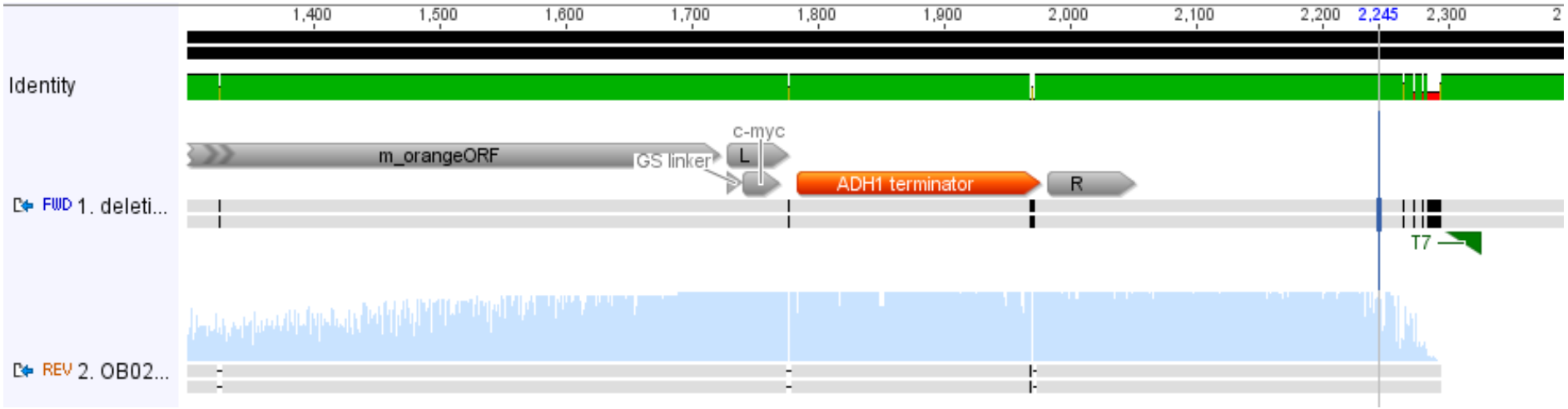

Figure D.10: The result indicating the sequence analysis of integration cassette being cloned into pETcon backbone with a reverse primer.

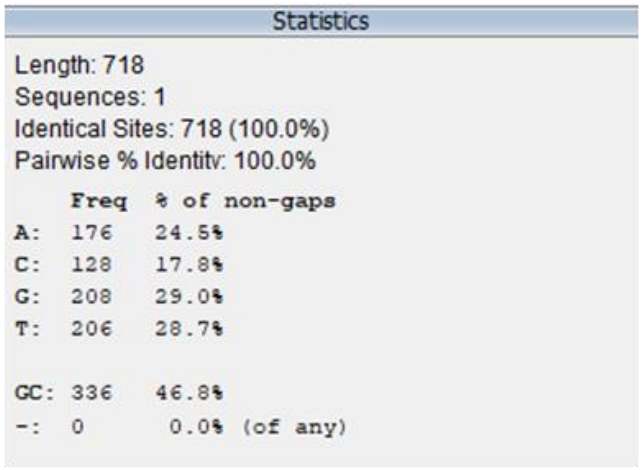

Figure D.11: Statistics of sequence analysis of Htt-25Q. A region which is 718 bp in length including Htt-25Q sequence was chosen for statistical analysis.

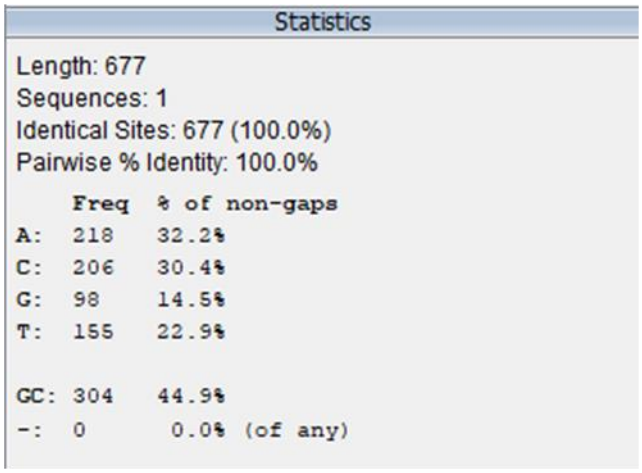

Figure D.12: Statistics of sequence analysis of Htt-46Q. A region which is 677 bp in length including Htt-46Q sequence was chosen for statistical analysis.

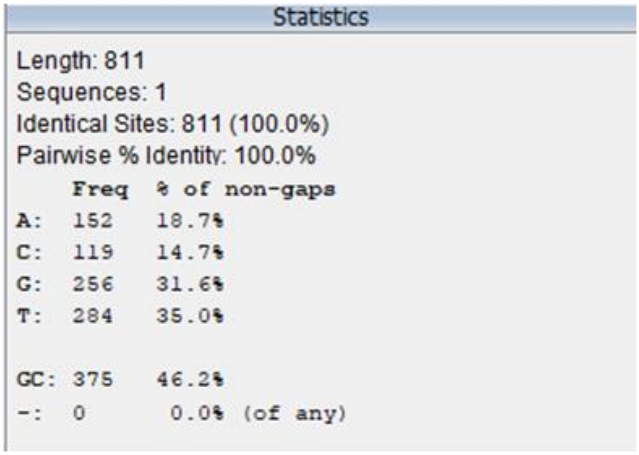

Figure D.13: Statistics of sequence analysis of Htt-103Q. A region which is 811 bp in length including Htt-103Q sequence was chosen for statistical analysis.

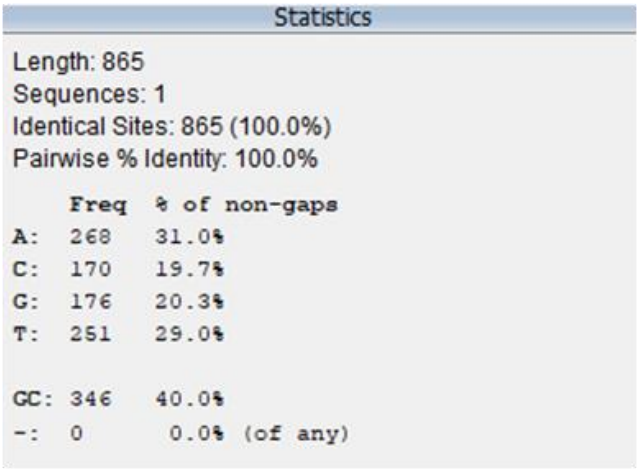

Figure D.14: Statistics of sequence analysis of amyloid β40. A region which is 865 bp in length including amyloid β40 sequence was chosen for statistical analysis.

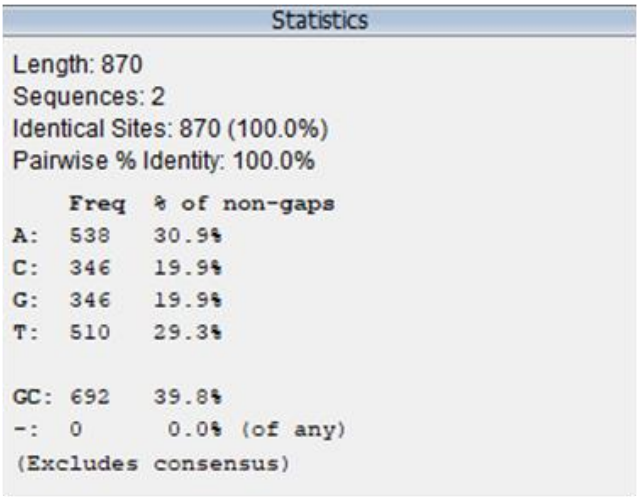

Figure D.15: Statistics of sequence analysis of amyloid β42. A region which is 870 bp in length including amyloid β42 sequence was chosen for statistical analysis.

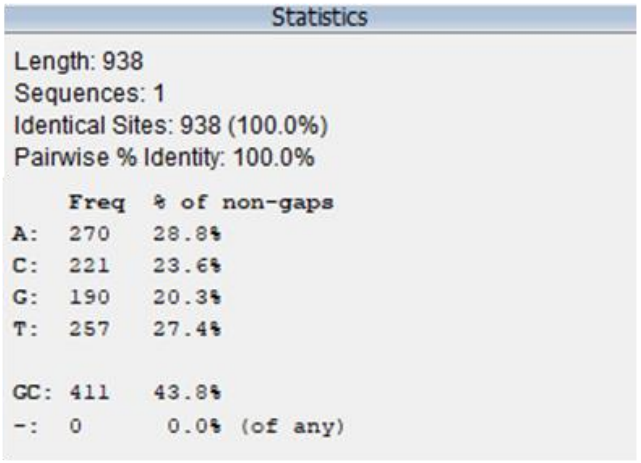

Figure D.16: Statistics of sequence analysis of repeated amyloid β40. A region which is 938 bp in length including repeated amyloid β40 sequence was chosen for statistical analysis.

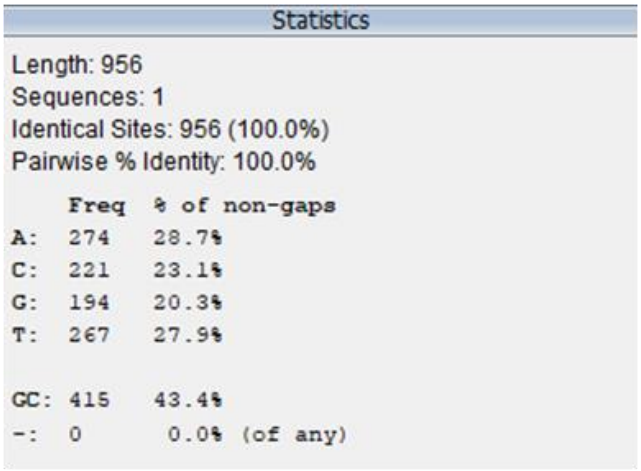

Figure D.17: Statistics of sequence analysis of repeated amyloid β42. A region which is 956 bp in length including repeated amyloid β42 sequence was chosen for statistical analysis.

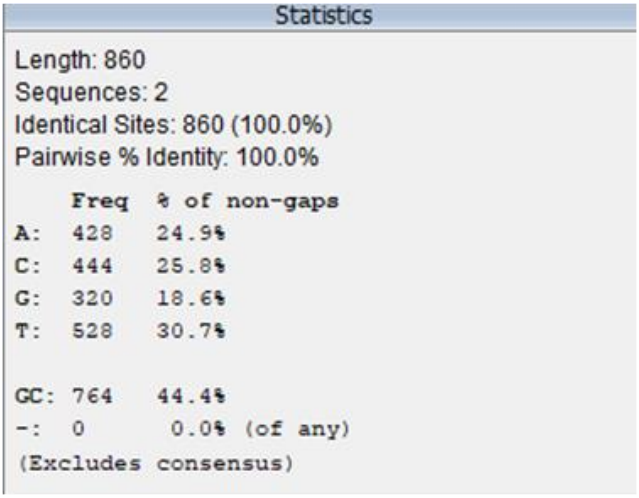

Figure D.18: Statistics of sequence analysis of repeated α-synuclein. A region which is 860 bp in length including repeated α-synuclein sequence was chosen for statistical analysis.

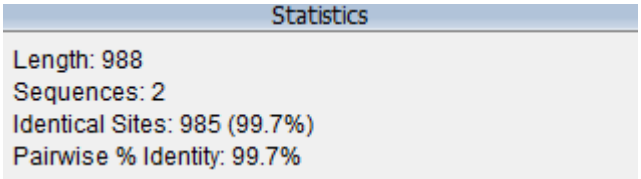

Figure D.19: Statistics of sequence analysis of integration cassette by using a forward primer. A region which is 988 bp in length including promoter and marker gene sequence was chosen for statistical analysis.

Statistics
Length: 1,000
Sequences: 1
Identical Sites: 992 (99.2%)
Pairwise % Identity: 99.3%

Figure D.20: Statistics of sequence analysis of integration cassette by using a reverse primer. A region which is 1000 bp in length including promoter and marker gene sequence was chosen for statistical analysis.

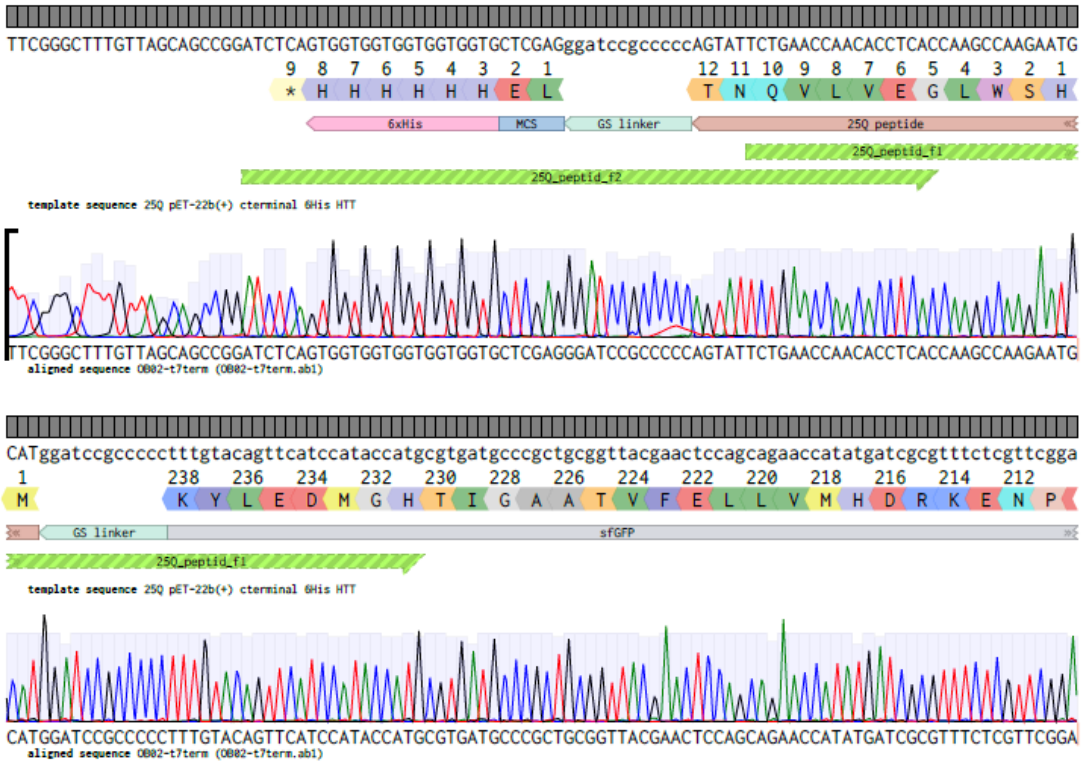

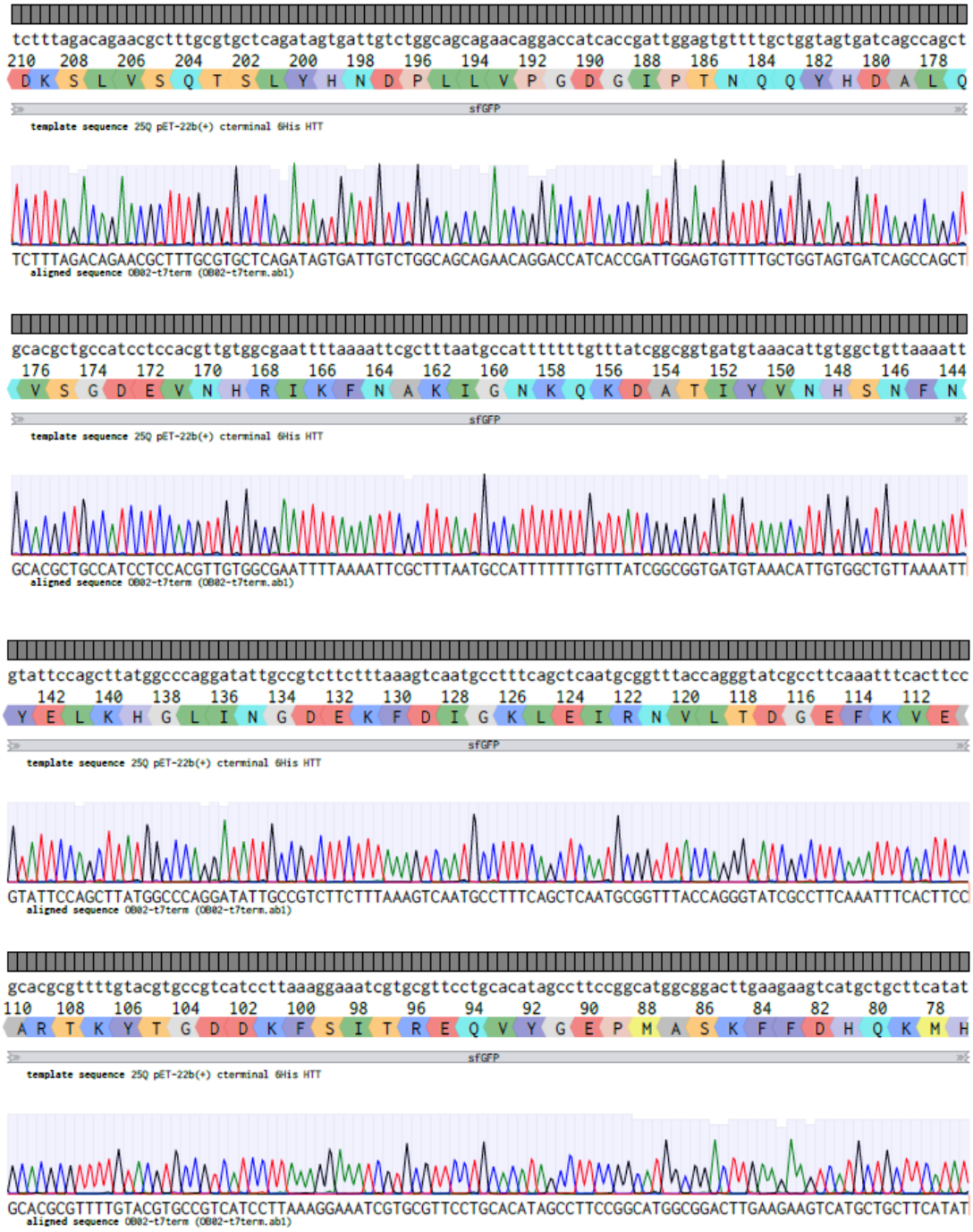
tctttagacagaacgctttgcgtgctcagatagtgattgtctggcagcagaacaggaccatcaccgattggagtgttttgctggtagtgatcagccagct
210 208 206 204 202 200 198 196 194 192 190 188 186 184 182 180 178
D K S L V S Q T S L Y H N D P L L V P G D G I P T N Q Q Y H D A L Q
sfGFP
template sequence 25Q pET-22b(+) cterminal 6His HTT
TCTTTAGACAGAACGCTTTGCGTGCTCAGATAGTGATTGTCTGGCAGCAGAACAGGACCATCACCGATTGGAGTGTTTTGCTGGTAGTGATCAGCCAGCT
aligned sequence 0802-t7term (0802-t7term.ab1)
gcacgctgccatcctccacgttgtggcgaattttaaaattcgctttaatgccatttttttgtttatcggcggtgatgtaaacattgtggctgttaaaatt
176 174 172 170 168 166 164 162 160 158 156 154 152 150 148 146 144
V S G D E V N H R I K F N A K I G N K Q K D A T I Y V N H S N F N
sfGFP
template sequence 25Q pET-22b(+) cterminal 6His HTT
GCACGCTGCCATCCTCCACGTTGTGGCGAATTTTAAAATTCGCTTTAATGCCATTTTTTTGTTTATCGGCGGTGATGTAAACATTGTGGCTGTTAAAATT
aligned sequence 0802-t7term (0802-t7term.ab1)
gtattccagcttatggcccaggatattgccgtcttctttaaagtcaatgcctttcagctcaatgcggtttaccagggtatcgccttcaaatttcacttcc
142 140 138 136 134 132 130 128 126 124 122 120 118 116 114 112
Y E L K H G L I N G D E K F D I G K L E I R N V L T D G E F K V E
sfGFP
template sequence 25Q pET-22b(+) cterminal 6His HTT
GTATTCCAGCTTATGGCCCAGGATATTGCCGTCTTCTTTAAAGTCAATGCCTTTCAGCTCAATGCGGTTTACCAGGGTATCGCCTTCAAATTTCACTTCC
aligned sequence 0802-t7term (0802-t7term.ab1)
gcacgcgttttgtacgtgccgtcatccttaaaggaaatcgtgcgttcctgcacatagccttccggcatggcggacttgaagaagtcatgctgcttcatat
110 108 106 104 102 100 98 96 94 92 90 88 86 84 82 80 78
A R T K Y T G D D K F S I T R E Q V Y G E P M A S K F F D H Q K M H
sfGFP
template sequence 25Q pET-22b(+) cterminal 6His HTT
GCACGCGTTTTGTACGTGCCGTCATCCTTAAAGGAAATCGTGCGTTCCTGCACATAGCCTTCCGGCATGGCGGACTTGAAGAAGTCATGCTGCTTCATAT
aligned sequence 0802-t7term (0802-t7term.ab1)

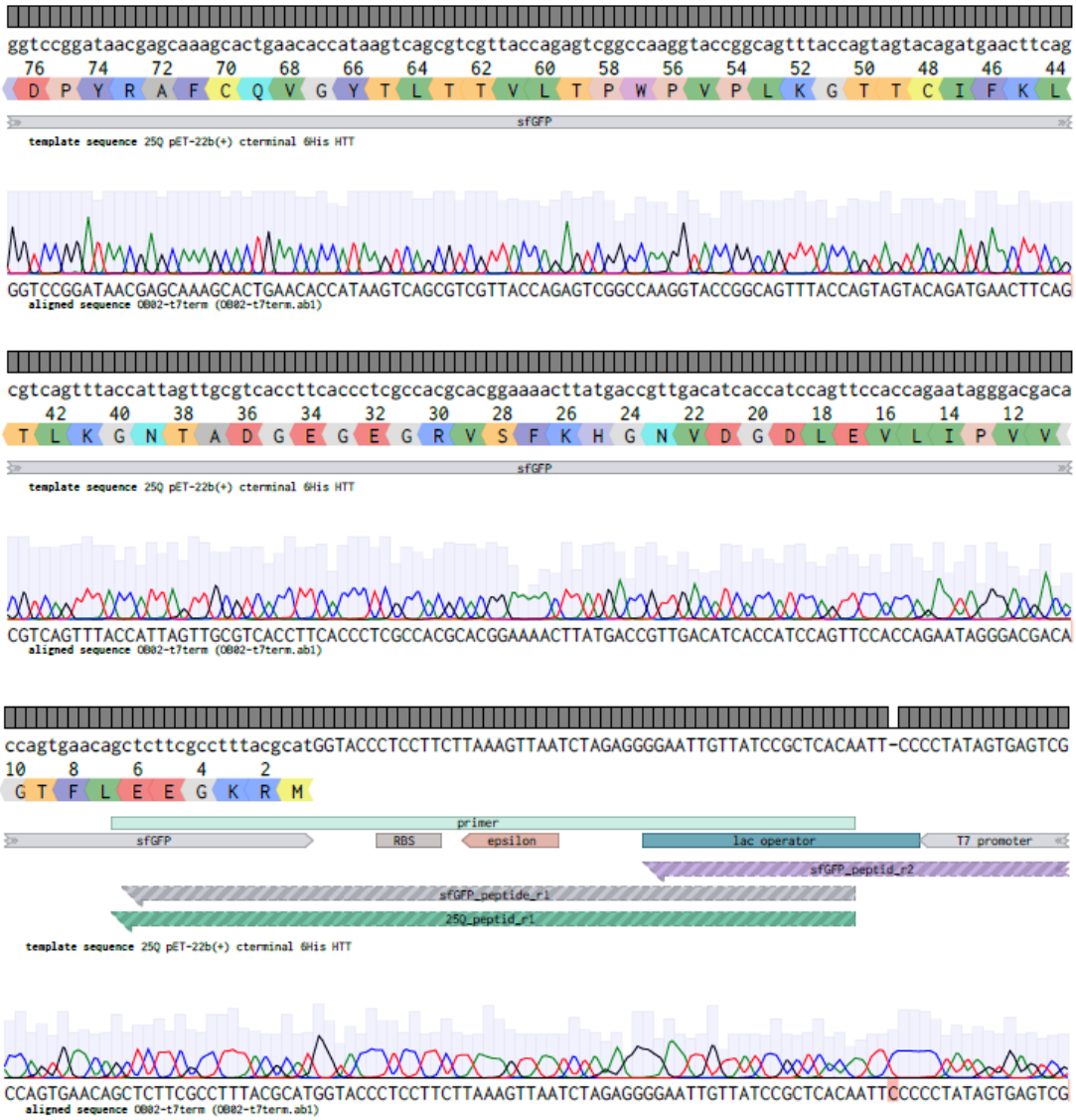

Figure D.21: The result indicating the sequence analysis of the peptide against Htt-25Q fused with sfGFP.

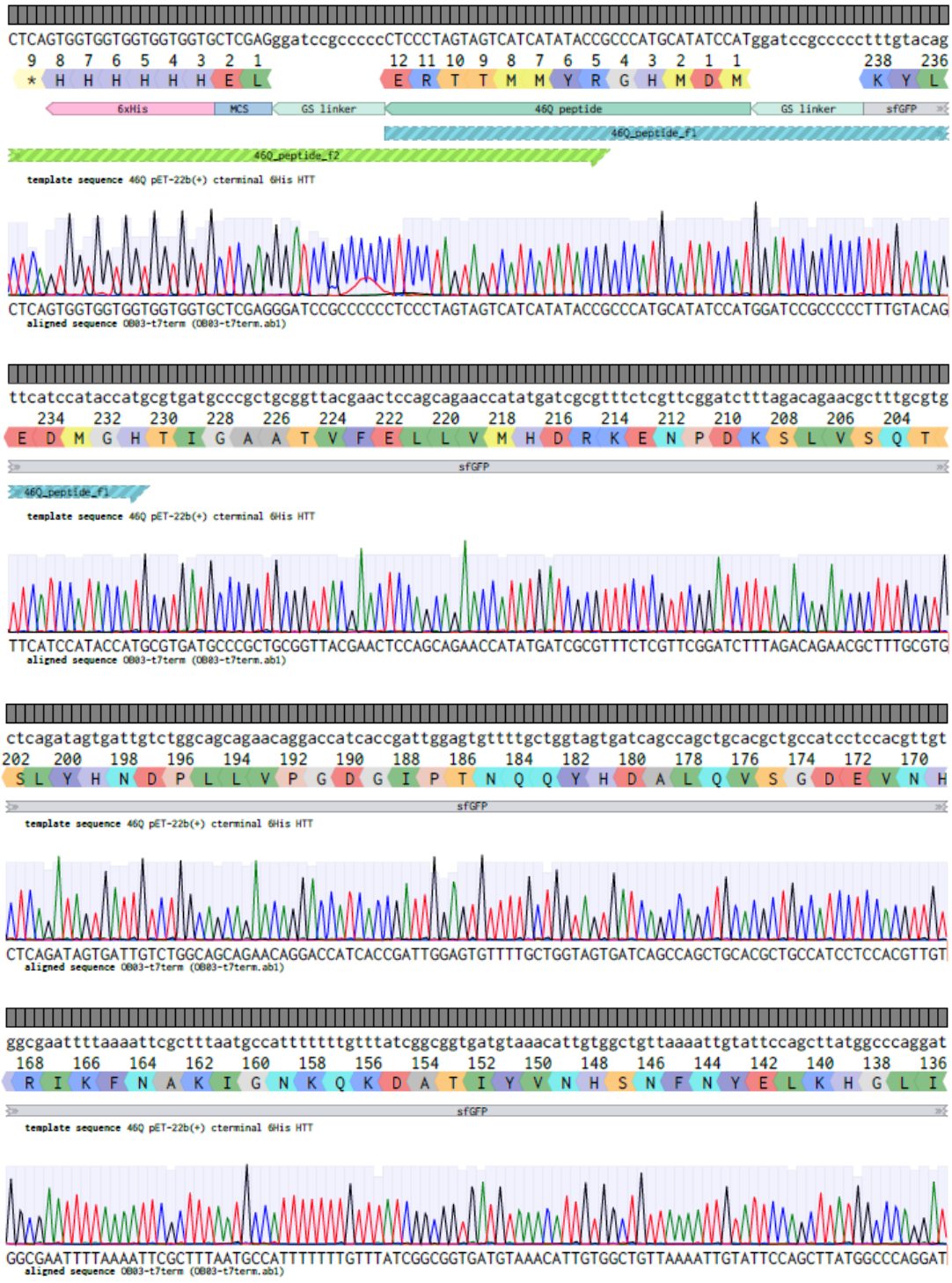
CTCAGTGGTGGTGGTGGTGCTCGAGggatccgcccccCTCCCTAGTAGTCATCATATACCGCCCATGCATATCCATggatccgccccctttgtacag
9 8 7 6 5 4 3 2 1
* H H H H H H E L
12 11 10 9 8 7 6 5 4 3 2 1 1
E R T T M M Y R G H M D M
238 236
K Y L
6xHis
MCS
GS linker
46Q peptide
GS linker
sfGFP
46Q_peptide_f1
46Q_peptide_f2
template sequence 46Q pET-22b(+) cterminal 6His HTT
CTCAGTGGTGGTGGTGGTGGTGCTCGAGGGATCCGCCCCCCTCCCTAGTAGTCATCATATACCGCCCATGCATATCCATGGATCCGCCCCCTTTGTACAG
aligned sequence OB03-t7term (OB03-t7term.ab1)
ttcatccataccatgcgtgatgcccgctgcggttacgaactccagcagaaccatatgatcgcgtttctcgttcggatctttagacagaacgctttgcgtg
234 232 230 228 226 224 222 220 218 216 214 212 210 208 206 204
E D M G H T I G A A T V F E L L V M H D R K E N P D K S L V S Q T
sfGFP
46Q_peptide_f1
template sequence 46Q pET-22b(+) cterminal 6His HTT
TTCATCCATACCATGCGTGATGCCCGCTGCGGTTACGAACTCCAGCAGAACCATATGATCGCGTTTCTCGTTCGGATCTTTAGACAGAACGCTTTGCGTG
aligned sequence OB03-t7term (OB03-t7term.ab1)
ctcagatagtgattgtctggcagcagaacaggaccatcaccgattggagtgttttgctggtagtgatcagccagctgcacgctgccatcctccacgttgt
202 200 198 196 194 192 190 188 186 184 182 180 178 176 174 172 170
S L Y H N D P L L V P G D G I P T N Q Q Y H D A L Q V S G D E V N H
sfGFP
template sequence 46Q pET-22b(+) cterminal 6His HTT
CTCAGATAGTGATTGTCTGGCAGCAGAACAGGACCATCACCGATTGGAGTGTTTTGCTGGTAGTGATCAGCCAGCTGCACGCTGCCATCCTCCACGTTGT
aligned sequence OB03-t7term (OB03-t7term.ab1)
ggcgaattttaaaattcgctttaatgccatttttttgtttatcggcggtgatgtaaacattgtggctgttaaaattgtattccagcttatggcccaggat
168 166 164 162 160 158 156 154 152 150 148 146 144 142 140 138 136
R I K F N A K I G N K Q K D A T I Y V N H S N F N Y E L K H G L I
sfGFP
template sequence 46Q pET-22b(+) cterminal 6His HTT
GGCGAATTTTAAAATTCGCTTTAATGCCATTTTTTTGTTTATCGGCGGTGATGTAAACATTGTGGCTGTTAAAATTGTATTCCAGCTTATGGCCCAGGAT
aligned sequence OB03-t7term (OB03-t7term.ab1)


attgccgtcttctttaaagtcaatgcctttcagctcaatgcggtttaccagggtatcgccttcaaatttcacttccgcacgcgttttgtacgtgccgtca
134 132 130 128 126 124 122 120 118 116 114 112 110 108 106 104
N G D E K F D I G K L E I R N V L T D G E F K V E A R T K Y T G D
sfGFP
template sequence 46Q pET-22b(+) cterminal 6His HTT
ATTGCCGTCTTCTTTAAAGTCAATGCCTTTCAGCTCAATGCGGTTTACCAGGGTATCGCCTTCAAATTTCACTTCCGCACGCGTTTTGTACGTGCCGTCA
aligned sequence OB03-t7term (OB03-t7term.ab1)
tccttaaaggaaatcgtgcgttcctgcacatagccttccggcatggcggacttgaagaagtcatgctgcttcatatggtccggataacgagcaaagcact
102 100 98 96 94 92 90 88 86 84 82 80 78 76 74 72 70
D K F S I T R E Q V Y G E P M A S K F F D H Q K M H D P Y R A F C Q
sfGFP
template sequence 46Q pET-22b(+) cterminal 6His HTT
TCCTTAAAGGAAATCGTGCGTTCCTGCACATAGCCTTCCGGCATGGCGGACTTGAAGAAGTCATGCTGCTTCATATGGTCCGGATAACGAGCAAAGCACT
aligned sequence OB03-t7term (OB03-t7term.ab1)
gaacaccataagtcagcgtcgttaccagagtcggccaaggtaccggcagtttaccagtagtacagatgaacttcagcgtcagtttaccattagttgcgtc
68 66 64 62 60 58 56 54 52 50 48 46 44 42 40 38 36
V G Y T L T T V L T P W P V P L K G T T C I F K L T L K G N T A D
sfGFP
template sequence 46Q pET-22b(+) cterminal 6His HTT
GAACACCATAAGTCAGCGTCGTTACCAGAGTCGGCCAAGGTACCGGCAGTTTACCAGTAGTACAGATGAACTTCAGCGTCAGTTTACCATTAGTTGCGTC
aligned sequence OB03-t7term (OB03-t7term.ab1)
accttcaccctcgccacgcacggaaaacttatgaccgttgacatcaccatccagttccaccagaatagggacgacaccagtgaacagctcttcgccttta
34 32 30 28 26 24 22 20 18 16 14 12 10 8 6 4
G E G E G R V S F K H G N V D G D L E V L I P V V G T F L E E G K
sfGFP
template sequence 46Q pET-22b(+) cterminal 6His HTT
ACCTTCACCCTCGCCACGCACGGAAAACTTATGACCGTTGACATCACCATCCAGTTCCACCAGAATAGGGACGACACCAGTGAACAGCTCTTCGCCTTTA
aligned sequence OB03-t7term (OB03-t7term.ab1)

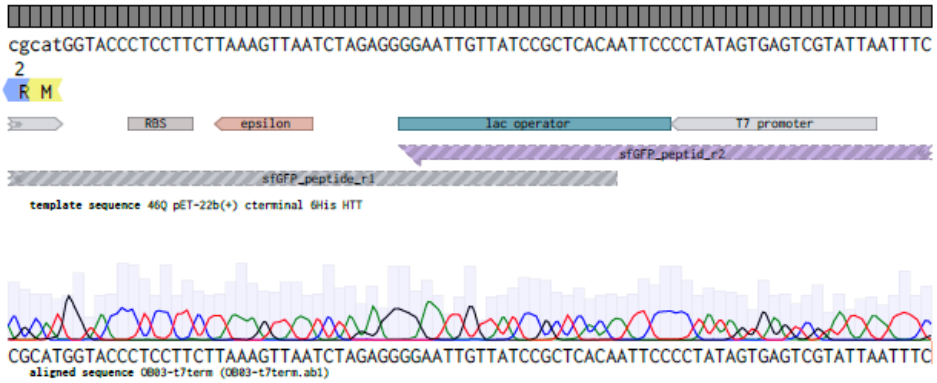

Figure D.21 1: The result indicating the sequence analysis of the peptide against Htt-46Q fused with sfGFP.

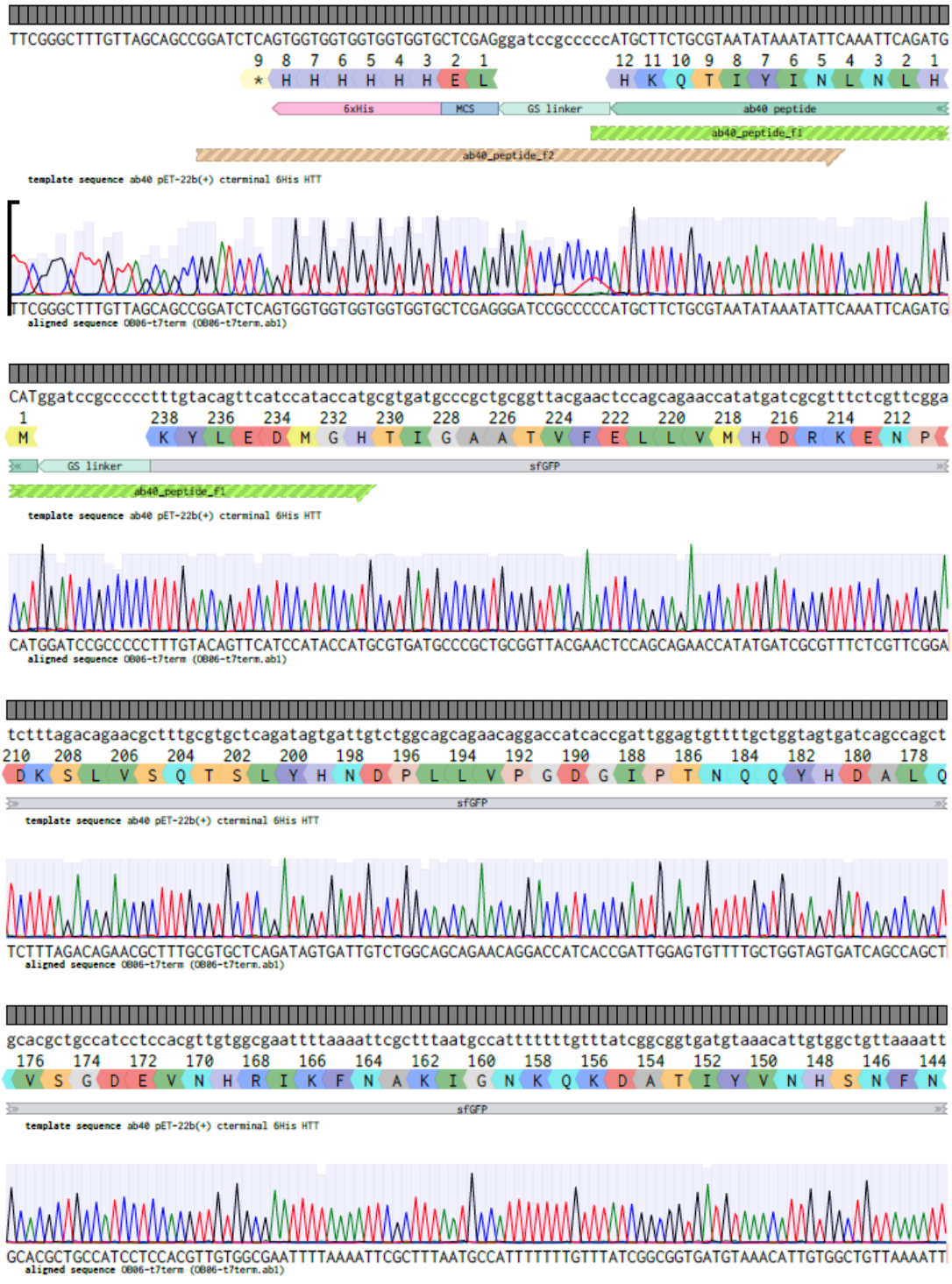
TTCGGGCTTTGTTAGCAGCCGGATCTCAGTGGTGGTGGTGGTGGTGCTCGAGggatccgccccATGCTTCTGCGTAATATAAATATTCAAATTCAGATG
9 8 7 6 5 4 3 2 1
12 11 10 9 8 7 6 5 4 3 2 1
* H H H H H H E L
H K Q T I Y I N L N L H
6xHis
MCS
GS linker
ab40 peptide
ab40_peptide_f1
ab40_peptide_f2
template sequence ab40 pET-22b(+) cterminal 6His HTT
TTCGGGCTTTGTTAGCAGCCGGATCTCAGTGGTGGTGGTGGTGGTGCTCGAGGGATCCGCCCCCATGCTTCTGCGTAATATAAATATTCAAATTCAGATG
aligned sequence OB06-t7term (OB06-t7term.ab1)
CATggatccgccccctttgtacagttcatccataccatgcgtgatgcccgctgcggttacgaactccagcagaaccatatgatcgcgtttctcgttcgga
1
238 236 234 232 230 228 226 224 222 220 218 216 214 212
M
K Y L E D M G H T I G A A T V F E L L V M H D R K E N P
GS linker
sfGFP
ab40_peptide_f1
template sequence ab40 pET-22b(+) cterminal 6His HTT
CATGGATCCGCCCCCTTTGTACAGTTCATCCATACCATGCGTGATGCCCGCTGCGGTTACGAACTCCAGCAGAACCATATGATCGCGTTTCTCGTTCGGA
aligned sequence OB06-t7term (OB06-t7term.ab1)
tctttagacagaacgctttgcgtgctcagatagtgattgtctggcagcagaacaggaccatcaccgattggagtgttttgctggtagtgatcagccagct
210 208 206 204 202 200 198 196 194 192 190 188 186 184 182 180 178
D K S L V S Q T S L Y H N D P L L V P G D G I P T N Q Q Y H D A L Q
sfGFP
template sequence ab40 pET-22b(+) cterminal 6His HTT
TCTTTAGACAGAACGCTTTGCGTGCTCAGATAGTGATTGTCTGGCAGCAGAACAGGACCATCACCGATTGGAGTGTTTTGCTGGTAGTGATCAGCCAGCT
aligned sequence OB06-t7term (OB06-t7term.ab1)
gcacgctgccatcctccacgttgtggcgaattttaaaattcgctttaatgccatttttttgtttatcggcggtgatgtaaacattgtggctgttaaaatt
176 174 172 170 168 166 164 162 160 158 156 154 152 150 148 146 144
V S G D E V N H R I K F N A K I G N K Q K D A T I Y V N H S N F N
sfGFP
template sequence ab40 pET-22b(+) cterminal 6His HTT
GCACGCTGCCATCCTCCACGTTGTGGCGAATTTTAAAATTCGCTTTAATGCCATTTTTTTGTTTATCGGCGGTGATGTAAACATTGTGGCTGTTAAAATT
aligned sequence OB06-t7term (OB06-t7term.ab1)

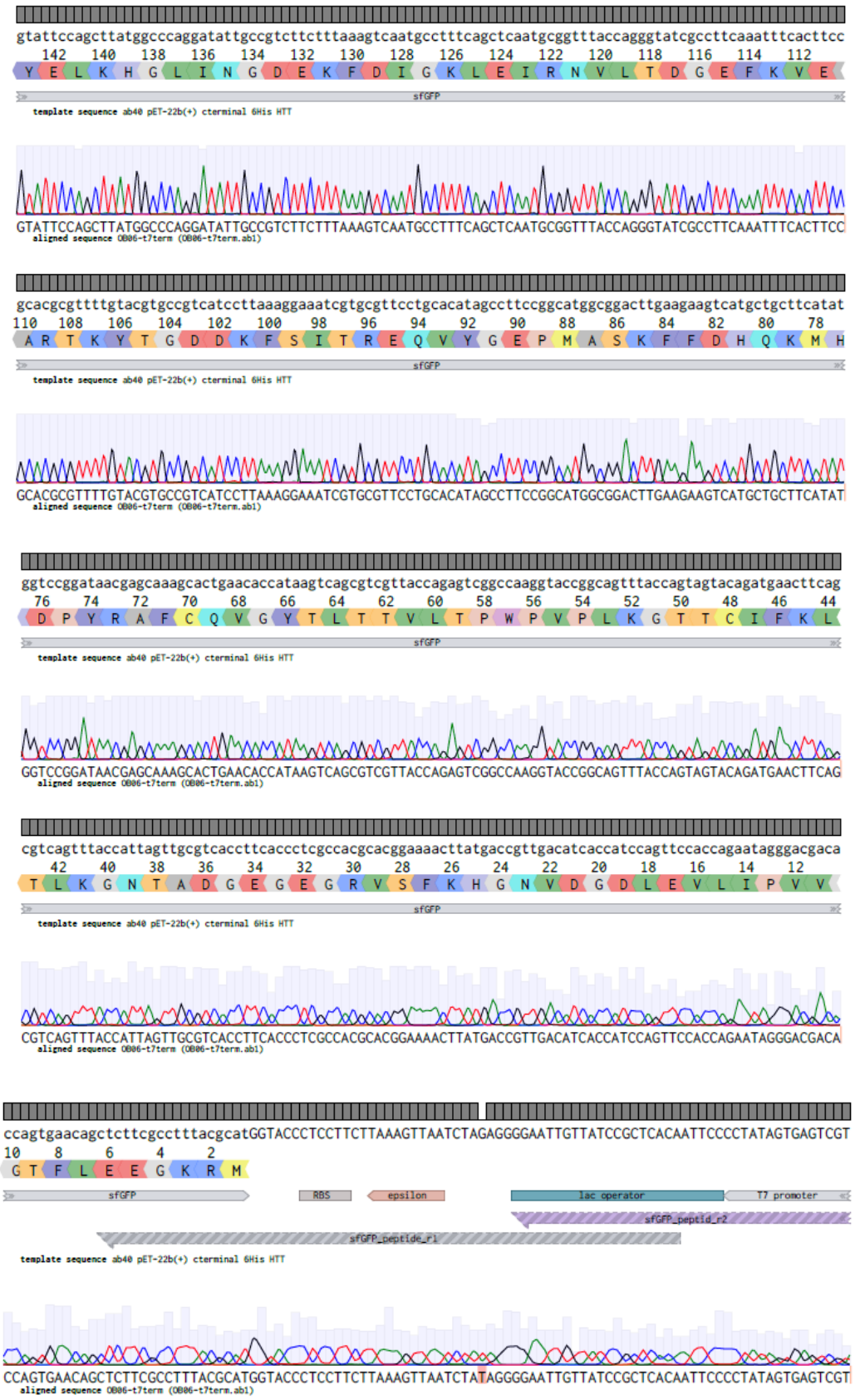

Figure D.21 2: The result indicating the sequence analysis of the peptide against aβ_{40} fused with sfGFP.